Ph.D. Dissertation

Polydimethylsiloxane Fabrication Methods using Polyvinyl Chloride Stencils and Manipulating Polymerization for a Drug Delivery Device

PDMS의 중합 억제와 Polyvinyl Chloride 패턴을 이용한 약물 전달 기기 공정 방법 제안

February 2019

Department of Electrical Engineering
and Computer Science
College of Engineering
Seoul National University

Hyun Kim

Polydimethylsiloxane Fabrication methods using Polyvinyl Chloride Stencils and Manipulating Polymerization for a Drug Delivery Device

Advisor Jong-mo Seo

Submitting a Ph.D. Dissertation of Public Administration

February 2019

Department of Electrical Engineering
and Computer Science
College of Engineering
Seoul National University

Confirming the Ph.D. Dissertation written by Hyun Kim

Chair	조동일	(Seal)
Vice Chair	서종모	(Seal)
Examiner	홍용택	(Seal)
Examiner	이종호	(Seal)
Examiner	구교인	(Seal)

Abstract

Effective drug therapy requires an adequate dosage control that can control the plasma concentration to be in between Maximum Tolerated Concentration (MTC) and Minimum Effective Concentration (MEC). The conventional drug administration methods fail to achieve effective drug therapy. Therefore, localized drug delivery devices have been devised to overcome the shortcomings of systemic drug administration, oral gavage and intravenous injection.

Localized drug delivery devices realize spatial control simply by installing it on desired sites. Challenges of drug delivery devices are precise control of dosage, exact time of release, and low power consumption. All of these can be achieved by controlling the actuation components of the device: microvalves and pumps. The proposed device utilizes a balloon-like inflatable and deflatable drug reservoir, which eliminates the use of a pump. Moreover, a normally closed magnetically actuated microvalve that requires power consumption only when it opens was constructed. Consequently, the device was designed to release drug substances driven by the tension and stress formed by the inflated drug chamber only upon the actuation of the microvalve.

Conventional PDMS patterning methods introduced in Micro Electromechanical Systems (MEMS) include photolithography and etching. Previous methods, however, require several steps and long processing time. A novel PDMS patterning method that only employs vapor deposition, oxygen plasma treatment, and stencil screen-printing was devised for simpler and faster procedure.

Vapor deposition of trichlorosilane is a commonly used method to coat a barrier between PDMS layers from bonding. In the contrary, oxygen plasma treatment is a method used to bond layers of polymerized PDMS. Coordinating the two methods, along with a polyvinyl chloride (PVC) stencil patterned using a cutting plotter or a diode pumped solid-state laser, selective bonding was implemented. Selective bonding of PDMS accounted for the formation of the drug reservoir and the pump. Moreover, inhibition of PDMS polymerization was exploited over PVC substrates to acquire results similar to PDMS etching. This new etching alternative was used to construct microchannels with widths ranging from approximately 200 to 1000 micrometers. These microchannels with varying cross-sectional area served as a secondary drug release rate regulator.

A magnetically actuated microvalve consist of two components. The opening mechanism of this normally closed valve was driven by an external magnet that produces magnetic field and a circular magnetic membrane with a neodymium magnet bonded on the surface with PDMS that deflects towards the external magnetic source. All the component of the microvalve were fabricated using only PVC stencils and PDMS-metal powder composites. Nickel powder-PDMS composite was used for the deflection membrane.

The completed device was evaluated on biocompatibility for implantation and durability for reusability. PDMS may be biocompatible, PDMS-metal powder may show different results. In the device, even though PDMS-metal powder composites were encapsulated with pure

PDMS, long-term use may increase cytotoxicity. Moreover, surface modification using trichlorosilane and oxygen plasma may also have an adverse effect on biocompatibility. Therefore, the device was tested for biocompatibility using elution and cell growth evaluation. Furthermore, the device was intended to be refillable and reusable. Thus, the durability of the microvalve and the inflatable chamber was evaluated by actuating the valve multiple times and whether or not the mechanical characteristic changed over the experiment.

Keywords : Polyvinyl Chloride (PVC) Stencil Patterning, Polydimethylsiloxane (PDMS) Polymerization Inhibition, Single and Multiple Layer PDMS Patterning, Conductive PDMS Polymer, Localized Drug Delivery Device

Student Number : 2012-30933

Table of Contents

Abstract ..... **i**

Table of Contents ..... **iv**

List of Figures ..... **vii**

List of Tables ..... **x**

Chapter 1. Introduction **1**

1.1 Drug Delivery Device in Microfluidics 2

1.2 Localized Drug Delivery Device 3

1.3 Microvalves and Pumps in Microfluidic Devices 5

1.4 Polydimethylsiloxane (PDMS) Etching 8

1.5 PDMS Surface Modification: Hydrophilic Alteration 10

1.6 Circular Cross-sectional Microchannels 12

1.7 Flexible Conductive PDMS 15

1.8 PDMS Adhesion 17

1.9 Previously Developed Drug Delivery Devices 19

1.9.1 Electro-actively Controlled Thin Film 19

1.9.2 Drug Release through Microchannel Configuration 20

1.9.3 Frequency Controlled Hydrogel Microvalve 21

1.9.4 Magentically Controlled MEMS Device 22

1.9.5 Electrochemical Intraocular Drug Delivery Device 23

1.9.6 Electrostatic Valve with Thermal Actuation 25

1.9.7 Transdermal Delivery through Microneedles 27

1.9.8 Osmotic Drug Delivery Devices 28

1.10 Summary 35

Chapter 2. Materials and Procedure 39
2.1 System Overview 39
2.2 Materials 41
2.2.1 Polydimethylsiloxane (PDMS) 41
2.2.2 Polyvinyl Chloride (PVC) Adhesive Sheets 42
2.2.3 Magnetic Microparticles and Neodymium Magnet 45
2.2.4 Silver Microparticles 46
2.3 Procedures 48
2.3.1 Spin Coating 48
2.3.2 Oxygen Plasma Treatment 49
2.3.3 Silanization (Self-Assembled Monolayer) 51
2.3.4 Plasma Bonding 53
2.4 Fabrication 54
2.4.1 PDMS Etching via PVC Stencils 54
2.4.2 Inflatable Chamber Fabrication 59
2.4.3 Full Fabrication of the Drug Delivery Device 63
2.4.3.1 Primary and Secondary Drug Chamber 64
2.4.3.2 Microvalve 67
2.4.3.3 Magnetic Actuation 71

Chapter 3. Results 74
3.1 PVC Stencil Preparation 74
3.2 Surface Modification and Selective Bonding 76
3.3 PDMS Polymerization Inhibition 83
3.4 PDMS Etching 86
3.5 Three Dimensional Microchannel Fabrication 91
3.6 Circular Cross-sectional Microchannel 94
3.7 Inflatable Chamber Fabrication 97

3.8 Conductive PDMS Fabrication.....99
3.9 Drug Delivery Device.....104
3.9.1 Dimensions and Profile of the Device.....105
3.9.2 Fluid Release Amount of the Device.....105
3.8.2.1 Case 1 105
3.9.2.2 Case 2 106
3.9.2.3 Case 3 107
3.10 *In Vitro* Cytotoxicity of the Device 110

Chapter 4. Discussion 116
4.1 Electromagnetic Actuation 116
4.2 Drug Substance Delivery.....118
4.3 Comparison with Similar Drug Delivery Devices 119
4.4 Integration of the Device with PDMS Electrodes.....121

Bibliography.....123

Abstract in Korean 143

List of Figures

Figure 1-1. Therapeutic Range of Drug Delivery 1
Figure 1-2. Micro-valves with Various Actuation Mechanisms .6
Figure 1-3. Previous PDMS Etching Methods 9
Figure 1-4. Existing Circular Microchannel Fabrication Methods (Micromilling) 13
Figure 1-5. Existing Ciruclar Microchannel Fabrication Methods (Sacrificial Layer) 14
Figure 1-6. Stretchable Conductive PDMS 16
Figure 1-7. Drug Delivery Devices in Development 26
Figure 1-8. Commercial Drug Delivery Devices 32
Figure 1-9. Components of the Proposed Drug Delivery Device 35

Figure 2-1. Polydimethylsiloxane Polymerized Formula..... 41
Figure 2-2. Oxygen Plasma Treatment of PDMS 50
Figure 2-3. Self-assemble Monlayer Coating of PDMS 52
Figure 2-4. Plasma Bonding of PDMS 53
Figure 2-5. PVC Stencil Fabrication Method to Achieve PDMS Etching Results 56
Figure 2-6. PVC Stencil Fabrication Method to Execute Selective Bonding 62
Figure 2-7. PVC Stencils Required to Fabricate the Drug Delivery Device 63
Figure 2-8. Fabrication of Chamber Layer of the Drug Delivery Device 65
Figure 2-9. Fabrication of Microvalve 68
Figure 2-10.Cross-sectional View of Microvalve and its Actuation 69

Figure 3-1. Stencil Comparison between DPSS Laser Ablation and Cutting Blade Plotter 74
Figure 3-2. PDMS Surface Modification via Silanization and Oxygen Plasma Treatment 77
Figure 3-3. Water Contact Angle Measurements of Modified PDMS Surfaces 78
Figure 3-4. Change in Water Contact Angle Overtime through Different Oxygen Plasma Recipe 80
Figure 3-5. Transferring PVC Stencils onto PDMS Surface via Transfer Paper 82
Figure 3-6. Implementation of Selective Bonding 83

Figure 3-7. Polymerization Inhibition of PDMS on PVC Stencils 84
Figure 3-8. Relationship between PDMS Polymerization Inhibition and PDMS Thickness on PVC Stencils 86
Figure 3-9. Vertical Profile of PDMS Microchannels 88
Figure 3-10 Diagram of Overcut Profile of PDMS Microchannels . 89
Figure 3-11. Overcut Profile of PDMS Microchannels 90
Figure 3-12. Fabrication of Three Dimensional Microchannels 92
Figure 3-13. Three Dimensional Microchannels 94
Figure 3-14. Circular Microchannel Fabrication via Selective Bonding 95
Figure 3-15. Cross-sectional Images of Circular Mirochannels 96
Figure 3-16. Inflatable Circular Chamber with Inlet and Bolting Microchannel 98
Figure 3-17. Maximum Tolerable Volume of the Inflatable Chamber with Respect to the Radius of the Chamber and Width of Bolting Microchannel 99
Figure 3-18. Silver PDMS Mixed in Different Ratios 101
Figure 3-19. Resistance and Conductivity of Silver PDMS with Different Ratios 102
Figure 3-20. Flexible Conductive PDMS 103
Figure 3-21. Diagram and Real Image of the Drug Delivery Device 104
Figure 3-22. Case 1: DI Water Delivery 106
Figure 3-23. Case 2: DI Water Delivery 107
Figure 3-24. Case 3: DI Water Delivery 108
Figure 3-25. Volume Change of the Chamber Over Time..... 109
Figure 3-26. Cell Viability of L-929 Fibroblast According to Concentration of the Extracts 113
Figure 3-27. Cell Morphology after 24 Hours 114
Figure 3-28. Cell Morphology after 48 Hours 115

Figure 4-1. Schematic of Electromagnetic Actuation 117
Figure 4-2. Comparison with other Magnetically Actuated Drug Delivery Device 119
Figure 4-3. Comparison with other Active Drug Delivery Device 121
Figure 4-4. Diagram of Electrode and Drug Delivery Device Integration 122

List of Tables

Table 1-1 Comparison of currently in development or commercially available drug delivery devices 33
Table 1-2 Comparison of currently in development or commercially available drug delivery devices 34
Table 3-1 Cross-sectional profile of PDMS microchannels 91
Table 3-2 Conductivity and Resistivity of Metals 100
Table 3-3 Case 1: Dimensions of the Device 105
Table 3-4 Case 2: Dimensions of the Device 106
Table 3-5 Case 3: Dimensions of the Device 107
Table 3-6 Quantitative Biocompatibility Evalutaion of the Drug Delivery Device 111
Table 3-7 Qualitative Biocompatibility Evaluation of the Drug Delivery Device 112

1. Introduction

Microfluidics grew into versatile technological applications since its advent in the 1990's: fluid mixing and separation, miniaturized sensors, lab-on-a-chip devices etc. [1]-[10]. These devices are normally fabricated using conventional Micro Electromechanical System (MEMS) fabrication methods. Through conventional Micro Electromechanical System (MEMS) fabrication procedures such as photolithography, deposition, and etching, the devices normally use polydimethylsiloxane (PDMS) for its biocompatibility, chemical compatibility, flexibility, easy fabrication, and optical transparency [11], [12]. Microfluidics developed into the drug delivery field as fabrication methods progressed to have higher resolution and a capability to build complex multi-layer designs.

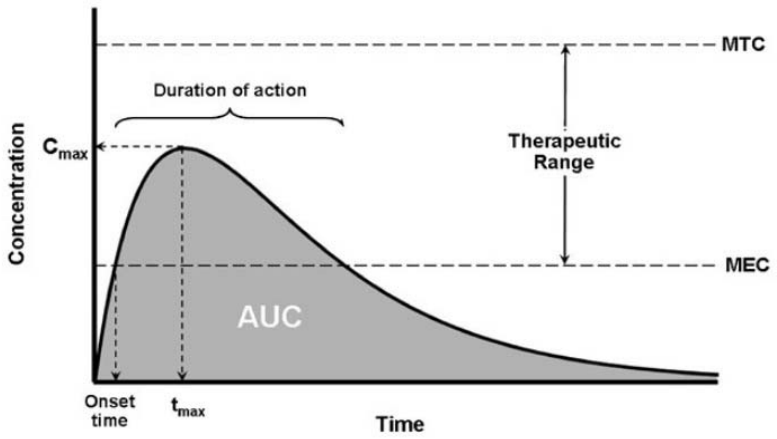

Figure 1-1. Therapeutic range drug delivery devices should aim for: between Maximum Tolerable Concentration (MTC) and Minimum Effective Concentration (MEC).

Therapeutic drug delivery requires adequate amount of drug release

to maintain a plasma concentration to a level between Maximum Tolerated Concentration (MTC) and Minimum Effective Concentration (MEC). Conventional drug administration methods, systemic and local, reach highest concentration shortly after injection. The duration of action of administered drug starts as soon as the concentration rises above and stops as it falls below MEC. Purpose of effective drug therapy is to prolong this duration as long as possible. However, oral and injection methods' concentrations rapidly decrease [13]. Consequently, higher dosage or periodic administration is necessary. Higher dosage can increase the risk of cytotoxicity and periodic administration may be problematic. Therefore, considerable efforts have been devoted towards developing 'smart' advanced drug delivery systems to realize effective drug therapy [14]-[16].

1.1. Drug Delivery Device in Microfluidics

Recently, various novel drug delivery platforms have been developed to target sites to improve the outcome of the treatment process [17]. These devices can be categorized into micro, nanoparticle size drug carriers made of biodegradable material [18]-[20] and localized drug delivery device by their mechanism on how they achieve spatial control [21]-[23].

Drug carriers generate reproducible release profile by encapsulating drug substances with degradable or withstanding materials in certain PH or temperature [24], [25]. For example, orally administered drug carriers

must survive pass through the low PH of the gastrointestinal tract to be released into the blood stream. Moreover, they have to be small enough to be able to pass through the intestinal mucosal barrier. Fabrication of drug carriers [17], [19], [20], self-assembly [26]-[30], droplet-based, non-spherical [31]-[37] etc. is plausible by recent advances in development of microfluidic systems. Drug carriers, like any other drug delivery devices, should adjust release rate, improve bioavailability, and reduce cytotoxicity.

Localized drug delivery devices realize spatial control by directly installing the device onto desired sites. Therefore, only temporal control is required. Microfluidic systems allow precise handling of nano-liter and pico-liter volumes. More importantly, these systems can be programmed to release a certain amount, which can be accurately reproduced assuming constant conditions. This direct delivery characteristic facilitates the use of drugs with short half-life or those that may be toxic when systemically administered.

1.2. Localized Drug Delivery Device

Localized drug delivery devices can be subcategorized into various types such as drug loaded polymeric devices and microfluidic implantable devices [38]. Drug loaded polymeric devices utilize diffusion or biodegradability of the composing material. Due to these release mechanisms, these devices have a few shortcomings. Drug release begins delivery as soon as drug is loaded in the device for devices

that utilize diffusion. For biodegradable devices, release begins when the device reaches a certain environment, PH, heat, or elapsed time [24], [25]. For localized drug delivery devices that utilized biodegradability, release initiates when they are installed on chosen locations.

The localized drug delivery devices focused in this paper are implantable microfluidic devices controlled by convective forces such as magnetic [40], [41], electromagnetic [42], [43], [49], electrostatic [44], [45], osmotic [46]-[48], and pneumatic [39], [50] etc. These devices are different from diffusion or degradation-based devices in that they are designed to be responsive to convective forces, therefore, which enable on demand drug delivery. Furthermore, release rate can also be controlled which has its advantage of diffusion-based delivery platforms with continuous and non-uniform release profile.

Microfluidic local drug delivery platforms are usually comprised of a drug reservoir, a pump, a valve and a microchannel [51]. The simplest design of these various platforms employ a mechanical pump and a valve that pushes and opens by an outside trigger: magnetic [40], [41], electromagnetic [42], [43], [49], electrostatic [44], [45], thermal [52], etc. Here, microchannels lie between other components such as valves and drug reservoirs not only connecting them, but also guiding drug flow to precise locations. Recently developed localized drug delivery devices attempt to simplify the design by eliminating crucial components such as pumps or valves. Since pumps and valves in this device are power-consuming components, reducing these components not only simplifies the design, but also reduces overall power-consumption.

While spatial control of drug delivery devices are realized by fixing the device on desired sites, temporal control is relatively more difficult. Temporal control can be achieved actively or passively. Polymeric devices that manipulate biodegradability and diffusion are passive devices. As mentioned above, passive devices fail to deliver exact quantities of drug to target sites. Active control can amend these shortcomings of passive control systems. These systems allow on demand drug administration and precise drug quantification in response to external stimuli such as electric or magnetic fields. However promising these systems may be, several challenges still remain. Micrometer-scale pump, channel, well, and valve fabrication technologies have been developed yet integrating them to build a single system is challenging.

1.3. Microvalves and Pumps in Microfluidic Drug Delivery Devices

Many types of miniaturized microvalves and pumps for lab-on-a-chip have been developed. Different types of actuation and modes exist in valve and pumps. To be applied on lab-on-a-chip devices, several complications in developing microvalves and pumps must be met.

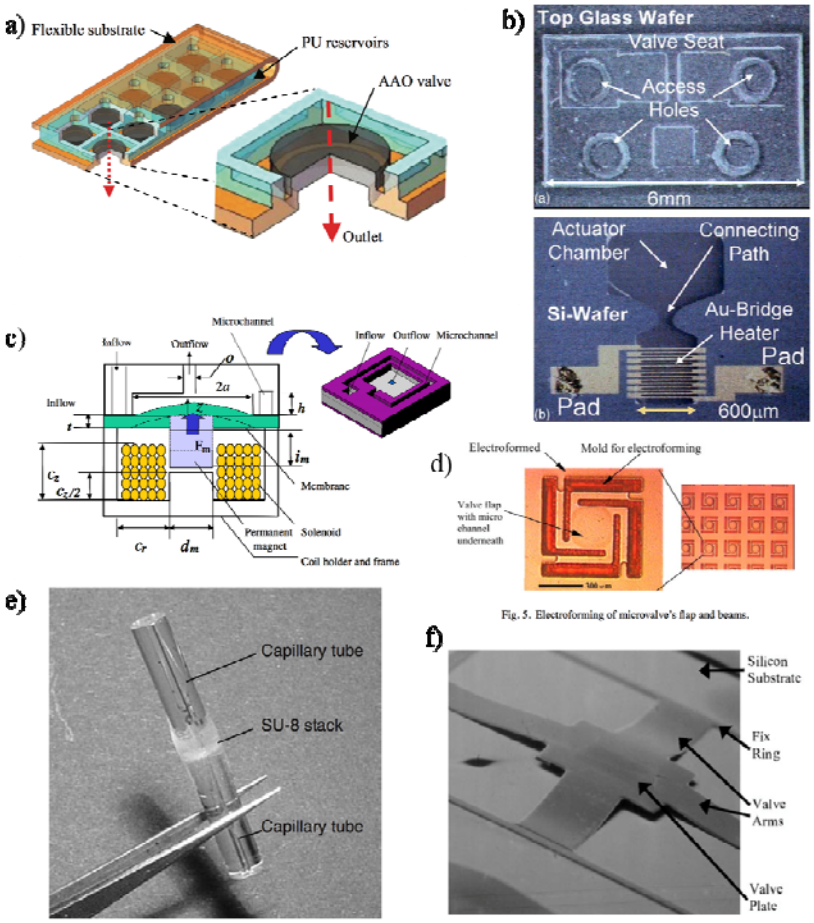

Fig. 5. Electroforming of microvalve's flap and beams.

Figure 1-2. Microvalves with various actuation mechanisms. a), b), c) are active microvalves and d), e), f) are passive microvalves. a) electro-active nanovalve array reusable for drug delivery [53]. b) thermos-pneumatic actuator valve for a blood test system [66]. c) electromagnetically actuated valve for glaucoma implant [54]. d) Passive check valves actuated piezoelectrically [69]. e) Full polymeric micro check valves [74]. f) Micromachined passive valve fabricated through polycrystalline silicon [70].

Microvalves can be categorized initially by active [53]-[68] and passive [69]-[79]. These passive and active microvalves can be further

categorized into their actuation originality. Passive and active microvalves can be subcatergorized into mechanical and non-mechanical components. Mechanical active microvalves are accomplished using conventional MEMS-based micromachining technologies where mechanically moveable membranes or components are coupled to magnetic, electric, piezoelectric or thermal actuation. Non-mechanical active microvalves actuate due to their functionalized smart materials such as phase change or rheological materials. Passive microvalves can also be classified into mechanical and non-mechanical categories. However, passive microvalves are regarded as micropumps since there is no fine line between them considering their actuation mechanism [80]-[82]. Microvalves can also be divided into their initial mode: normally open [67], [83]-[85] and normally closed [68], [86]-[87]. The design of the microvalve determines the initial mode. Normally closed mode requires energy consumption only when it needs to be opened. Normally open mode requires energy only when it needs to be closed. Therefore, normally closed mode is more desirable for it requires less energy consumption.

Typical operation range of micropumps lies in between a few microliters to tens of microliters. Micropumps can also be classified into mechanical and non-mechanical pumps. Mechanical pumps utilize moving parts such as check valves, oscillating membranes, or turbines for delivering a constant fluid volume in each cycle. Non-mechanical pumps add momentum to the fluid for pumping effect by converting another energy form into kinetic energy. All micropumps, mechanical or

non-mechanical, require energy consumption.

With the energy consumed in the microvalve and the micropump, installing a power source large enough to handle them both on a localized drug delivery device is difficult for its millimeter-size device. Therefore, localized drug delivery devices must minimize the power consumption throughout the device.

1.4. Polydimethylsiloxane (PDMS) Etching

PDMS is a polymeric material used in a variety of fields for its biocompatibility, chemical resistance, optical transparency, flexibility, and ease in fabrication. Its innate ability to convert from liquid form to solid form just by applying heat makes it so prevalent over other materials used in similar fields. Conventional MEMS fabrication methods such as spin coating, photolithography, several surface modification techniques are commonly used methods to produce patterned PDMS [88]-[92]. However, there are also some drawbacks. Since the polymerization process of PDMS is irreversible once PDMS solidifies, re-patterning is possible only with certain defects or shortcomings. Moreover, PDMS is frequently used to replicate by developing hard molds. Therefore, only single layer patterning is possible. Consequently, complex designs with multiple layer fabrication can only be realized by bonding fully polymerized PDMS layers. In this process, difficulties rise in handling thin layers of patterned PDMS and alignment of patterns of different layers.

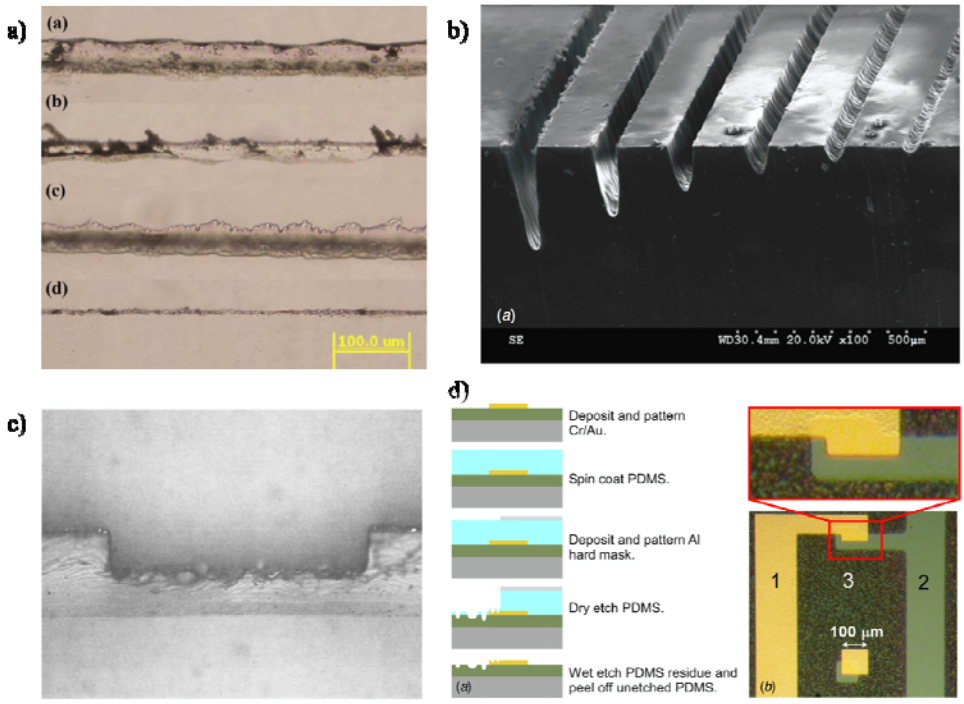

Figure 1-3. Previous PDMS etching methods. a), b) are PDMS etching using high powered CO_2 laser [95]. c) is an image of PDMS dry etching using only fluorine based reactive ion etching [96]. d) is fabrication steps for PDMS etching by combination of wet and dry etching [97]

. Patterning polymerized PDMS can be plausible by a few methods: direct laser cutting, wet and dry etching. High-powered laser such as CO_2 laser or Diode Pumped Solid State (DPSS) can be used to cut out grooves on fully polymerized PDMS [93]-[95]. Since patterning is achieved by burning off polymerized PDMS, the resulting surface is not smooth enough and microscale residue may be difficult to wash off. Dry and wet etchings of PDMS are also fabrication methods that can pattern fully polymerized PDMS. Dry etching is performed by fluorine-based reactive ion etching (RIE) [96]. Regulating the gas ratio between oxygen and

tetraflouromethane can control the etching rate of RIE. Relatively simple, however, the procedure demands long hours of processing time just to etch a few tens of micrometers of PDMS and is incapable of meeting precise amount of etching depth. The process produces significant surface roughness, which is inadequate for microfluidic applications. Wet etching of PDMS is a type of chemical etching [97]. A mixture of tetrabutylammonium fluoride (TBAF) and n-methyl-2-pyrrolidion (NMP) with a ratio of 1:3 can melt off PDMS on contact areas. However, severe undercutting is unavoidable due to lateral etching. Moreover, PDMS that has undergone chemical etching process does not sustain the physical and chemical characteristics of normal PDMS. Complete removal of microscale, even nanoscale residue or arbitrary patterns on PDMS surfaces caused by wet and dry etching is vital since they can cause turbulent fluid flow in microchannels. Furthermore, both wet and dry etchings require photo-resistive hard baked patterns developed by photolithography prior to the etching process. This does not only increase steps in developing photoresist patterns, but also steps in removing photoresist patterns after PDMS etching.

1.5. PDMS Surface Modification: Hydrophilic Alteration

PDMS polymerization starts with mixing PDMS pre-polymer with a curing agent in 10:1 ratio. After mixing and degassing for uniformity,

PDMS is spin coated onto a silicon wafer or a patterned surface. PDMS takes on a liquid form before it undergoes hydrosilylation process. Therefore, spin coating and replica molding is easily achievable. The hydrosilylation process solidifies liquid PDMS into solid PDMS, which can be accelerated with the aid of heat stimuli. Fully polymerized PDMS preserves its advantageous characteristics such as biocompatibility, high chemical resistance, optical transparency etc., however, gains one crucial disadvantage inadequate in biomedical applications: hydrophobicity. Hydrophobicity of native PDMS hinders bonding between PDMS and other materials such as glass, silicon and other PDMS, disrupts liquid delivery and decreases the possibility of proteins or cells from binding to the surface.

In recent years, there have been many PDMS surface modification methods such as plasma treatment, silanization, ultraviolet treatment, chemical vapor deposition (CVD), layer-by-layer (LBL) deposition, metal and metal oxide coatings, partial curing methods, suspended gel methods, protein absorption, graft polymer coating and hydrosilylation-based surface modification [98], [99]. Many of these methods require multiple steps and long processing time. Oxygen plasma treatment is the most common method used to enhance hydrophilicity of PDMS. However, oxygen plasma treated surfaces starts reverting back to hydrophobic state minutes after treatment. A more permanent method increasing hydrophilicity of PDMS surfaces is silanization. Silanization, also known as Self Assembled Monolayer (SAM) coating, is normally used to rende PDMS surfaces superhydrophobic. Unlike oxygen plasma

treatment, SAM coatings form covalent bonds on the surface of PDMS, thus, the modification is permanent. Therefore, a combination of these two procedures can achieve moderately hydrophilic PDMS surfaces.

Oxygen plasma treatment is commonly used to bond two polymerized PDMS together. On the other hand, silanization builds an anti-bonding layer on the surface so that PDMS replica molding on PDMS mold can be realized. Here, an adequate mixture of oxygen plasma treatment and silanization using trichlorosilane was used to increase hydrophilicity, increase adhesiveness, and bonding.

1.6. Circular Cross-sectional Microchannels

The conventional method of fabricating microchannels produces channels with rectangular cross-sectional areas. Whereas, these rectangular cross-sectional channels may be used for fluid mixing and separation, they are inadequate for biomedical and microfluidic applications. In microfluidic applications, viscous fluid flow through rectangular microchannels produce a laminar flow where the velocity ranges from zero at the walls to highest towards the center of the channel. Due to the rectangular shape, when the laminar flow reaches equilibrium, the velocity around the four corners of the channel is zero and fluid there remain untouched. However, circular cross-sectional microchannels do not have corners where residual fluid remains. Therefore, for biomedical and microfluidic applications, circular cross-sectional microchannels are more preferable.

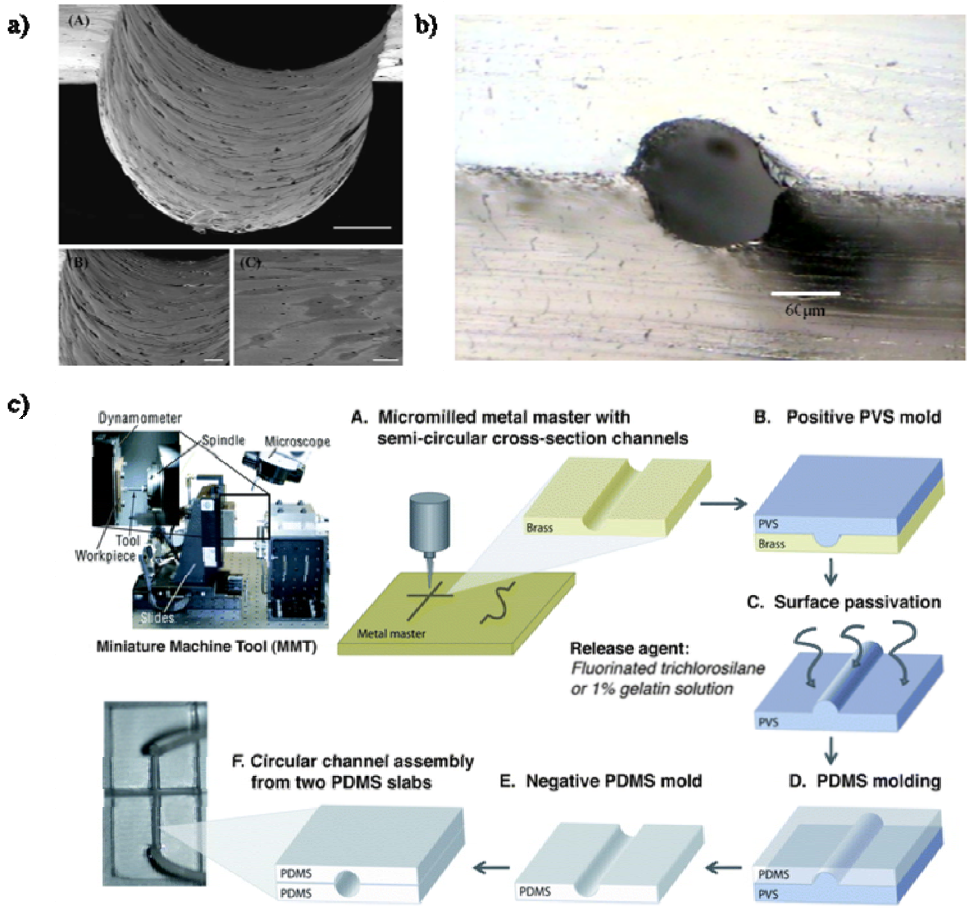

Figure 1-4. Circular PDMS microchannel fabrication methods. a) [100] and b) [101] are thermal reflow methods utilized to develop PDMS microchannels. c) is an image of molds fabricated through micromilling [102]. All these methods require bonding of two half-cylindrical molds.

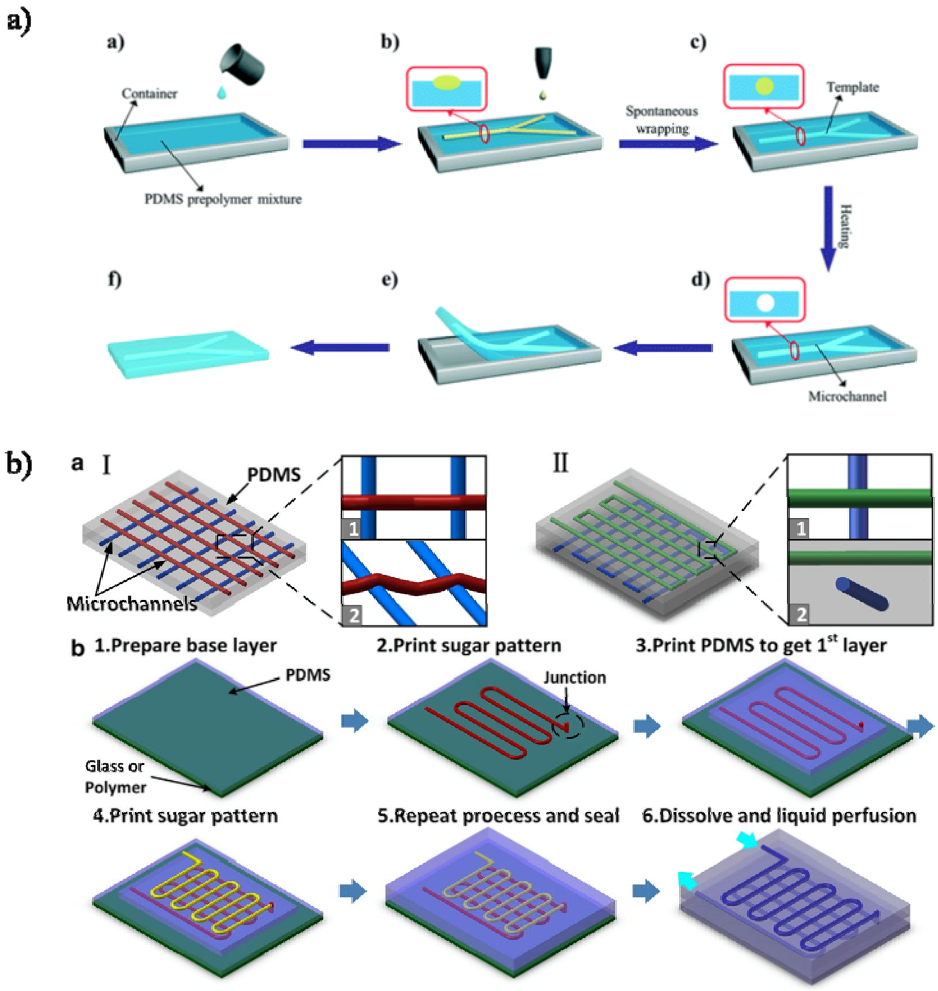

Figure 1-5. Circular microfluidic channel fabrication method using sacrificial templates by inkjet printers [103] and sugar templates [104].

Previously developed circular cross-sectional microchannel fabrication methods employ conventional MEMS fabrication methods: photolithography patterning with thermal reflow [100], [101], and micromilling [102]. The typical fabrication methods produce two open semi-circular cylinders where the two are bonded to construct a cylindrical channel. Since the constructed channels are tens or hundreds of micrometers thick, alignment to realize perfect cylindrical shape is

very difficult. Many novel circular cross-sectional microchannel fabrication methods have been devised. An inkjet printer was used to pattern microchannels on pre-polymerized PDMS bath. The ink printed on the PDMS bath was then immersed. PDMS was then polymerized and the ink was removed [103]. Another example of a novel circular cross-sectional microchannel fabrication was by a sugar printer [104]. A three dimensional structure was printed using a 3D printer that uses sugar filaments. The structure is then immersed in a PDMS bath and polymerized. Similarly, the structures can be easily oxidized or melted through to construct microchannels. Both methods are examples of fabricating circular cross-sectional microchannels. However, both methods produce slightly dented circular channels due to the softness of the filaments or the ink used.

1.7. Flexible Conductive PDMS

Conductive line fabrication over rigid surfaces is achievable using conventional MEMS fabrication methods. Deposition, photolithography patterning, and etching steps are required to accomplish lift-off processes to pattern metals. Most of these metal conductive lines are deposited over hard substrates such as silicon wafers and glass plates for several reasons. Flexible materials such as PDMS, polyimide, parylene, etc. have weak adhesion to metal substances [105]. However malleable metals may be, deposited metal on PDMS and parylene easily tear off. Moreover, metals cannot stretch like polymeric materials. When metal-coated PDMS is

bent, deposited metals crack and disconnect. Consequently, considering it durability, metal deposition patterning on flexible materials may be inadequate.

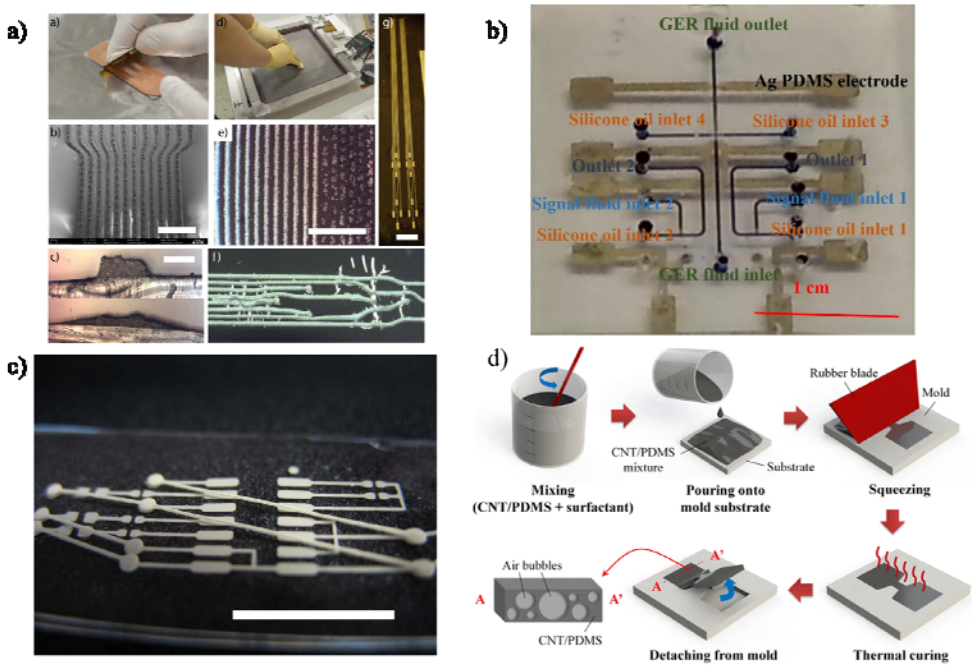

Figure 1-6. Stretchable conductive PDMS using silver and CNT particles. a) [106], b) [107], c) [106] silver PDMS composites used with metal stencils or SU-8 mold. d) Carbon nanotube conductive PDMS designed using polymeric molds [125].

Alternative conductive line fabrication methods on flexible polymeric materials have been devised. A composite of conductive particles with polymers were investigated and tested. Silver, nickel, copper, iron, nano, microparticles, and carbon nanotubes (CNT) [125] were mixed with PDMS in several different weight ratios to manufacture conductive lines on polymeric devices [106], [107], [123]. These

conductive lines were mounted on other polymeric flexible substrates. However, since the mixture contains PDMS, an insulating material, high conductivity was difficult to achieve. Higher ratios of conductive powder can be a solution to increase the conductivity. However, as the volume ratio goes over 25% of conductive powder to PDMS the mixture becomes too slurry consequently raises difficulties in molding into desired shapes [106], [107].

Another drawback in applying PDMS and metal particle composite to developing conductive circuit on PDMS substrate is the unreliability of composite mixing method. Conductivity of PDMS-metal powder composite is determined by the uniform distribution of particles in the PDMS solution. Manual mixing fails to achieve uniform distribution and thus results in inconsistent conductivity [106], [107].

1.8. PDMS Adhesion

PDMS has received attention because it is stretchable and flexible. Consequently, PDMS is appropriate for attaching onto surfaces like skin and implanting into the body. However, completely polymerized PDMS has hydrophobic surface properties. Thus, attaching and securely fixing a PDMS based device on skin or implanting into a body requires an additional adhesive layer fabrication step.

In previous studies, securely fixing biomedical devices such as electrodes and drug delivery devices onto hydrophilic and hydrophobic surfaces was realized by applying tape [108], polymeric adhesives, or

sutures [109]. Using tape has been the easiest method many biomedical devices utilize. However, using tapes leaves a messy result. Therefore, using tapes were only implemented on prototype testing. Polymeric adhesives that are used mainly on bandages have also been used to position devices. The adhesives are pre-manufactured and have a rather thick profile to it. The adhesives can be easily cut using blades or scissors. Manufacturing and mounting onto fabricated devices is simple. Recently, adhesive PDMS (Dow Corning, MG7-9900) was also used to increase adhesiveness to paste on the epidermis [110]. Suturing device onto skin or organs has also been investigated [109]. Localized drug delivery devices are invasive in their nature. Suturing is not only invasive but it also increases discomfort to the subject. Furthermore, retrieving the device requires an additional invasive procedure. Also, a biomimetic approach to realize adhesion of PDMS on hydrophilic and hydrophobic surfaces has been investigated. A physical characteristic inspired by geckos and mussels were tested [111]. Mussel-mimetic polymer coated micropillar fabrication was implemented to increase adhesion. The increase in adhesion of biomimetic micropillars remains a controversy, still.

Previously developed adhesive methods and materials all have simple fabrication processes. However, the manual process results in a messy and sloppy implementation of the device. Moreover, these methods increase bulkiness to the device and long-term biocompatibility has not yet been tested intensively.

1.9. Previously Developed Drug Delivery Devices

In this subsection, drug delivery devices available commercially, or in its research level are investigated. Fabrication methods, composition, actuation methods, drug delivery rates, advantages, disadvantages etc. were analyzed to compare the results with the proposed drug delivery device.

1.9.1. Electro-actively Controlled Thin Films [112]

This active control drug delivery device utilizes electroactive thin films actuated by the presence of a small-applied voltage of 1.25 V. This drug delivery device is an example of a layer-by-layer release actuation device. These electroactive films, also known as Prussian Blue (PB), are nontoxic, FDA-approved inorganic hexacyanoferrate compound. Fabrication of the device is rather simple. A glass substrate is coated with a conducting film of indium tin oxide (ITO). This is then dipped in a solution containing a cationic drug or drug carriers then rinsed with deionized water. Next, the substrate is dipped in an aqueous PB solution and again rinsed with deionized water. This process is repeated many times to build a layer-by-layer profile of drug/drug carriers and electroactive particles. Deconstruction of the films is initiated when an electrochemical potential of 1.25 V is applied. PB particles switch to the neutral Prussian Brown (PX) state and destabilize the film to release the encapsulated drug components.

This device runs on low voltage. The low power consumption of the

device increases its potential applicability to implantable pharmacy-on-a-chip applications. The device can be easily switched on and off by applying and disconnecting the power source. Experimental results show no release of drug substances while no voltage is applied. The device releases micrograms of drug substances or carriers, as a localized drug delivery device should. For the device to activate and release micrograms of drug substances, however, voltage has to be applied for minutes. When voltage is applied, drug release rate rapidly increases. However, drug release does not “switch off” when applied voltage is removed. A few minutes is required for the electroactive films to stop releasing drug substances.

1.9.2. Drug Release Control through Microchannel Configuration [113]

This drug delivery device is designed to deliver drug loaded nanoparticles through microchannel configuration with the pressure gradient of fluid flow. Delivery rate of nanoparticles is determined by the maximum number of nanoparticles in the outlet region after a certain time limit. Drug release rate can be regulated through different nanoparticles sizes and different microchannel configurations. Nano-particles is also advantageous in that they can easily cross tissue barriers.

This device was designed to be applied for an ocular drug delivery device that utilize PLA (Polylactide) to deliver bFGF or Rh-6G to the retina. From the drug delivery device mechanism explained above, it can be induced that the device is a passive drug delivery device with no

apparent microvalve that enables the device to actively deliver drugs. In other words, drug release begins with the device's installment and the ends with the drugs emptying the reservoir. This drug delivery device, like many other passive devices, required rather long response time until nanoparticles reached the outlet region. Moreover, due to the pressure driven fluid gradient, as the release started depletion of the reservoir was achieved rather quickly. In other words, the release rate increase rather steeply with respect to time.

1.9.3. Frequency Controlled Wireless Hydrogel Microvalve [114]

This active drug delivery device is a polyimide based. The fabrication requires polyimide films, polyimide liquid prepolymer, copper conductive lines, and hydrogel microvalves made of poly-(N-isopropylacrylamide) (PNIPAM). The fabrication process requires photolithography with the usage of photomasks, and electroplating of copper and titanium. This device utilizes microvalves made of hydrogels responsive to heat activated by resonant radio frequency. These hydrogel microvalves that cover the cavities are thermally actuated through the copper conductive lines that release heat when actuated by its resonant radio frequency. These hydrogel microvalves are designed to be normally closed. To decrease the response time of these hydrogel microvalves, they were designed to be small and thin. Therefore, the overall thickness of the device was approximately 1 mm. However, to increase the volume storage of liquid drug substances, the device inevitably required a broad

profile. By using heaters actuated by resonant frequency, the device could be stimulated wirelessly. The hydrogel microvalves achieved 38% shrinkage at a temperature of 20 degrees Celsius. This drug delivery device successfully demonstrates on-demand release with wireless actuation which is a critical characteristic an implantable device must acquire. However, the resonant frequency mechanism of the device's actuation method required minutes of response time. Moreover, the experiment did not specify the release rate of the device itself. However, the device merely locks the drug chamber with a hydrogel valve with no other pumping mechanism that pushes substances out of the chamber. Consequently, the release rate of the device would highly depend on the density of the surrounding material.

1.9.4. Magnetically Controlled MEMS Device [115], [116]

This drug delivery device is an active device that realizes temporal control by magnetic actuation. The device merely consists of a cylindrical reservoir with 6 mm in diameter and 550 μm depth sealed with a thick surrounding of PDMS opened only at the top. A thin magnetic PDMS (iron oxide nanoparticle-PDMS composite) covers the top of the reservoir. This magnetic PDMS has thickness of approximately 40 μm with an aperture of approximately 131.7 μm in diameter. The releasing mechanism is also simple. Magnetic field either induced by an external coil or a permanent magnet from the bottom of the device pulls the magnetic PDMS membrane towards the reservoir. The membrane

pulls toward the drug substances in the reservoir subsequently pushing substances out of the reservoir through the aperture in the membrane. As simple as the overall process of the device, the fabrication method is relatively simple, too.

Photolithography was implemented to develop the reservoir. On a different wafer, magnetic PDMS was spin coated with a sacrificial layer. Merely bonding the two with drug loaded in the reservoir and drilling a hole with a UV laser completes the device.

The device is developed using only PDMS and PDMS composites which guarantee biocompatibility. Each actuation with an external magnetic field releases a few microliters of substances filled in the reservoir. From the properties mentioned above, some disadvantages can be deduced. First, the device does not have a valve that locks the device's aperture which inevitably results in minor leakage of substances. Second, magnetic field originating a few millimeters away from the device can only deflect the membrane to a few hundred micrometers. In other words, the device cannot completely deplete the reservoir. Moreover, the device can only withhold tens of micro-liters, hundred microliters at most. Lastly, magnetic field must originate from the bottom of the device. Consequently, the orientation of the device is a crucial factor in the device's actuation mechanism.

1.9.5. Electrochemical Intraocular Drug Delivery Device [117]

This drug delivery device is developed for incurable ocular diseases

such as retinitis pigmentosa, age-related macular degeneration, diabetic retinopathy and glaucoma. All these diseases are incurable and absence of treatment may lead to blindness. This active drug delivery device utilizes parylene bellows that act as a micropump. This parylene based micropump is sealed, filled with DI water and inserted in the drug reservoir. Pump electrodes are positioned under this micropump which induce electrolysis in the parylene pump. Electrolysis of water results in volume expansion due to phase change of liquid substances to gas. Drug substances are then released from the reservoir through the cannula with the volume change of the pump.

This device has centimeter scale overall size. Intricate layers of MEMS fabrication methods such as photolithography, deposition, and lift-off are executed. Moreover, alignment and bonding using epoxy is required. Above all, for the precise drug release of the parylene pump, the device has a rather rigid base. This rigid profile of the device is a major drawback since the device was intended to be implanted in the eye. 0.2 mA to 1 mA was applied to the electrodes for actuation and 2 μL/min to 6.5 μL/min release rate could be achieved. However, the actuation response relied on the electrolysis chemical reaction. Therefore, minutes of actuation time was required. More importantly, when the electrodes were turned off, the parylene pump slowly returned to its normal shape. With the actuation of the device, the drug reservoir already released a certain amount. Consequently, when the device is turned on, the device will not release substances from the reservoir until the pump reaches the volume before the actuation was turned off. This active device requires

longer processing time as the reservoir depletes to release consistent amounts.

1.9.6. Electrostatic Valve with Thermal Actuation [118]

This implantable drug delivery device is designed to release vasopressin, a peptide hormone synthesized in the hypothalamus and stored, secreted in the posterior pituitary. Administration of vasopressin induces changes in the arterial blood pressure. This administration may have no effect on healthy individuals. However, for patients in hemorrhagic shock, administrating vasopressin can be a critical mechanism for restoring blood pressure. This condition requires precise dosing and rapid delivery. This device utilizes gold electrode pads that are positioned below and above the pyramid shaped reservoir. This reservoir can hold up to 15 μL of substances and is covered and locked by a thin gold membrane. An electric potential is applied to the electrodes that induce electrochemical reactions. Gold membrane that locks the reservoir dissolves and the electrolysis of water in the reservoir develops microbubbles that consequently propel drug contents in the reservoir out. Apparently, higher electrostatic potential applied to the electrodes results in faster and higher dose of drug release. However, once the gold membrane dissolves, it cannot be restored. Therefore, the device is disposable and cannot be used again.

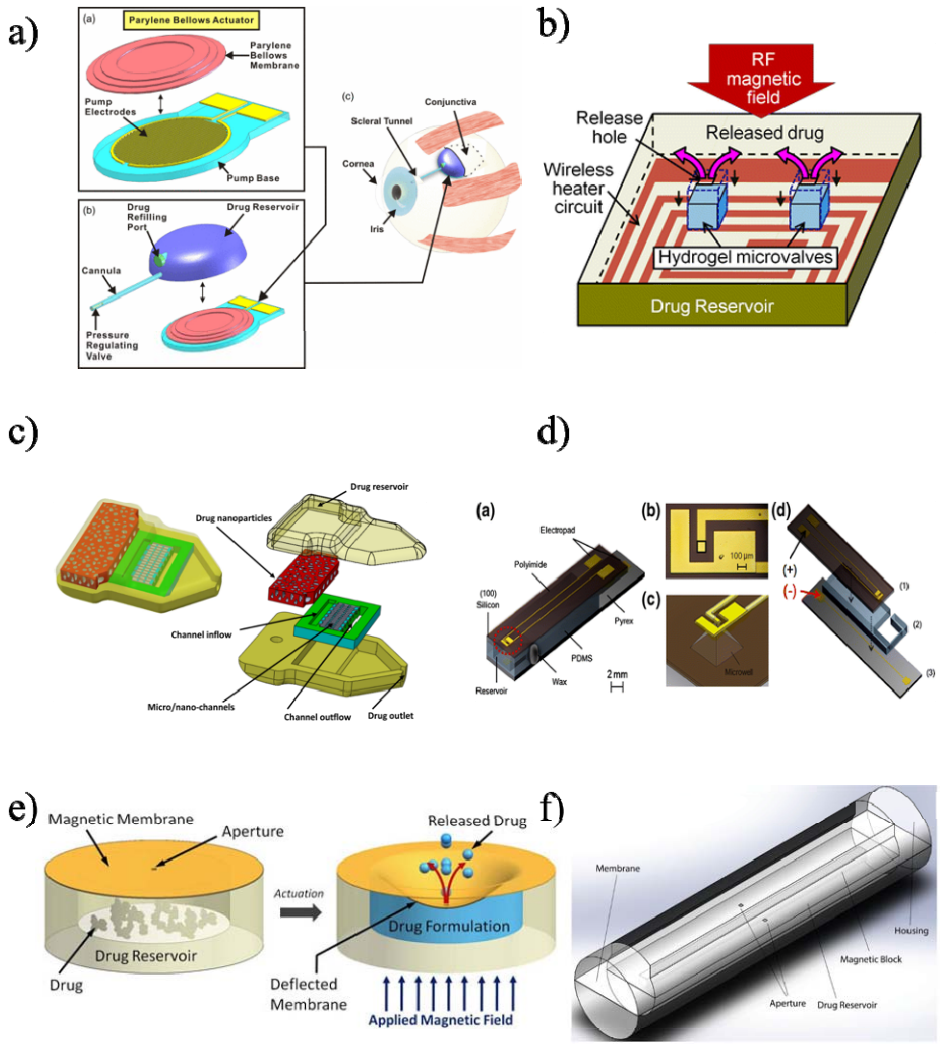

Figure 1-7. Drug delivery devices in development or in research level. a) Electrochemically actuated drug delivery device for ocular delivery [116]. b) Drug delivery device with hydrogel microvalves controlled via wireless actuation [114]. c) Passive drug delivery device utilizing drug loaded nanoparticles controlled through microchannel designs [113]. d) Electrostatically actuated drug delivery device where the actuation compensates for both valve and pump [117]. e) Magnetically actuated drug delivery device that release drugs from the reservoir through deflecting flexible membrane [115]. f) Magnetically actuated drug

delivery device for prostate cancer [116].

1.9.7. Transdermal Delivery through Microneedles [119]

Transdermal delivery that offers a number of advantages such as improved patient comfort, sustained release, avoidance of gastric irritation, and elimination of pre-systemic first-pass effect [118]. However, only a handful of medications can be delivered through the skin with therapeutic amounts. Many types of microneedles exist and are in development.

Hollow microneedles can be easily fabricated using the commercially available 30 gauge hollow needles. Polyetherentherketone mold [122], polylactic acid (PLA) sheet [123], polyimide resin [124] were used to hold the hollow needles in a array. Other materials such as silicon microneedles were also used for their biocompatibility. However, silicon needles are too fragile and require high production costs. To compensate for the fragility of the silicon needles, sputter deposition of titanium and gold were also considered. The fragility of the needles was amendable, however, the overall production cost of the device increase with the presence of extra deposition steps. Stainless steel microneedles are also widely used. Hollow microneedles are rather invasive, however, have advantages in delivering substances directly into the epidermis or the dermis by penetrating through the stratum corneum. Moreover, substances with high molecular weight such as proteins, oligonucleotides, and vaccines can also be delivered. Hollow microneedles would be

desirable if they had adequate mechanical strength and bores that do not clog while transdermal delivery. However, the hollow microneedles in development and commercially available still need research to meet these requirements. Solid microneedles are made of silicon, metal and polymeric materials. These systems delivery drug via passive diffusion. Not only drugs, solid microneedles show promising results in delivering vaccines. These microneedles are designed to be a few hundred micrometers thick to penetrate the stratum corneum. Dissolving microneedles are of great interest for a number of advantages. Above all, one-step application which is convenient for patients. These microneedles are made of polysaccharides or other polymers. Most of these dissolving microneedles are made using micromolding. Pouring polysaccharides or polymers in female molds and curing under centrifugation or pressure.

There are many advantages of various types of microneedle arrays listed above. However, there are still disadvantages of these devices. Transdermal delivery requires penetration through stratum corneum into the dermis. This method can raise local inflammation and skin irritation for patients with allergy or sensitive skin. Moreover, the needles are designed to be much thinner than the normal hair. Hollow microneedles or coated microneedles can break off while removing the device.

1.9.8. Osmotic Drug Delivery Devices [120]

Osmotic micropump based drug delivery devices require no additional power consuming stimulus consequently are applicable in a

variety of fields. Osmotic pumps consist of three compartments: osmotic agent, solvent, and drug. In contrast to common tablets or drug injection, these systems provide long-term and constant release in either implanted in desired sites or systemic way. These systems can handle drug substances in solid and liquid form. First osmotic pumps were developed more than 50 years ago. Recently, osmotic pump based drug delivery devices are commercially available, and are under active development. Here, some of commercially available osmotic drug delivery

The fundamental principle of osmotic pump is generated by two solutions with different solute concentrations separated by a semi-permeable membrane. Through osmosis, solvents from lower concentration travel across the permeable membrane to high concentrated solution. This applies to the fabrication of osmotic drug delivery device. There are devices with one, two, and three compartments. For one compartment osmotic device, drugs are stored in a chamber with semi-permeable membrane. Solvents, for example bodily fluids, travel across this membrane dissolving drugs that later leaves the device through the outlet. One compartment osmotic devices' release rates depend on the physical properties of the drug. Two compartment osmotic devices have a chamber filled with drug substances and another chamber with osmotic agents. These two chambers are divided with a movable barrier. As solvents travel in to the osmotic agent chamber and expand in size, the barrier moves toward the drug chamber physically pushing out drug substances through the outlet. Through this compartmentalization, drugs stored in the drug chamber have little

limitations. Main drawbacks of two compartment devices are complicated design, and reduced drug storage compared to one compartment devices.

1.9.8.1. ALZET® [130]

This commercially available osmotic drug delivery device is probably the most prominent example until today. This device is designed and fabricated for research purposes by DURECT Corp., Cupertino, CA, USA. This device can be implanted in multiple animal species as small as mice in multiple anatomical sites. This cylindrically shape device is comprised of a collapsible reservoir made of impermeable thermoplastic hydrocarbon elastomer which is surrounded by a coating layer of osmotic driving agent. The device's geometry minimizes diffusive release or accidental spill and ensures constant delivery solely controlled by osmosis. Water enters the osmotic layer generating pressure in the drug chamber which then pushes stored drug out of the device. Three different sizes with chambers with 100 μL, 200 μL, and 2 mL and delivery rates ranging from 0.11 μL/h to 10 μL/h. This device can be operated for 1 day to 6 weeks depending on the device choice. A catheter can be connected to the release orifice of the device which then can specifically target organs or tissues.

1.9.8.2. DUROS® [131]

This osmotic drug delivery device is developed by ALZA Corporation, Mountain View, CA, USA in 2001. The device is very small

comparable to a size of a matchstick and made of titanium alloy. One side of this cylindrical device incorporates a semi-permeable membrane while the other side has an outlet port. Osmotic agent and drug substances are divided with a movable piston. The fluidic substances pass through the semi-permeable membrane pressurizing the osmotic chamber slowly moving the piston toward the drug chamber. This then effectively push drugs out of the chamber through the outlet port. This outlet port can also be connected to a catheter to specific sites. Drug release can be maintained for a time period of 3 to 12 months. The device has overall device dimensions of 4 mm in diameter, 44 mm in length and has a drug reservoir of 155 μL. This device has been applied to many *in vivo* studies along with toxicity and safety tests. This device was used in many long-term clinical trials that managed chronic conditions, pain therapy, diabetes mellitus, obesity etc.

1.9.8.3. BuccalDose [132]-[134]

This disposable osmotic drug delivery device was specifically designed to treat Parkinson's disease. Advanced stages of Parkinson's disease have a narrow therapeutic window which consequently require frequent intake of drug whether it is administered orally or invasively using a syringe. This device was designed to release constant amounts of dopamine agonists to the buccal mucosa and subsequently to the bloodstream. The device is implanted in the mouth attached to the gums. Once the device is attached to the gums, disposable drug cartridges can be easily attached and removed from the device repeatedly. These

cartridges contain micro injection molded housing made of cyclic olefin copolymer, semi-permeable polyamide thin film, hyperelastic styrenic copolymer barrier that separates drug and osmotic agent, and fluidic capillaries for drug release. Neodymium cubic magnets are embedded in the cartridges for easy attachment and detachment.

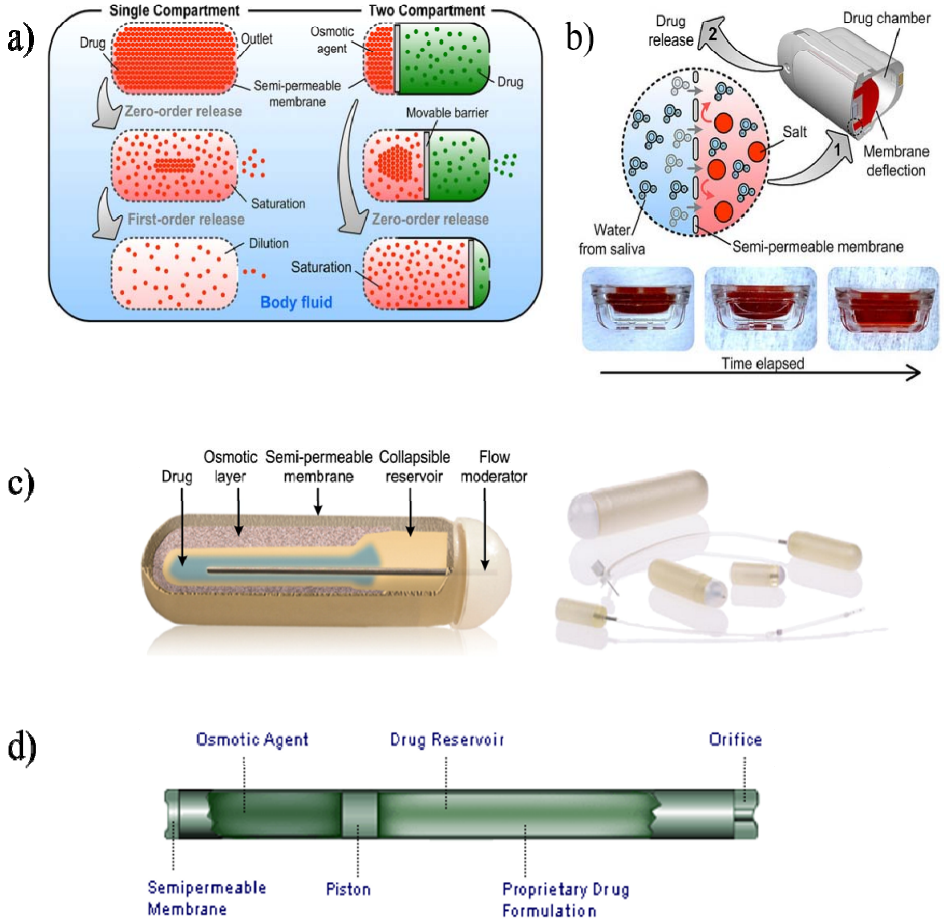

Figure 1-8 Osmotic drug delivery devices. a) Release mechanism of drug osmotic drug delivery devices with one or two compartments. b) BuccalDose intraoral drug delivery device. c) ALZET® drug delivery device. d) DUROS® drug delivery device.

Table 1-1. Comparison of currently in development or commercially available drug delivery devices

Journal or Device	Year	Reservoir Volume	Pump Rate	Power	Material Composition	Disadvantages
Wood et al. [112]	2008	Depend on fabrication	0.5~0.6 mg/min	1.25 V	Prussian Blue Electroactive Film Indium Oxide	Slow response time
Morimoto et al. [50]	2016	Max 1mL	25~45μL /min	No power	PDMS/Parylene PEGDA floating valve	Passive delivery Inconsistent release Dispense rate decrease rapidly over time
Rahimi et al. [114]	2011	Depend on device size	Non-specified	External coil heater	Polyimide Hydrogel valve	Slow response in on and off
Pirmoradi et al. [115]	2011	15.7 μL	2.1~3.3 μL	Magnetic field	PDMS Magnetic PDMS (iron oxide particle)	Inconsistent dispense rate Reservoir is too small, after 5 to 6 deliveries Non refillable/non reusable
Gensler et al. [117]	2010	100 μL	2 μL/min to 3.4 μL/min	Electrolysis 0.2 mA to 1 mA	Parylene Platinum/Titanium	
Struss et al. [116]	2017	800 μg	1.5 μg per actuation	External magnetic field	PDMS Neodymium Magnetic	Different release rate according to magnetic field (magnet distance) Approximately 1ug background leakage

Table 1-2 Comparison of currently in development or commercially available drug delivery devices

Journal or Device	Year	Reservoir Volume	Pump Rate	Power	Material Composition	Disadvantages
Ma et al. [113]	2014	1100 NP	Non-specified	Pressure gradient fluid flow	Polylactide (PLA) PDMS	Passive delivery Inconsistent release
Chung et al. [118]	2009	15 μL	15 μL	Electrochemically driven ejection	PDMS, Polyimide, Pyrex, Gold	Rigid device Non-reusable Instant release of the reservoir at once
ALZET® [130]	2000	100μL, 200μL, 2 mL	0.11 μL/hr ~ 10 μL/hr	Osmotic pump	Thermoplastic hydrocarbon elastomer	Last up to 6 weeks depending on size Passive delivery
DUROS® [131]	2001	155 μL		Osmotic pump	Titanium Casing	Small but rigid device Passive delivery
BuccalDose [133]	2011		1.85 ± 0.02 μL /hr	Osmotic pump	Cyclic olefin copolymer (COC) Polyamide film Hyperelastic styrenic copolymer (SEBS)	Saliva secretion is crucial for osmosis Implant in the mouth that can increase inconvenience

1.10. Summary

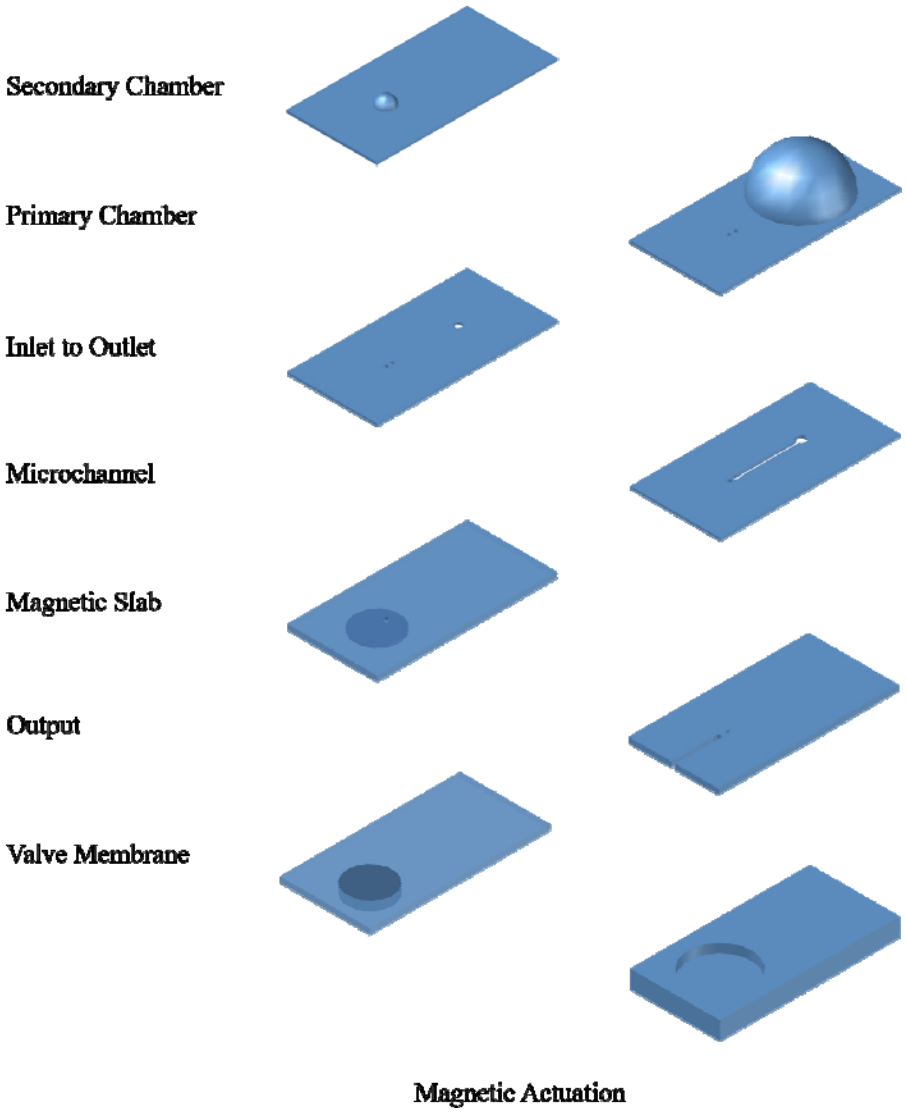

Figure 1-9. Components of the drug delivery device separated layer by layer.

Drug administered through oral gavage and syringe injection fails to achieve therapeutic drug delivery since sustaining the plasma

concentration in between MEC and MTC requires consistent and periodic administration. Moreover, the typical administration has a systemic effect on the user. To prolong effective drug therapy, administering larger doses of drugs or periodic injection may be a solution. However, larger doses of drugs may increase the cytotoxicity and periodic administration is challenging. Therefore, an increase in usage and demand of localized drug delivery devices to substitute conventional drug administrating methods such as invasive syringes and oral gavage is imminent.

Localized drug delivery devices achieve both temporal and spatial control relatively simply. Spatial control is realized by installing the device on locations drug delivery is required directly. Temporal control is accomplished by its actuation mechanism. Since the device has to be implanted, several conditions have to be met. The device must maintain a small profile, be flexible, and be less invasive when it is fixed onto skin or other organs to assure patient's comfort. Localized drug delivery devices usually comprise of a drug reservoir, pump, and a valve. Furthermore, these components require a power source. All these components and the actuation power source have to fit in a miniature device. Therefore, the device was designed to consume minimum power. For the device to be implantable, only biocompatible materials must be used.

The drug delivery device proposed in this paper attempts to realize all the requirements listed above. Firstly, the device uses a mechanical pump that does not require a power source. Utilizing oxygen plasma

treatment and vapor deposition onto PDMS surfaces, selective bonding of PDMS and zero-volume chamber fabrication is realized. Zero-volume chambers have flexible walls that have no volume when the chamber is empty. When the internal pressure increases via input substances through a syringe, the chamber expands. The output mechanism of the device is implemented using an output microchannel that connects the chamber and the microvalve. This normally closed valve remains closed when no external stimulation is present. When the valve is actuated to open via electromagnetic actuation, the chamber would deflate and push out loaded drug substances through the chamber outlet. Secondly, to minimize power consumption, a secondary pump is in necessary. This drug delivery device with one inflatable chamber inevitably pumps drug substances exponentially. The chamber pumps with higher release rate when the chamber is full. The release rate rapidly decreases with respect to time. Therefore, consistent drug release and periodic administration of drug substances through this device with one pump can be difficult to achieve. A secondary pump is used to revise this weakness. A microchannel is constructed to connect the chamber with the secondary pump. The primary chamber fills the secondary pump to a certain limit. When the valve opens, for a couple of seconds, the secondary pump is depleted releasing drug substances into the medium. This process can be repeated until the primary chamber depletes or reaches a saturation state where it cannot further pump substances into the secondary pump. By integrating the secondary pump to the primary chamber relatively consistent drug amounts could be released. Lastly, a combination of

PDMS and microparticles were employed to fabricate magnetically responsive PDMS membrane and conductive PDMS composite designs that compose the electromagnetically actuated microvalve. These composites were used to preserve the flexibility and fabrication simplicity of the device.

The proposed device was designed to be implanted in the body or adhered on the skin. The device is PDMS based. However, microparticles such as nickel and silver were used. Therefore, the device's biocompatibility required analysis. The completed device was tested for *in vitro* quantitative and qualitative cytotoxicity according to International Standards.

2. Materials and Procedures

In this chapter, materials and fabrication procedures required to construct the proposed drug delivery device. The fabrication method proposed in this thesis eliminates the usage of conventional MEMS procedures such as photolithography, wet and dry etching. Instead, patterning and fabrication of microstructures were executed by only using processes such as spin coating, oxygen plasma treatment, vapor coating and designed polyvinyl chloride (PVC) adhesives that substitute the function of photomasks.

2.1. System Overview

The proposed drug delivery device consists of four components: primary drug chamber, secondary drug pump, release rate controlling microchannel, and an electromagnetically actuated microvalve. Many drug delivery devices' working mechanisms have issues in releasing consistent amount of drugs until the reservoir is completely depleted. Most of them release larger amounts when the reservoir is completely full. As the chamber drains, the device actuation either requires longer actuation time or stronger power to release consistent amounts. The proposed device realizes consistent delivery through the secondary pump. Both the primary chamber and the secondary pump are inflatable and

deflatable. They inflate as fluidic substance fills up increasing the internal pressure and deflate as the substance leaks out from the chamber. A microchannel connects the primary chamber to the secondary pump. Fluidic drug substance is filled in the primary inflatable/deflatable drug chamber via a syringe. As the primary chamber fills up, drug substance slowly fills the secondary pump. The secondary pump is filled until a certain threshold, determined by their size and thickness of the primary reservoir and the secondary pump. When the microvalve opens via electromagnetic actuation, the secondary pump starts to drain first. Subsequently, the inflated thin membrane of the secondary pump returns to its normal shape. Once the secondary reservoir depletes, the microvalve is closed. Slowly the secondary pump is filled again through the primary chamber. This process can be repeated until the primary chamber completely drains. The device delivers relatively consistent amount each time the microvalve opens.

The conventional PDMS microstructure fabrication process includes PDMS patterning via photoresist lithography and etching. This process produces rectangular shaped microstructures with fixed width and height. Therefore, a new fabrication method was necessary to develop the components of the device. Here, a non-lithographic approach was taken. A combination of oxygen plasma treatment, silanization, and polyvinyl chloride (PVC) stencil masks were used to develop each component. Utilizing stencils designed and cut using a Diode Pumped Solid State (DPSS) laser system, the proposed procedure introduces a novel PDMS fabrication method that produce flexible PDMS structures that can

change its shape and size in response to the internal pressure.

2.2. Materials

2.2.1. Polydimethylsiloxane (PDMS)

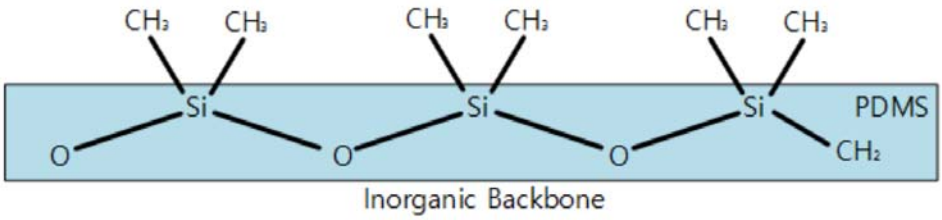

Figure 2-1. Chemical formula and structure of fully polymerized PDMS

PDMS is one of many silicone polymers frequently used in various biomedical applications. It has its prevalence over other polymers in optical transparency, biocompatibility, easy fabrication, and good mechanical and chemical characteristics. Furthermore, PDMS has Young's Modulus of approximately 1.0MPa which is relatively similar to body tissues such as nerves, muscles and brain. Thus, implantation onto those tissues is plausible. Aside from these numerous advantages, there are a few challenges PDMS has to overcome to be perfectly suitable for biomedical applications such as multi-electrode array (MEA) for brain machine interface (BMI) applications, and localized drug delivery device: low surface energy and chemical stability.

Low surface energy, hydrophobicity, of PDMS may be its critical flaw that raises a couple of problems when PDMS is put into use for

MEMS fabrication. PDMS is fabricated by mixing a curing agent (Sylgard® 184B, Dow Corning, USA) to liquid pre-polymer (Sylgard® 184A, Dow Corning, USA) in a 1:10 ratio. PDMS sustains a hydrophilic solution even with the curing agent mixed. When heat stimulus is applied to the mixture, the hydrosilylation reaction begins with the platinum catalysts abundant in the solution form ethylene bond between silicon hydrides and silicon vinyl. When the hydrosilylation reaction is complete, PDMS attains a solid form with high flexibility and optical transparency. However, the process renders the surface hydrophobic. Hydrophobicity of PDMS raises issues in many applications due to the incompatibility with other metal materials. For example, implantable MEA's developed using PDMS require high adhesion between PDMS surfaces and conductive channels to acquire strong signal and increase durability. However, deposition of gold directly over PDMS forms weak adhesion. Therefore, patterning through photolithography and etching is impossible. To ensure strong adhesion between PDMS and metals, a series of surface treatment procedures are necessary []. Furthermore, in some cases surface treatment does not ensure strong adhesion. Therefore, titanium deposition before gold deposition can also be performed. In other cases, to increase hydrophilicity of PDMS surfaces oxygen plasma treatment and vapor coating can be implemented.

2.2.2. Polyvinyl Chloride Adhesive Sheets

Fabrication processes devised here eliminates the usage of photolithography, and etching. Subsequently, photo-masks and acidic

etching solutions are unnecessary. Rather, photo-masks and etching solutions were substituted using PVC adhesive sheets. Two types of PVC sheets with different thickness were used: 80 μm (Matte PVC, Silhouette, USA) and 150 μm (Inductive Tape, Taeyoung Chemical Inc. Co. LTD., Korea) thick sheets. PVC sheets are widely produced and used synthetic plastic. PVC sheets are very versatile and cost-effective thermoplastic material that has good dimensional stability, good impact strength and excellent weathering properties. PVC sheets can be easily extruded, calendered, and cut using a sharp blade. Depending on the composition, these sheets can be manufactured in a variety of colors, and even transparent. Above all, depending on the thickness of the sheets, they can be rigid or flexible. PVC adhesive films commonly refer to flexible films. These flexible PVC films were used in this thesis. This flexible nature of PVC films is essential to the proposed fabrication method because it allows the films to be easily transferred and removed to and from PDMS surfaces. Similar to photo-mask preparation, PVC stencils were designed using AutoCad program. These designs were cut out using two types of machines. A blade plotter (Silhouette Cameo, Silhouette, USA) that uses a sharp blade to cut out the PVC stencils. This blade plotter device works very much like an inkjet printer. With two step motors each controlling the horizontal and vertical movement of the blade, it cuts out the designs. The preciseness of the blade plotter differed relative to the cut out speed of the blade movement. The other device is the Diode Pumped Solid State (DPSS) laser cutter. This laser system (Samurai UV Marking System, DPSS Lasers Inc., USA) uses UV lasers at 355 nm. This system

was designed to be a marking system. However, by controlling the power of the laser, the system could also execute UV ablation and engravings on many materials such as wires, metals, sapphire, glass, silicon wafers, plastics, paper, polyimides, etc. This ablation property of the system could also cut PVC stencils. With the adequate power and wavelength, the PVC adhesives could be precisely cut. Both devices used in the procedure were analyzed to evaluate the preciseness and accuracy of the device.

PVC sheets have a chemical formula of $(C_2H_3Cl)n$. PDMS polymerization process relies on the platinum catalyst induced hydrosilylation process. This process cross-links silicon hydride with vinylsiloxane groups with the aid of platinum catalysts abundant in the solution. There has been an experiment conducted to inhibit this polymerization process by immobilizing the platinum catalyst which in result hinders the hydrosilylation process. Amine group was coated over a glass plate which acted as a chelating agent that trapped the platinum atoms [129]. Platinum atoms have positive charge. Hence, this positive atom binds to the negatively charged amine group. However, inhibition also depended on the thickness of the PDMS. Similarly, this inhibition process was reproduced by other possible chelating agent. Here, PVC stencils were used as chelating agent to reproduce this phenomenon. Similar to the negatively charged amine group, PVC sheets can act as a chelating agent due to the negatively charged chloride atoms in PVC stencils. The negatively charged chloride atoms in PVC stencils attract platinum atoms consequently resulting in the inhibition of

polymerization of PDMS. Similar to the reaction in [129], the inhibition process depended on the thickness of the PDMS deposited over the PVC stencils.

2.2.3. Magnetic Microparticles and Neodymium Magnet

Nickel microparticles were used in this paper to manufacture magnetically actuated PDMS membranes. PDMS normally act as an inductor. It is non-conductive and non-responsive to magnetic fields. For this polymeric material to be responsive to magnets or magnetic fields induced by conductive coils, the precured liquid PDMS needs to be mixed with metal microparticles.

There are many magnetic microparticles in use for MEMS fabrication. Iron oxide particles, nickel particles, copper particles, neodymium particles, etc. Since the proposed drug delivery device is designed to be biocompatible for in-body implantation or skin adhesion, copper particles are inadequate. Therefore, nickel, iron oxide, and neodymium particles were tested and analyzed whether the particles cause any problems during the fabrication process. Nickel powder (APS 2.2-3.0 micron, 99.9% (metal basis), S.A ≈ 0.68 m^2/g, Apparent density = 0.5-0.65 g/cm2, USA), iron oxide (Fe_3O_4) powder (5 micron, 99%, US Research Nanomaterials, Inc., USA), and neodymium (NdFeB) microparticles (150μm, Xin Chang, China) were used. PDMS has high tensile strength and flexibility. Depending on the composition of PDMS and metal microparticles, the tensile strength and flexibility of can

change accordingly. The higher the composition of the microparticles are the tensile strength and flexibility of the film decreased.

Neodymium magnets are also used in this device. Tensile strength of magnetic PDMS membrane fabricated through nickel or iron oxide particles is greater than PDMS itself. In this paper, membrane deflection of this magnetic PDMS was tested through magnetic actuation and electromagnetic actuation. However, due to limited power consumption, electromagnetic actuation could not produce enough power to deflect the membrane. PDMS's tensile strength, Young's Modulus, is thickness dependent as the thickness increases over 200 μm [126]. Magnetic PDMS's tensile strength does not change if the composition is less than 10% volume percentage [127]. Magnetic membrane with 162 μm thickness with 6 mm, 8 mm, 10 mm, diaphragm could be deflected approximately 96 μm, 141 μm, 251 μm, respectively, using a permanent magnet. Therefore, for magnetic actuation via a permanent magnet, the magnetic PDMS could be used for releasing substances. However, for electromagnetic actuation, a millimeter size neodymium magnet was used for releasing substances. Here, magnetic PDMS was also used for fast recovery to lock the microchannel.

2.2.4. Silver Microparticles and Silver Ink

Both silver powder (APS 4-7 micron, 99.9% (metal basis), S.A. 0.1-0.4m/g, USA) and silver ink (Elcoat, Jin Chemical, Korea) were tested to develop conductive PDMS composites. This silver ink is composed of 60~70% silver mixed into ethyl lactate 20~30%. The ethyl lactate is there

for ease in application so that it can be used as paint. Many PDMS based electronic devices such as flexible sensors, and multi-electrode arrays (MEA) require conductive lines. These conductive lines, whether the device is biocompatible or not, are made out of gold, silver, lead, etc. The conventional gold, silver, and lead conductive lines lack durability in many aspects. As the lines become thinner, they become more flexible. However, with increased flexibility, the lines are more susceptible to crack when they are stretched. Moreover, as mentioned earlier, metal deposition over PDMS is challenging due to the lack of hydrophilicity of PDMS surfaces. However, bonding between fully polymerized PDMS and uncured liquid PDMS is rather simple. PDMS is hydrophilic before polymerization and hydrophobic after polymerization. When pre-cured PDMS solution is poured over fully polymerized PDMS, the two build into one PDMS slab. Therefore, PDMS mixed with other metal particles can easily be dispensed over the surface with high adhesion strength. Above all, due to the PDMS in the conductive mixture, the conductive lines produced using this mixture inherits the flexibility of PDMS. Yet, the flexibility and stretchability depends on the composition of the mixture.

As mentioned earlier, there are many conductive microparticles used and applied in MEMS fabrication methods. There is nickel, silver, gold, iron oxide, copper, etc. Again, copper particles were not adequate for they are non-biocompatible. Other materials can also be used. Here, however, silver was used because silver has highest conductivity among all the other microparticles. Since PDMS is an insulating material, to

achieve high conductive lines with PDMS-microparticle composite, metal particles with high conductive properties were necessary.

2.3. Procedures

2.3.1. Spin Coating

Spin coating is a commonly used MEMS fabrication method. This procedure produces thin films with uniform thickness. Usually, silicon wafers are placed on a chuck and securely fastened with a pump. Small amounts of spin coating materials are dispensed on the center of the substrate. The substrate then spins the substrate, silicon wafer, at a programmed speed. Due to the centrifugal force produced by the spinning motion, the dispensed material spreads over the surface of the substrate developing a uniform thickness. The thickness of the material is determined by the rotating speed, time and viscosity of the material itself. In some cases, the surface energy of the substrate itself and the dispensed solvent's hydrophilicity and hydrophobicity also has an effect on the thickness of the result.

Fabrication process of the proposed drug delivery device utilizes spin coating of PDMS on various substrates with different surface energy. PDMS is spin coated over PVC adhesives, silanized wafer, silanized PDMS, and oxygen plasma treated PDMS. The thickness of PDMS spin coated over each substrate was investigated. Through the results depicted through the experiment, the relationship between PDMS thickness and substrate hydrophilicity was analyzed.

2.3.2. Oxygen Plasma Treatment

Two types of surface treatment procedures are used. Figure depicts the chemical formula of PDMS. This chemical formula presents PDMS's physical characteristics. The methyl group abundant in the PDMS surface decreases the attractive force, thus results in low surface tension. These are reasons to why PDMS has low surface tension, and low surface energy hence combination with other metallic materials is challenging. However, surface modification of PDMS is rather simple. Oxygen plasma treatment, silanization, and HEMA (2-hydroxyethyl methacrylate) processes are frequently used procedures that render the surface's hydrophobicity. In this paper, only oxygen plasma treatment and vapor coating trichlorosilane will be used.

Plasma is one of four state of matter. Under normal conditions, only solid, liquid and gas exists. Solid is the state of matter with lowest energy. With increase energy induced to the subject, the state of matter changes from solid to liquid to gas. Plasma cannot exist under normal conditions. Plasma can only be artificially generated by subjecting neutral gas to strong electromagnetic field to a point where the ionized gas become electrically conductive. In MEMS fabrication, this plasma generation process is used for plasma etching, and Plasma Enhanced Chemical Vapor Deposition (PECVD). Oxygen plasma treatment or etching is frequently used to increase surface energy of many materials.

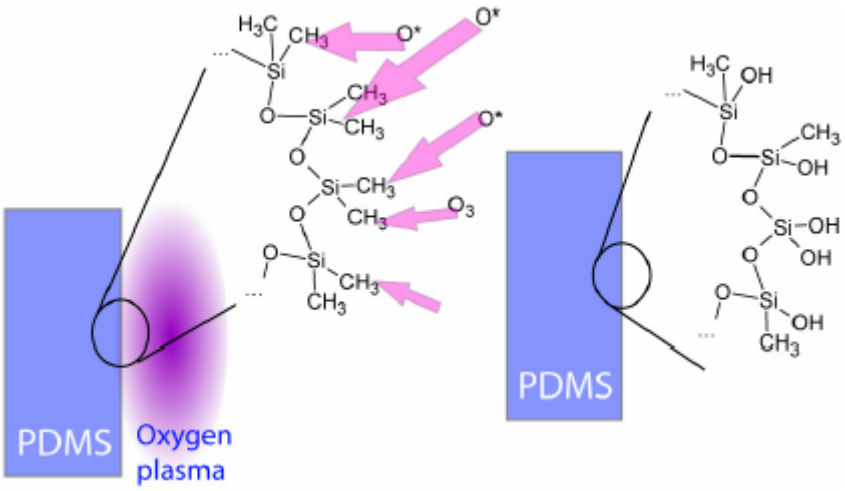

Figure 2-2. Oxygen plasma treatment of PDMS surfaces.

Oxygen plasma treatment renders PDMS surface hydrophilic. The methyl groups abundant on PDMS surfaces are substituted with hydroxyl groups and carboxyl groups through oxygen plasma treatment. Consequently, the surface energy increase and the surface is now hydrophilic. Moreover, oxygen plasma treatment not only renders the surface hydrophilic, but also increases adhesion strength, too. For this reason, oxygen plasma treatment can also be used to bond PDMS to other substrates such as other PDMS, glass or silicon wafer. However, hydrophilic modification through oxygen plasma treatment is not permanent [121]. Hydrophobic recovery of plasma treated PDMS begins in a matter of minutes. The time it takes for full recovery differs due to several aspects such as oxygen concentration, RF power, and treatment time. In most cases, PDMS fully recovers its hydrophobicity after several days. Volatile modification of PDMS surface energy alone is not adequate for the selective bonding process required to fabricated the

proposed drug delivery device. However, selective bonding is implemented by executing a series of oxygen plasma treatment and silanization. Moreover, oxygen plasma treatment was also used as a bonding mechanism permanently adhering fully polymerized PDMS structures.

2.3.3. Silanization (Self-Assembled Monolayer)

Vapor coating using trichloro (1H, 1H, 2H, 2H-tridecaflfluoro-n-octyl) silane is a type of self-assembled monolayer (SAM) coating over polymeric surfaces. SAM coating is a process that bonds one molecular thick layer of material to the surface in a manner that satisfies with its physical or chemical forces during deposition. Above all, SAM coating is different to oxygen plasma treatment in that the process does not bear volatile rendering of surface modification. SAM coated PDMS surface can be permanently rendered hydrophilic. SAM coating is not necessarily implemented to increase hydrophilicity of PDMS surfaces. SAM coating is implemented over molds, especially PDMS, for easy peel-off of polymerized PDMS from the mold. PDMS is hydrophobic when it fully polymerizes. Moreover, if uncured PDMS is poured over fully cured PDMS, the two form an irreversible bond. For the mold to successfully act as a mold, newly poured uncured liquid polymer must be easily removable. Therefore, if PDMS molds are treated with SAM coating, the surface can be rendered hydrophilic. Hence, when new PDMS is poured

over the treated surface and cured, the discrepancy in hydrophilicity of surfaces make them easily separable. Consequently, desired patterned PDMS can easily be removed.

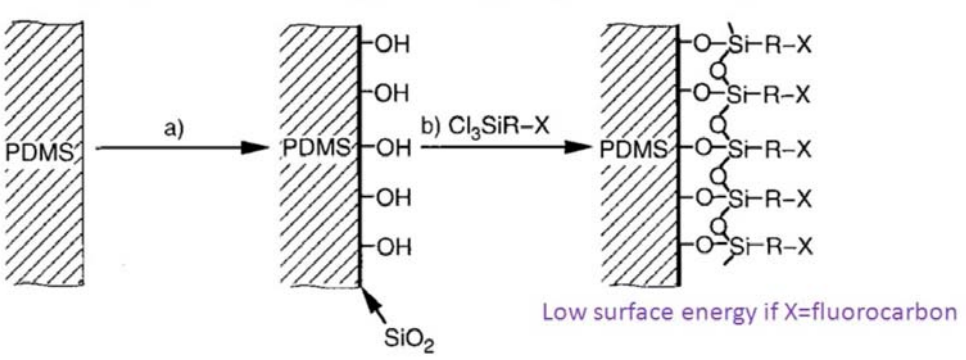

Figure 2-3. Self-assembled monolayer of PDMS surfaces. a) oxygen plasma treatment. b) silanization.

Silanization of PDMS layer is a two-step process. The hydrophobic surface of PDMS is composed of methyl groups. By oxygen plasma treatment of the surface, the methyl gourds break to form hydroxyl groups. Since oxygen plasma treatment, forming hydroxyl groups on the surface, is a volatile process, the treated PDMS is placed in a vacuum chamber with a drop of trichlorosilane. SAM coatings are normally implemented to increase hydrophobicity of PDMS surfaces. This hydrophobic modification of PDMS substrates depended on the duration, power and oxygen concentration of the oxygen plasma treatment that was implemented prior to vacuum deposition. Here, short duration, low

power, low oxygen concentration was tested to render PDMS surfaces slightly hydrophilic. In doing so, precaution steps are necessary since vaporized trichlorosilane releases toxic gas harmful in many ways. Moreover, trichlorosilane liquid used in this process is harmful in liquid state too. Oxygen plasma treatment is harmless. However, during silanization, all procedures must be handled in a fume hood with protective gloves and garments.

2.3.4. Plasma Bonding

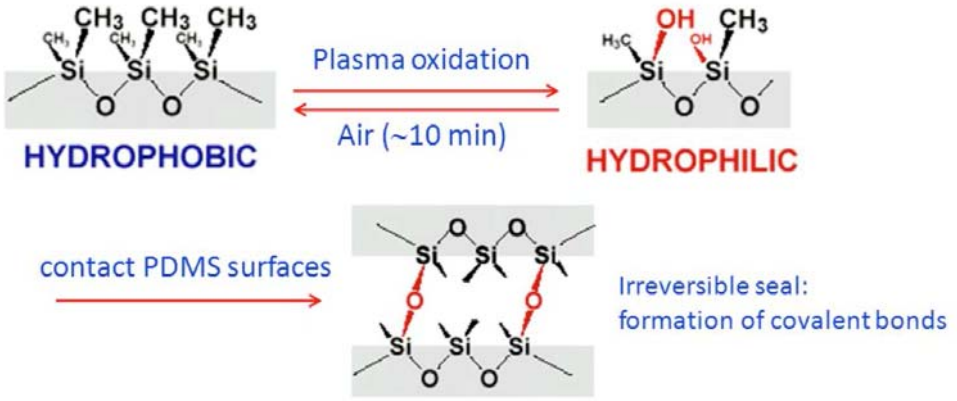

Figure 2-4. Plasma bonding of two fully cured PDMS.

PDMS to PDMS bonding can be executed through two methods. As mentioned above, when liquid PDMS is poured over fully polymerized PDMS, the two combine as one. Here, liquid PDMS was used as a bonding agent. However, this method can only be applied in a few applications. Plasma bonding via oxygen plasma treatment can be used in

a variety of fields. Moreover, bonding onto other surfaces such as glass can also be implemented. As mentioned above, oxygen plasma treatment removes hydrocarbon groups and forms hydroxyl bonds on the surface. When two treated PDMS surfaces come in contact with each other, this allows strong silicon to oxygen to silicon bonding.

2.4. Fabrication

In this section, fabrication methods to develop inflatable PDMS chambers and alternative methods to achieve PDMS etching results are introduced. PVC stencils were prepared using the DPSS Laser system and a blade plotter. With the stencils that act as masks, only oxygen plasma treatment and silanization were implemented to fabricate the structures.

2.4.1. PDMS Etching via PVC Stencils

PVC stencils were prepared using both a DPSS laser system and a blade plotter. Stencils with length 2 cm and widths ranging from 100 μm to 1 mm were tested to execute PDMS etching. PVC adhesive sheets have a thickness of approximately 80 μm. For the DPSS laser system settings were fixed to 100% laser power, frequency of 20.00 Hz, mark speed of 100.00mm/s, and pulse width of 20 μs. Even with this laser setting, single pass over PVC stencil does not fully cut out the designed stencil. Multiple passes were implemented to completely cut out the stencils with desired designs. A minimum of 30 passes were require to cut the PVC stencils. However, the polyacrylic adhesive side of the PVC

sheets were not completely trimmed. Therefore, for the polyacrylic adhesive side to be completely trimmed, an additional 20 times and a total of 50 passes were executed. The Silhouette blade plotter cut stencils with a physical blade. The settings possible with the device is plotting speed and blade depth. With the stencils prepared, the stencils' widths and lengths were investigated in depth to analyze the preciseness of each device.

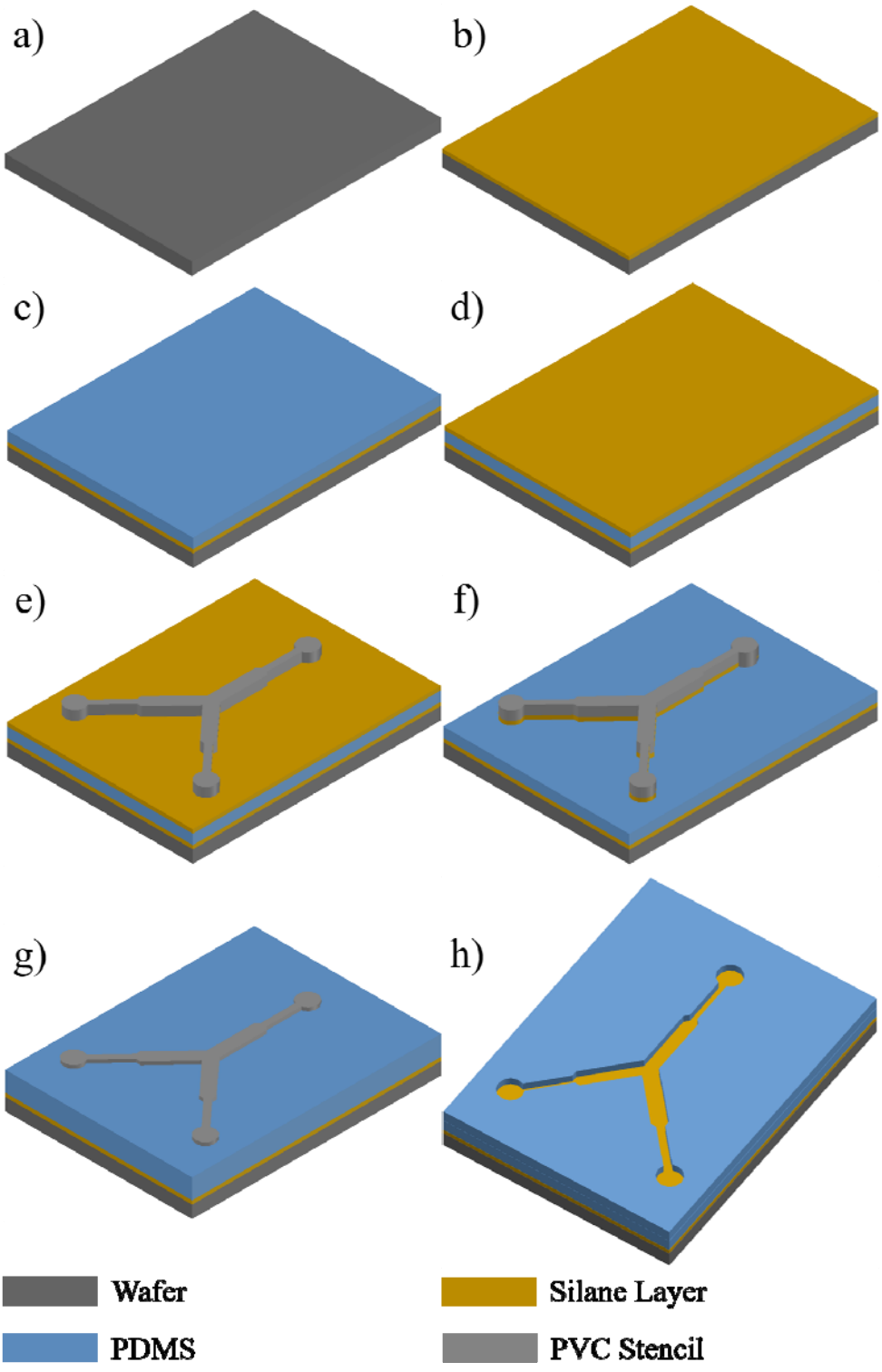

Figure 2-5. Fabrication steps to acquire etching results on PDMS surfaces.

The fabrication process starts with preparing a wafer (Figure 2-5a). Single side polished wafers with 100 mm diameter, 525 μm thickness, Boron doped and resistivity of 1-10 Ω·m. If PDMS is spin coated over this wafer, PDMS forms irreversible bonds with the wafer surface and retrieving PDMS structures is impossible. Therefore, this wafer is silanized for easy retrieval. Prior to silanization, to promote strong adhesion of vapor deposition, the wafer was treated with oxygen plasma treatment at an RF power of 5W, 10.0 sccm (standard cubic centimeter per minute), for 60 seconds. Then, this wafer was placed in a vacuum chamber with two to three drops of trichlorosilane. The chamber is degassed and locked. The wafer is left in the chamber overnight (Figure 2-5b). This process is very important throughout the proposed fabrication process because layers of PDMS structures may not be retrievable. Before the next step, a thin layer of PDMS was spin coated over the wafer to test if the layer could be peeled off without damaging the structures. After silanizing the wafer and tested, PDMS of arbitrary thickness is spin coated over the wafer (Figure 2-5c). This layer should be at least 100 μm thick for later steps to come. The designed stencils have to be pasted on this layer. These designed stencils are removed from the sheet using a transferable application tape. Even without this application tape, simple stencils with thick fragments can be easily transferred onto the PDMS surface. However, when the stencils become smaller with micrometer scale size fragments, without the application tape, the design cannot be sustained during the transferring process.

Therefore, a transferable application tape (Silhouette Trans Paper, Silhouette, USA) is cut out sufficiently larger than the stencil design. This application tape is pasted over the designed and cut out stencil. When the application tape is peeled off, the design is peeled off taped on the adhesive side of the application tape. This application tape is then pasted on the PDMS surface and peeled off. The intension of this process is so that the stencil designs are left in on the PDMS surface while only the transfer tape is removed. Moreover, weak adhesion of the PVC stencil with PDMS surface can cause problems during oxygen plasma treatment. Oxygen plasma treatment requires a medium vacuum (25 to 10^{-3} Torr) chamber, approximately 7.0~8.0 × 10^{-2} Torr before oxygen injection. With weak adhesion strength between PVC adhesives and PDMS surface, PVC stencils can be lifted off the PDMS surface in low pressurized chamber. However, the hydrophobic surface of the fully polymerized PDMS has low energy. Therefore, the PVC stencil adhesives and the PDMS surface form very weak bonds. The application tape and the PVC form stronger bonds than PVC adhesives do with the PDMS surface. Therefore, an additional process that increase surface energy of PDMS is necessary. Oxygen plasma is not adequate for this process because the plasma treated PDMS surface and the PVC adhesive side form irreversible bonds like PDMS to PDMS bonding. Successive steps of this process requires the stencils to be peeled off without damaging the underlying substrate. Therefore, silanization is implemented using trichlorosilane on this PDMS surface prior to stencil transferring (Figure 2-5e). After the stencil is securely pasted on the

PDMS surface, liquid PDMS is spin coated over this surface with desired thickness. However, to promote strong adhesion of PVC adhesives on PDMS substrates, silanization was performed. As mentioned earlier, silanization is usually performed to build a barrier between fully polymerized PDMS and newly deposited uncured PDMS. When uncured PDMS is deposited over this silanized surface, the two detach easily. Moreover, PDMS etching is completed with the removal of the stencil which too removes PDMS that covers the stencil. Here, with silanization still intact, when the stencil is removed from the surface, the whole layer peels off. So, to ensure strong bonding between silanized surface and newly deposited layer, oxygen plasma treatment is executed with the stencils pasted on the first PDMS layer (Figure 2-5f). Oxygen plasma treatment is executed at an RF power of 5W, 10 sccm, for 45 seconds. After plasma treatment, PDMS is coated over this layer (Figure 2-5g). This layer is then cured on a hot plate at 100°C for 15 minutes. After full polymerization is achieved, the device is placed in room temperature for at least 15 minutes. Cooling down time is necessary because the stencil's adhesive side slightly melts in 100°C. When the stencil is peeled off without cooling down, adhesive residue may be left on the PDMS surface (Figure 2-5h). This etching process was designed to bear smooth surface. Adhesive residue left on the surface may increase surface roughness which is not what is expected through this process.

2.4.2. Inflatable Chamber Fabrication

Inflatable chamber is too fabricated only using oxygen plasma

treatment, silanization and PVC stencils. Stencils and wafers are prepared similarly as the previous PDMS etching procedure. Selective bonding of PDMS surfaces is implemented to fabricate the inflatable chamber. To test the selective bonding process, circular stencils with various size ranging from 2 mm to 8 mm in radius were tested. These circular stencils all have a concentric circular engraving in the center with a radius of 750 μm. This small circular stencil is there to make an entry point into the detached area.

With silanized wafer, PDMS is spin coated with desired thickness (Figure 2-6a). To test selective bonding, the layer was fixed to 100 μm. Moreover, if the thickness dropped below 100 μm substantially, problems may happen in successive steps. PDMS is spin coated over the wafer with a series of spin coating recipes: 500 rpm for 5 seconds, 1000 rpm for 15 second, and 500 rpm for 5 seconds. After curing on a hot plate with 100°C for 5 minutes. After full polymerization, this PDMS is silanized with the same recipe mentioned above (Figure 2-6b). Similarly, the circular stencil is pasted on this PDMS surface and treated with oxygen plasma treatment (Figure 2-6c). Different from the previous etching method, the larger circular stencil is removed (Figure 2-6d). Removing this stencil must be done in a careful manner so that this action does not damage the PDMS layer. Slightly lift an edge of the stencil using a sharp blade, then with a tweezer, peel off the stencil slowly. As mentioned above, the PDMS substrate must be thicker than at least 75 μm and close to 100 μm just to be safe. If the thickness of PDMS substrate drops below 75 μm, the strong adhesion strength formed

between PVC adhesives and silanized PDMS may peel the substrate off the wafer or even worse tear the thin PDMS layer. The smaller circle is left on the surface (Figure 2-6d). After peeling off the stencil, PDMS is spin coated over this layer with a recipe of 500 rpm for 5 seconds, 1500 rpm for 15 seconds, and 500 rpm for 5 seconds (Figure 2-6e). This developed approximately 75 μm thick PDMS. Curing on a hot plate for 5 minutes at 100°C, the wafer is removed and cooled for 15 minutes. Similar to the etching process elaborated above, the smaller circular stencil is peeled off from the wafer tearing off the new deposited PDMS layer (Figure 2-6f). This process bears two PDMS layers only detached on surfaces covered by the circular stencil. The second PDMS layer is punctured at the center with a size equal to the smaller circular stencil. Finally, this inflatable chamber is finished by bonding a thick slab (at least 3 mm thick) of PDMS (Figure 2-6g) with a hole with diameter of 1.75 mm punctured using a biopunch. This hole and the hole in the PDMS double layer is aligned and bonded via oxygen plasma treatment at RF power of 5W, 10 sccm, for 60 seconds. To test the detachment of the membrane, a syringe is connected to the hole. The chamber is inflated by injecting DI water (Figure 2-6h).

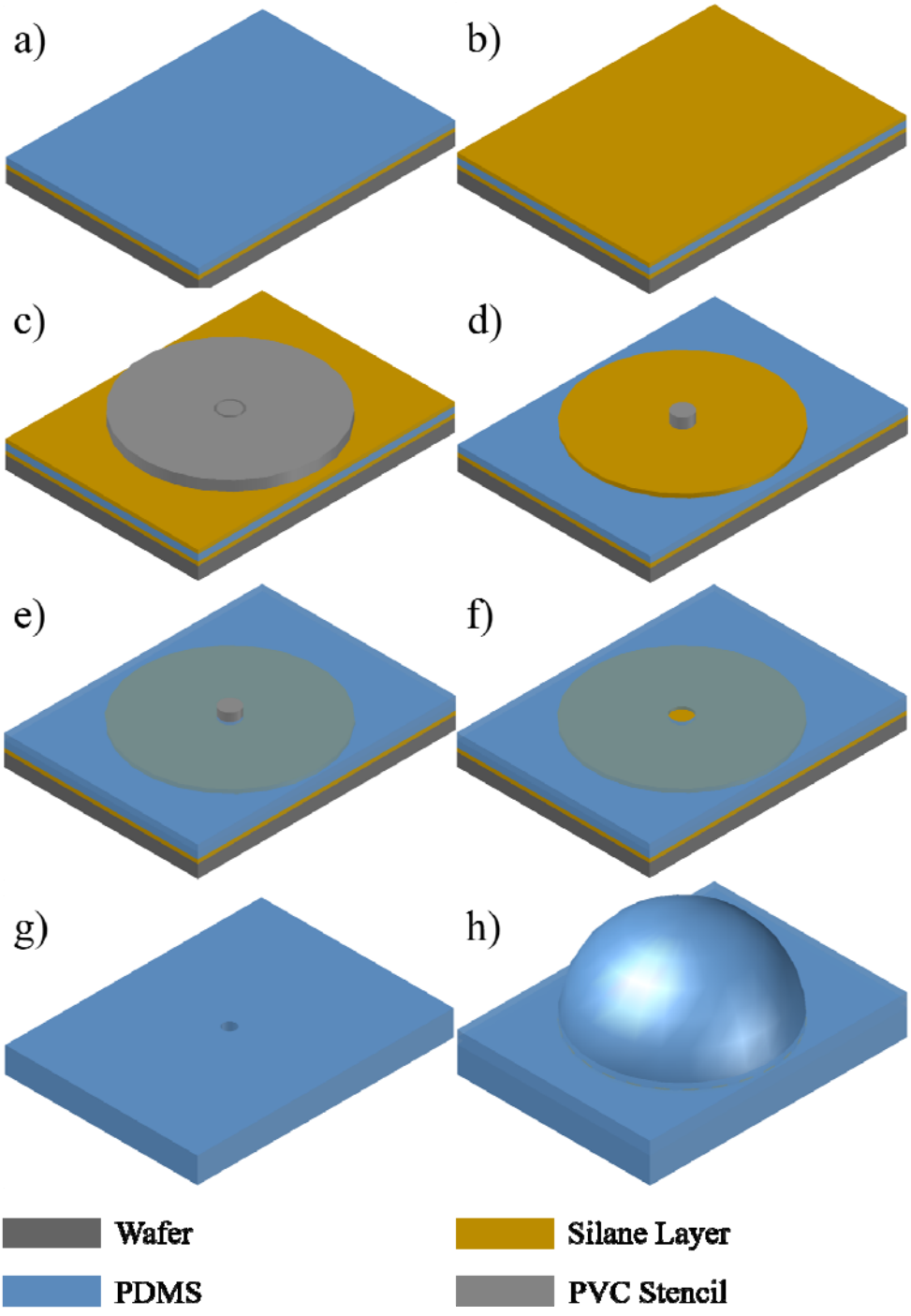

Figure 2-6. Fabrication steps of selective bonding to develop inflatable chambers

2.4.3. Full Fabrication of the Drug Delivery Device

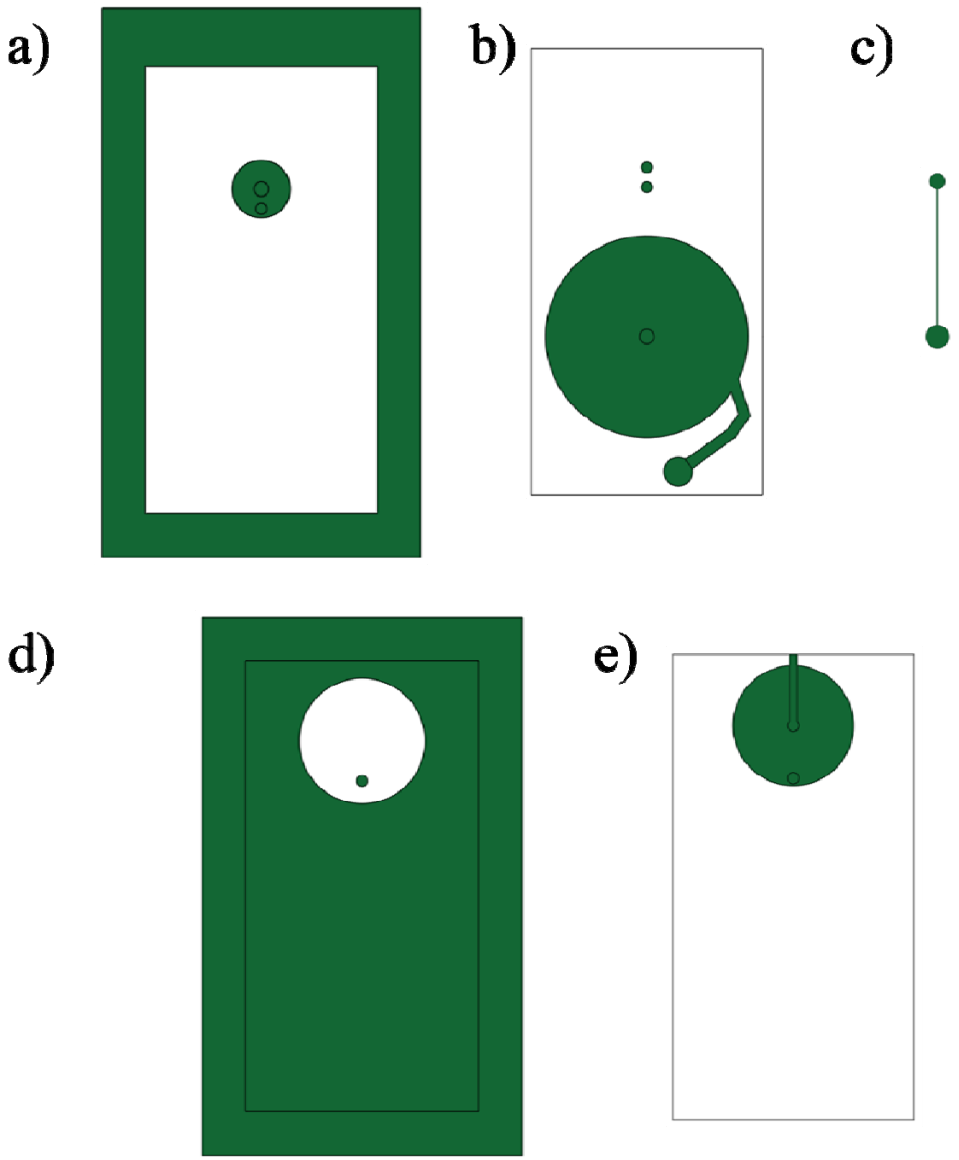

Figure 2-7. PVC stencil designs required to fabricate the device

In this section, full fabrication of the proposed drug delivery device is elaborated. The fabrication of the device can be divided into three or

four parts depending on the actuation mechanism. Four separate wafers are required for both magnetic and electromagnetic actuation of the device. Primary, secondary chamber and a microchannel that connects the primary and secondary chambers are fabricated on one wafer. A microvalve that utilize a neodymium magnet is fabricated on another wafer. A magnetic membrane that attracts the magnet to ensure closure of the microvalve is fabricated on another wafer. For magnetic actuation, a thick slab of PDMS (thickness ≈ 1.5 mm) with a cylindrical groove with depth of 1 mm and radius ranging from 3 to 5 is prepared on the last wafer. Fabrication steps of each component are illustrated and explained in depth. PDMS etching and selective bonding processes are used along with the PVC stencil designs in Figure 2-7 shows all the PVC stencil designs that are required to fabricate the drug delivery device. Figure 2-7a = secondary pump layer, Figure 2-7b = primary chamber layer, Figure 2-7c = microchannel layer, Figure 2-7d = microvalve layer_1, and Figure 2-7e = microvalve layer_2.

2.4.3.1. Primary and Secondary Drug Chamber

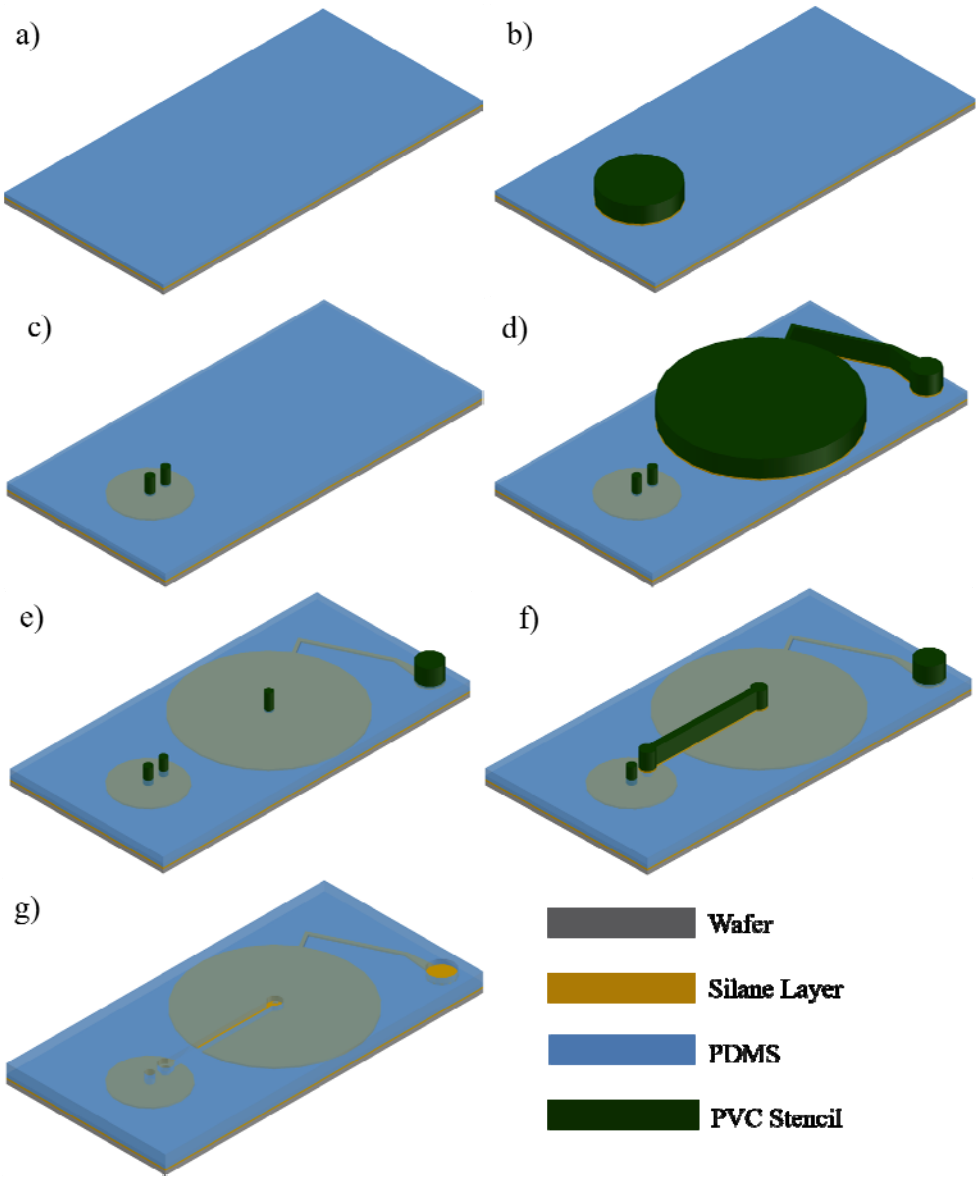

Figure 2-8. Fabrication of the chamber layer of the drug delivery device.

Fabrication of the reservoir layer starts with silanizing the wafer. The first PVC stencil, rectangular band stencil is pasted on the wafer using an application tape. This rectangular band works as an alignment key for successive layers that require precise positioning. Silicon wafer is

naturally hydrophilic. Therefore, pasting PVC stencils over the wafer does not require silanization. However, to easily remove PDMS structures from the wafer without damaging them require a silanized layer coating over the wafer surface. Over this layer, 3 mL of procured PDMS is spin coated with a series of coating recipes: 500 rpm for 5 seconds, 1500 rpm for 15 seconds, and 500 rpm for 5 seconds (Figure 2-8a). This first PDMS layer is approximately 75 μm thick. After curing on a hot plate at 100°C for 15 minutes, the layer is silanized using trichlorosilane. Retrieving the wafer from the vacuum chamber after a couple of hours, the secondary pump PVC stencil is pasted. This second stencil is aligned with the rectangular band and pasted. This second stencil is a circular shaped stencil with radius 1.5 mm to 2.0 mm. Two smaller circles with radius 375 μm are trimmed within this circle. These circles are the inlet and outlet of the secondary pump. Using this stencil, selective bonding is executed over this first PDMS layer (Figure 2-8b). With the stencil pasted on the first layer, the surface is treated with oxygen plasma at 5W RF power, with 10 sccm for 60 seconds. After plasma treatment, the larger circular stencil is removed. Here, the small inlet and outlet stencils are still intact on the surface. Over the PDMS and PVC stencil, PDMS is spin coated with consecutive recipe of 500 rpm for 5 seconds, 1000 rpm for 15 seconds, and 500 rpm for 5 seconds and cured on a hot plate at 100°C for 15 minutes (Figure 2-8c). This surface is then silanized again. Retrieving the wafer from the chamber after a couple of hours the primary pump stencil is aligned and pasted. This stencil is composed of three components: inlet, outlet, inflatable chamber,

and inflatable microchannel. After oxygen plasma treatment, the chamber, and microchannel portions are removed from the surface while the inlet and outlet portions are intact (Figure 2-8d). Then, PDMS is spin coated over this surface and cured (Figure 2-8e). Silanization of this surface is executed again and the microchannel stencil is pasted on this surface aligned with the inlet of the secondary pump and the outlet of the primary chamber. Finally, after oxygen plasma treatment, uncured PDMS is spin coated over this surface (Figure 2-8f). The chamber layer is finished with removing all the remaining stencils from the wafer. Removing the stencil removes the PDMS coated over the stencil. Thus, this action produces results similar results to PDMS etching.

2.4.3.2. Microvalve

The microvalve utilized in the drug delivery device is composed of two compartments. A thin membrane that can be deflected with the presence of a magnetic field, and a magnetic PDMS composite embedded PDMS slab that tightly encloses the deflectable membrane compose the microvalve used in the device. A neodymium permanent magnet is bonded on to the deflectable membrane on the opposite side of the PDMS slab.

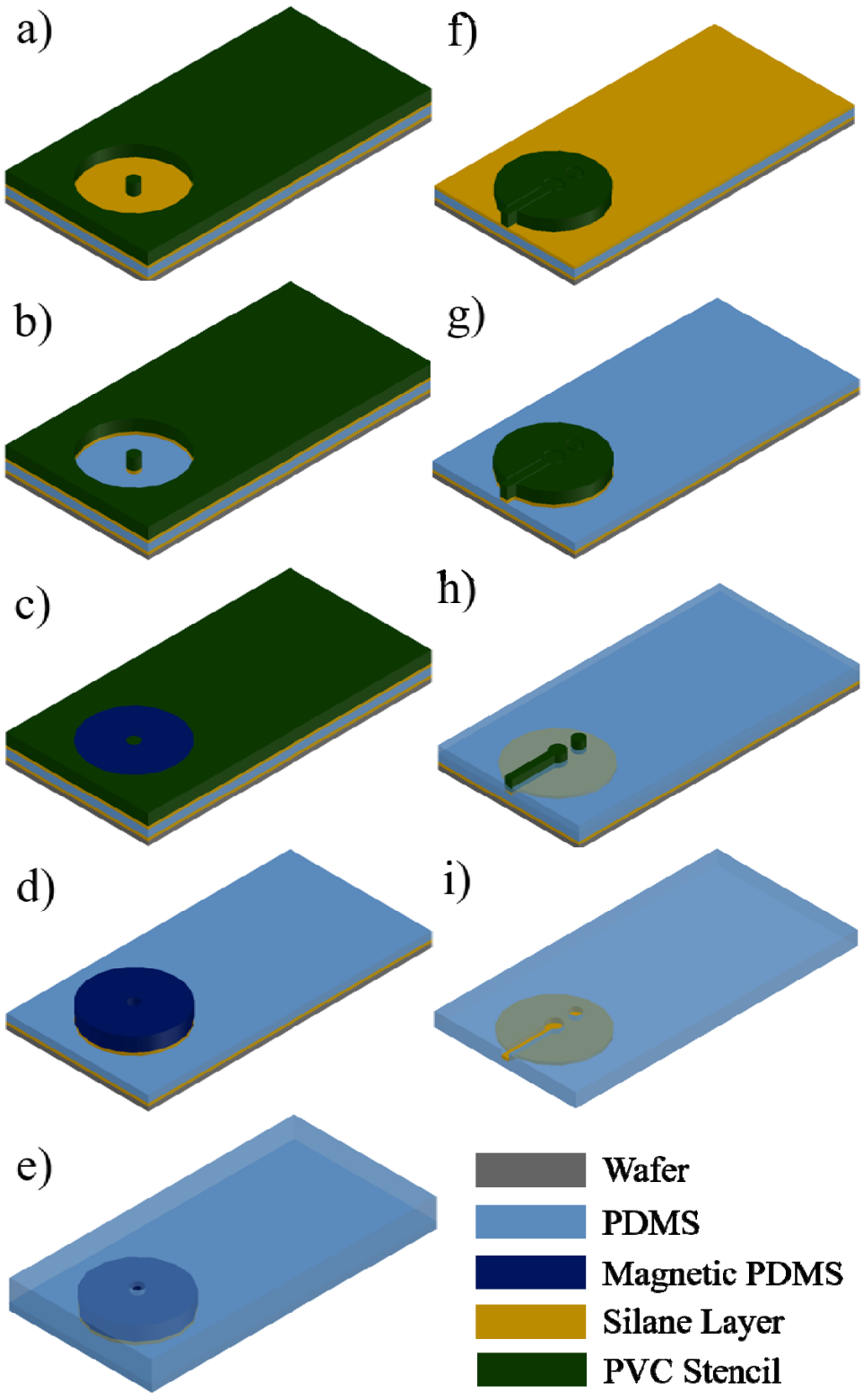

Figure 2-9. Fabrication of microvalve

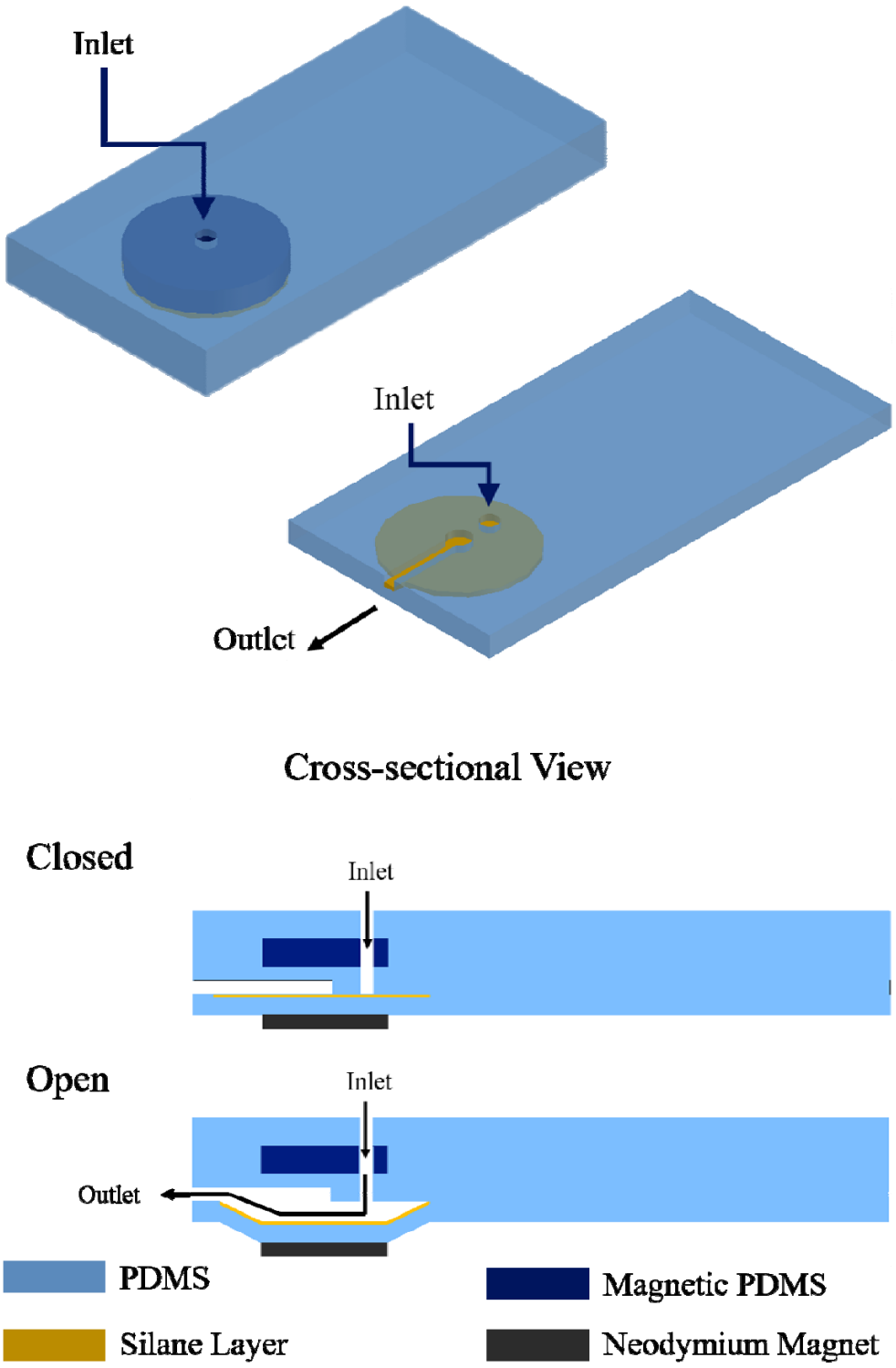

Figure 2-10. Plasma bonding of the two compartments that compose the microvalve and cross sectional view and deflection mechanism of the

valve.

Fabrication of the microvalve layer again starts with two silanized wafer. Each compartment of the device is developed on a separate wafer. First, fabrication of the magnetic slab is elaborated. Over a silanized wafer, a thin layer of approximately 95 μm PDMS was spin coated. This PDMS surface is then silanized with the same recipe introduced above. PVC stencil (Figure 2-7d) is pasted over this surface and the larger circular band stencil is peeled off (Figure 2-9a). This surface is then treated with oxygen plasma at 5W of RF power, 10 sccm, for 60 seconds (Figure 2-9b). The empty void of the PVC pattern is now filled with PDMS and nickel composite. PDMS and nickel composite was mixed with a weight ratio of 5:3.5. The composite prepared earlier is poured over the stencil. With a sharp blade, excess volume of the composite is removed by scraping off the surface. As the composition of nickel particles increase, this scraping motion can lead to inconsistent formation within the membrane. To avoid this inconsistency, a strong permanent magnet is placed right beneath the wafer aligned with the stencil to hold magnetic particles in place (Figure 2-9c). After curing, the remaining PVC stencils are removed from the wafer (Figure 2-9d) and PDMS is poured over to develop a PDMS slab with approximately 500 μm thick profile. A hole with 1 mm diameter is drilled through the center of the circular composite (Figure 2-9e). The second part of the microvalve is the deflection membrane with inlet and outlet. Similarly, a layer of PDMS is spin coated over the silanized wafer with a recipe of 500 rpm for 28 seconds. Curing at 100 °C for 15 minutes, the surface is silanized.

PVC stencil (Figure 2-7e) is pasted over this surface (Figure 2-9f). This stencil is composed of three parts. A circular patch that accounts for deflection membrane, circular inlet and a channel shaped outlet. This surface is treated with oxygen plasma with the stencil intact. Then, only the large circular stencil is removed and another layer of PDMS is spin coated over with the same recipe (Figure 2-9h). After curing, the remaining stencils are removed (Figure 2-9i). Fabrication of the microvalve is completed by plasma bonding the two compartments aligning them with the inlets of each compartment. Figure 2-9 shows the two compartments of the microvalve. The two are aligned with the inlets and bonded through oxygen plasma treatment. The cross-sectional view of the valve in Figure 2-10 show the working mechanism of the valve.

2.4.3.3. Magnetic Actuation Component

This last component of the device differs whether the device is actuated with a permanent magnet wirelessly or electromagnetically with a power source connected. For a magnetically actuated device a rather thick slab of PDMS approximately 1.5 mm in thickness with a cylindrical furrow with radius equal to the size of the deflection membrane and depth of 1 mm. This slab of PDMS is plasma bonded over the deflection membrane completely encapsulating the deflection membrane and the permanent magnet. This is necessary to enforce stronger closure of the valve. As the pressure in the primary and secondary pump increase and exceeds the valve's threshold, there is a chance the valve will open and leakage of drug substances out of the

device can ensue. Bonding the slab over the valve produces a cylindrical void encapsulated with PDMS all around. This air tight capsule promotes higher pressure over the deflective membrane that consequently require the valve a higher actuation force to open.

Fabrication of the flexible conductive coil starts with a silanzied wafer. This wafer is then coated with PDMS with approximately 150 μm. This can be achieved by dispensing 3 mL of pre-cured liquid PDMS mixture over the wafer and spinning with a recipe of 500 rpm for 30 seconds (Figure 2-11a). PDMS is cured and silanized. Positive PVC stencil of the coil is pasted on this surface and treated with oxygen plasma (Figure 2-11b). Then, PDMS is spin coated over this stencil to have thickness of approximately 250 μm (Figure 2-11c). After curing, this PDMS surface silanized. Over this surface, negative PVC stencil of the stencil is aligned with the positive stencil and pasted (Figure 2-11d). Then, the positive stencil is peeled off bearing etching results on the surface. The groove produced in this procedure is approximately 330 μm deep. Over this surface, silver micropowder and PDMS is mixed in a ratio of 5 to 1. The mixture produces a composite too lumpy to execute screen printing. Screen printing is a procedure used when magnetic PDMS patterning was implemented in previous procedures. The composite is dispensed over the surface. However, the lumpy composite cannot be injected into the microgrooves by scraping off the composite using a sharp blade. Therefore, highly volatile solvent was mixed in a 1 to 1 volume ratio with the composite to temporarily develop a slurry mixture. 80% ethanol mixed with 20% DI water was used here. Highly

volatile solvents such as n-Hexane can also do the job. However, PDMS swells up when it comes in direct contact with highly volatile substances [134]. Now the mixture is slurry enough to be screen printed (Figure 2-11f). Finally, the negative PVC stencil is removed from the layer and the PDMS surface is treated with oxygen plasma treatment. An encapsulation layer is dispensed over the surface completing the conductive flexible coil.

3. Results

3.1. PVC Stencil Preparation

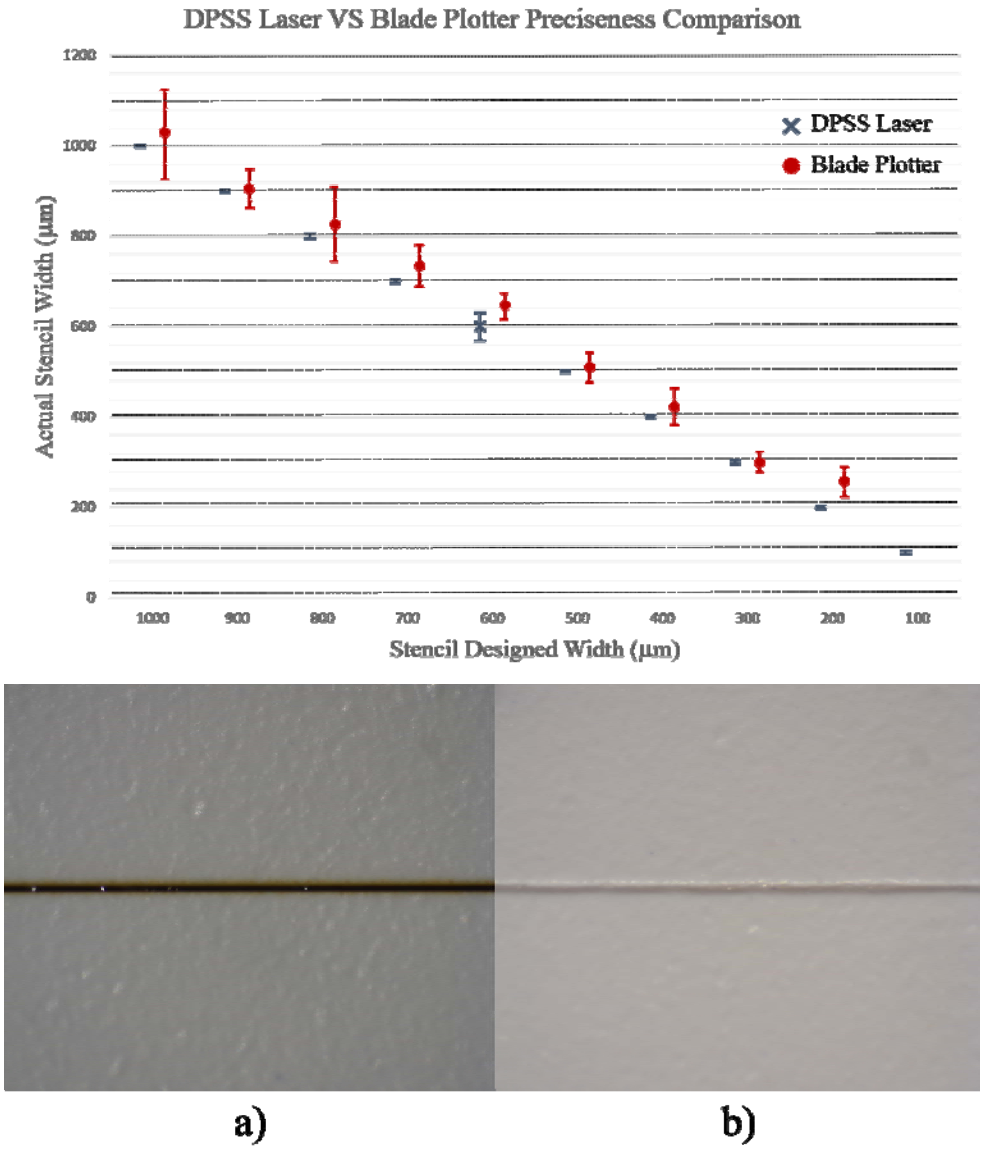

Figure 3-1. DPSS laser and blade plotter preciseness comparison.

Figure 3-1 is a chart analyzing both stencil preparation devices. Each

device was programmed to cut out stencils with width ranging from 1 mm to 100 μm. The widths of stencils cut out using each devices were measured using a Scanning Electron Microscope (SEM). Figure 3-1 a and b shows cutting profile of a DPSS laser and a blade plotter. DPSS laser system uses a high power laser that burns through the PVC material while blade plotters cut through with a physical blade. Figure 3-1a manifests the burned surface of PVC. The burning width can be controlled by the number of passes over the stencil. However, a certain amount of passes are required to burn through the 80 μm thick PVC sheet. At least 30 passes are required to burn through the PVC and the polyacrylic adhesives. 30 passes may be enough to cut through the PVC sheet. However, it may not be enough to clearly cut through the polyacrylic adhesives. At least 50 passes are required to cut through the polyacrylic adhesives. When 50 passes are burned through the PVC sheet, the width is approximately 20 μm. Therefore, thickness error of the DPSS laser device does not only arise from the device itself but also from the burning nature of the laser. Figure 3-1b manifests a groove made by the blade that passed over through the PVC sheet. Blade plotters do not burn through the PVC. Thus, thickness error produced by blade plotters arise from the devices' mechanism only.

Chart in Figure 3-1 shows the thickness preciseness of both devices. DPSS laser analysis is depicted in blue (x) and blade plotter is depicted in red (o). Stencil preparation was repeated 20 times for analysis. DPSS laser's analysis shows that the results are slightly smaller than desired and designed size. However, deviations from the average value was very

small. Blade plotters, however, use two motors that control the vertical and horizontal movement of the blade. These motors are not precise enough to cut down to a few hundred micrometer size fragments. The chart shows an average value slightly larger than desired and designed size. Moreover, the deviation of cut out stencils were too large. Therefore, the results were not reliable. Upcoming experiments and procedures were all implemented using PVC stencil acquired using only DPSS laser system.

3.2. Surface Modification and Selective Bonding

Fabrication of the inflatable chamber begins with surface modification and selective bonding using this surface modification method. PDMS surface modification is critical to the PVC fabrication methods proposed in this paper: increased surface energy to enable secure fixation and transfer of PVC stencils onto innately hydrophobic surface, and a barrier formed between two PDMS layers for selective bonding process.

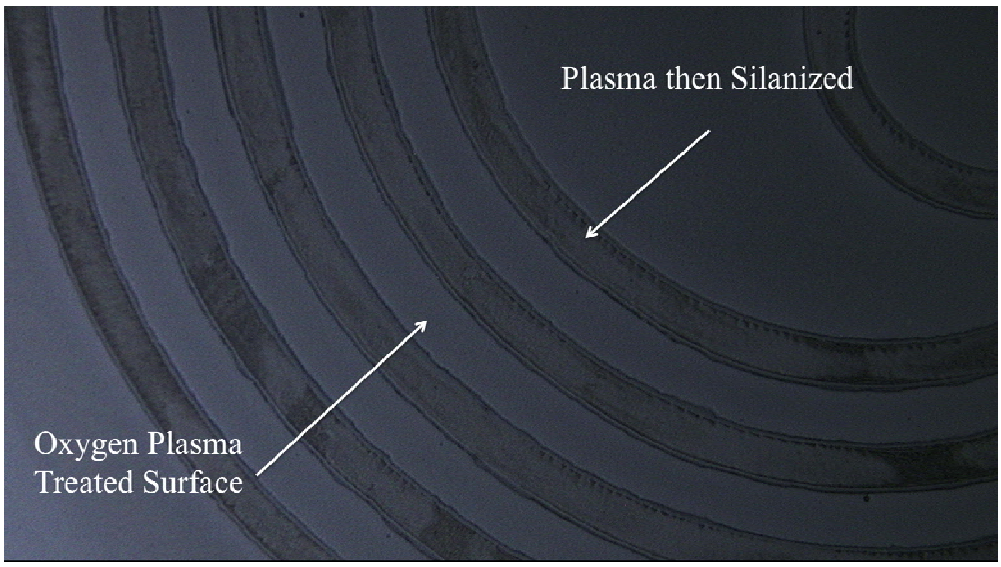

Figure 3-2. Surface modified PDMS surface using PVC stencils.

Figure 3-2 is an image of PDMS surface treated with oxygen plasma treatment and silanization to render the surface hydrophilic. A concentric design of PVC stencil was pasted on a silanized PDMS surface. This then was treated with oxygen plasma at an RF power of 5W, with oxygen concentration of 5 sccm for 30 seconds. The stencil was removed and the surface was place in a freezer for a minute. When it is retrieved from the freezer, the rapid change in temperature from below zero to room temperature, allows thin layer of frost to form on the surface. This only happens on hydrophilic surfaces. The image in Figure 3-2 shows the degree of hydrophilicity of the treated PDMS surface depending on whether it was treated only with oxygen plasma or silanized. Oxygen plasma treatment gives surfaces with higher hydrophilicity than silanized surfaces as the thicker frost layer in Figure 3-2 verifies.

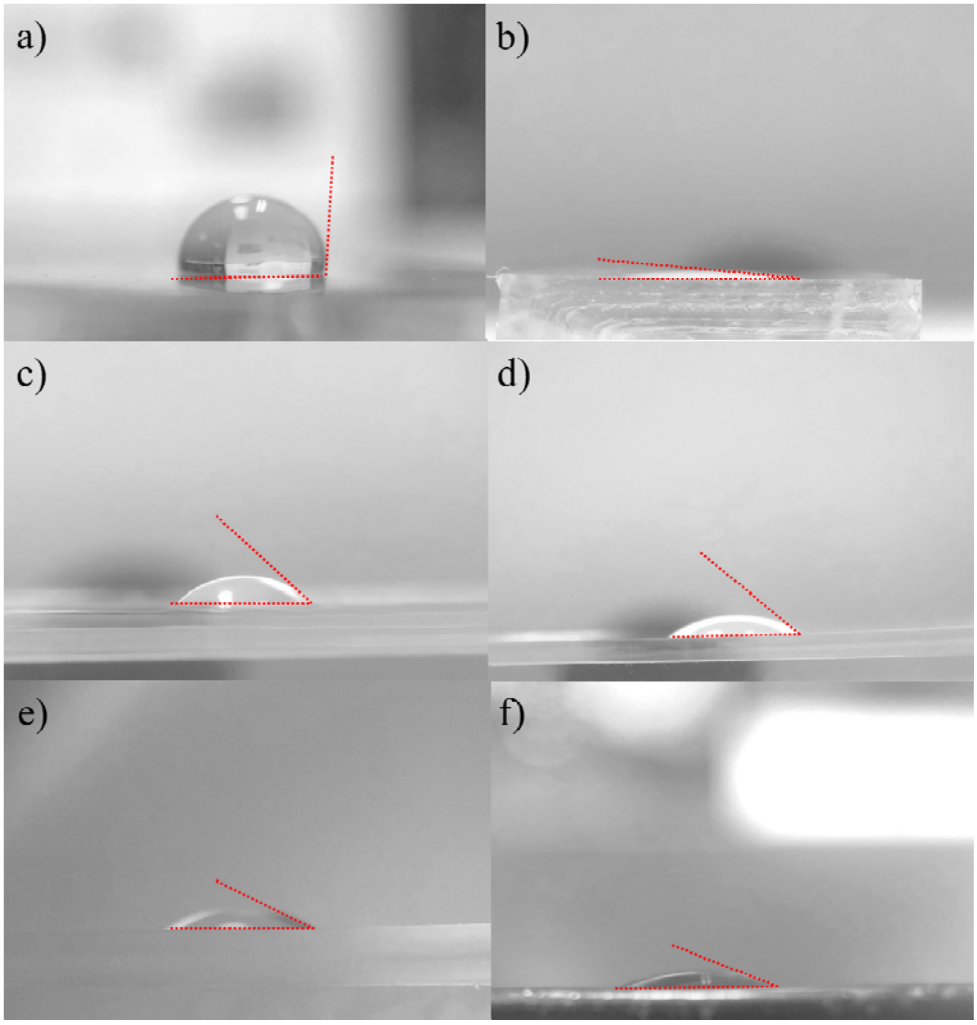

Figure 3-3. Water drop test on hydrophilic altered PDMS surfaces with varying oxygen plasma treatment duration.

Figure 3-3 are images of water drop test on bare, oxygen plasma treated, three different durations of oxygen plasma treated, and silanized then oxygen plasma treated PDMS surfaces. Oxygen plasma treatment was implemented with three different RF power states, 5W, 50W, and 150W. The duration of oxygen plasma treatment was varied from 30 seconds, 2 minutes, and 5 minutes. Here, the oxygen flow rate was fixed

to 10 sccm. Water drop test was executed to investigate how the surface properties of PDMS was modified. Water drop angle was measured for each oxygen plasma duration to show how much the surface was modified. Bare PDMS surface has a water contact angle of approximately 99 degrees (Figure 3-3a). Oxygen plasma treated surfaces have a contact angle of less than 10 degrees (Figure 3-3b). As many experimental results show, the oxygen plasma treatment implemented prior to vapor coating trichloro (1H, 1H, 2H, 2H-tridecafluoro-n-octyl) silane gives variance in how much the PDMS surface is modified. The silanized PDMS surfaces manifest change in surface energy as the oxygen plasma treatment duration increases, or the plasma treatment RF power increases. From 99 degrees of bare PDMS water contact angle, as the duration of oxygen plasma treatment increased, the water contact angle first begins to degrease down to 44.25 degrees. As the RF power increases, the contact angle increased up to 77.88 degree. Here, the plasma treatment duration was fixed to 2 minutes. Under same conditions in power and oxygen flow rate, when duration was increased to 5 minutes, PDMS surface was modified slightly more hydrophobic. The contact angles were increased up to 110 degrees. As the duration of plasma treatment increases, PDMS surfaces display hydrophobic return.

Figure 3-4 shows two charts that depict the change in water contact angle on different PDMS surfaces. Figure 3-4a is a chart with 4 types of PDMS surfaces: three types of treated and one untreated PDMS. Treated PDMS surfaces were treated with oxygen plasma with a flow rate of 10 sccm for two minutes. The difference in each surfaces was the RF power

of the process was 5W, 50W, and 150W. Figure 3-4b, similarly, depicts 4 different types of surface modified PDMS. The difference between Figure 3-4a is the oxygen plasma treatment duration. The process time was increased to 5 minutes. Longer processing time shows the increase in contact angle.

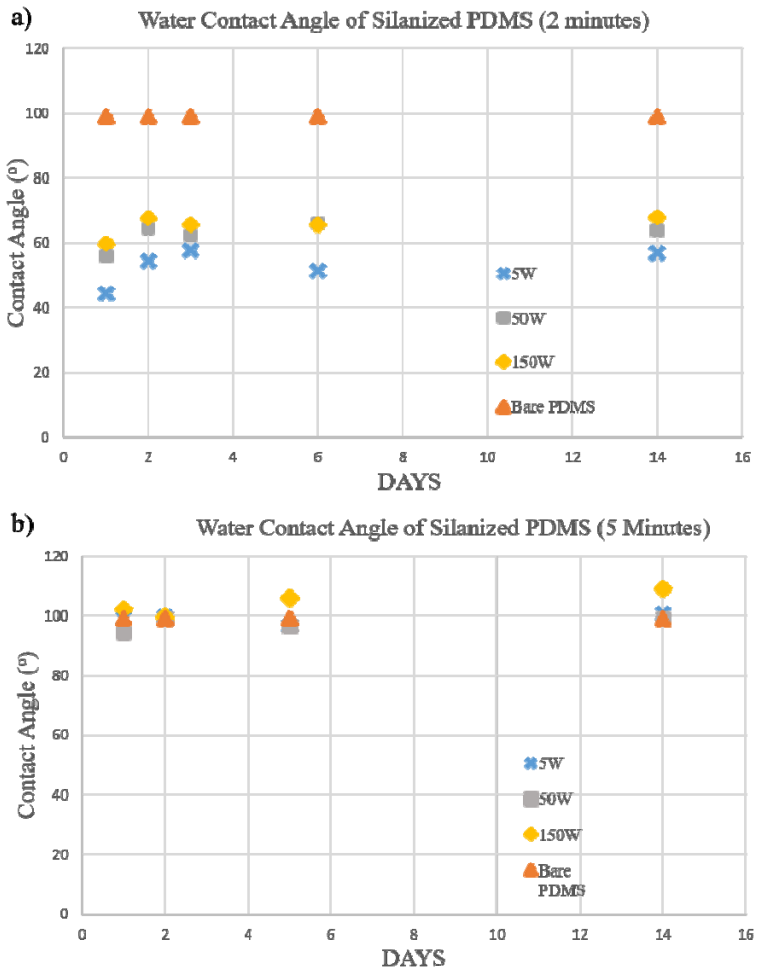

Figure 3-4. Surface modified PDMS via silanization with variance in oxygen plasma treatment.

Higher power and longer duration of oxygen plasma treatment was

not implemented because the process does not only render the surface hydrophilic, but also produces small and large cracks on the surface. The high temperature induced by the plasma treatment for longer duration and higher power can increase the degree of crack produced on the treated surface. The problem to this crack surface is that it does not only modify the surface properties, but also the tensile strength of the film itself.

The surface modification is crucial in this procedure in that the patterned PVC stencils can be securely fixated on the surface using the transfer paper. Figure 3-5 shows the difference in surface modification of PDMS when transferring PVC stencils using the transfer paper. Figure 3-5b shows that the stencil cannot be transferred onto the PDMS surface because of its low surface energy. When the transfer film is peeled off, the stencil design is still intact on the film rather than on the PDMS surface. On the other hand, Figure 3-5c shows successful transfer of PVC stencils onto the PDMS surface due to increased PDMS surface energy. Figure 3-5d are examples of more complex designs that could be successfully transferred onto the treated PDMS surface.

Selective bonding of PDMS surfaces is shown in Figure 3-6. A circular stencil with a microchannel stencil connected to an inlet stencil was used to test the surface modification. Figure 3-6a is the surface treated PDMS with the stencil peeled off. The stencil boundary can be visualized due to the difference in surface properties after oxygen plasma treatment and silanization.

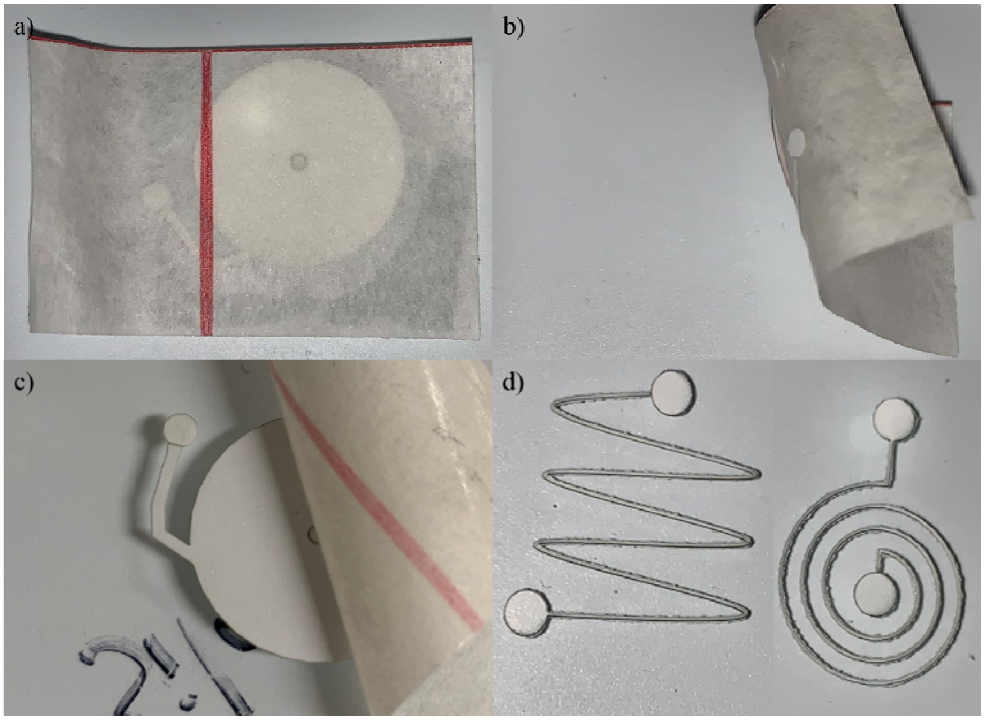

Figure 3-5 Transferring PVC stencils onto PDMS surfaces.

On the surface in Figure 3-6a, PDMS is spin-coated and cured. The surface covered by the stencil, thus not treated with oxygen plasma treatment, is detached while the other surface, treated with oxygen plasma treatment, is strongly bonded. Figures 3-6 c and d show images of selectively bonded PDMS double layer. A thick slab (≈5 mm) of PDMS is pasted on the selectively bonded PDMS. This slab has a hole punctured to connect a syringe tube to inject fluid into the detached area. A tube is injected into the hole and through a syringe, red-dyed DI water was injected. The thin membrane inflates verifying the detached and bonded surface by selective bonding process.

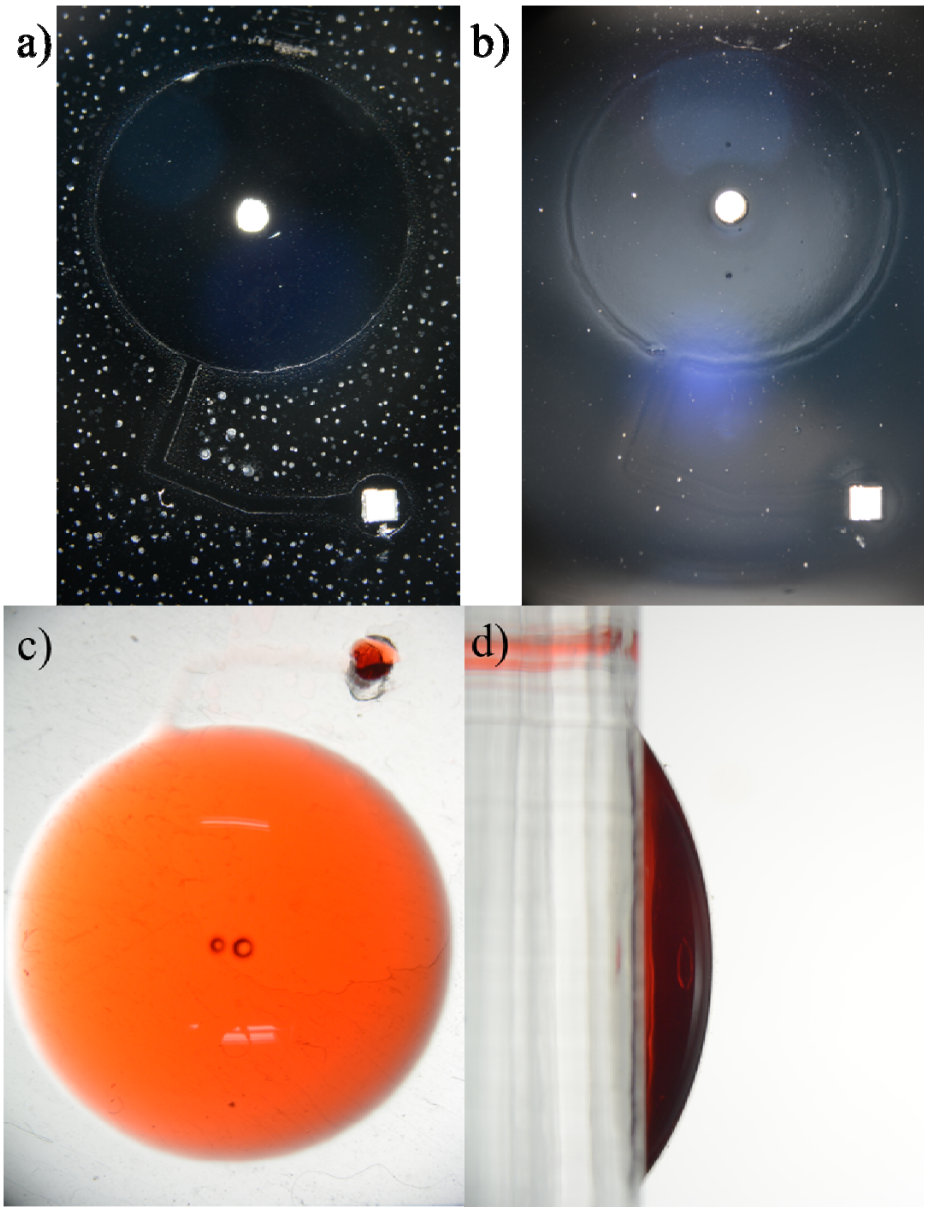

Figure 3-6. Selective bonding of PDMS surfaces. Selective bonding testing by injecting red-dyed DI water and inflating the chamber.

3.3. PDMS Polymerization Inhibition

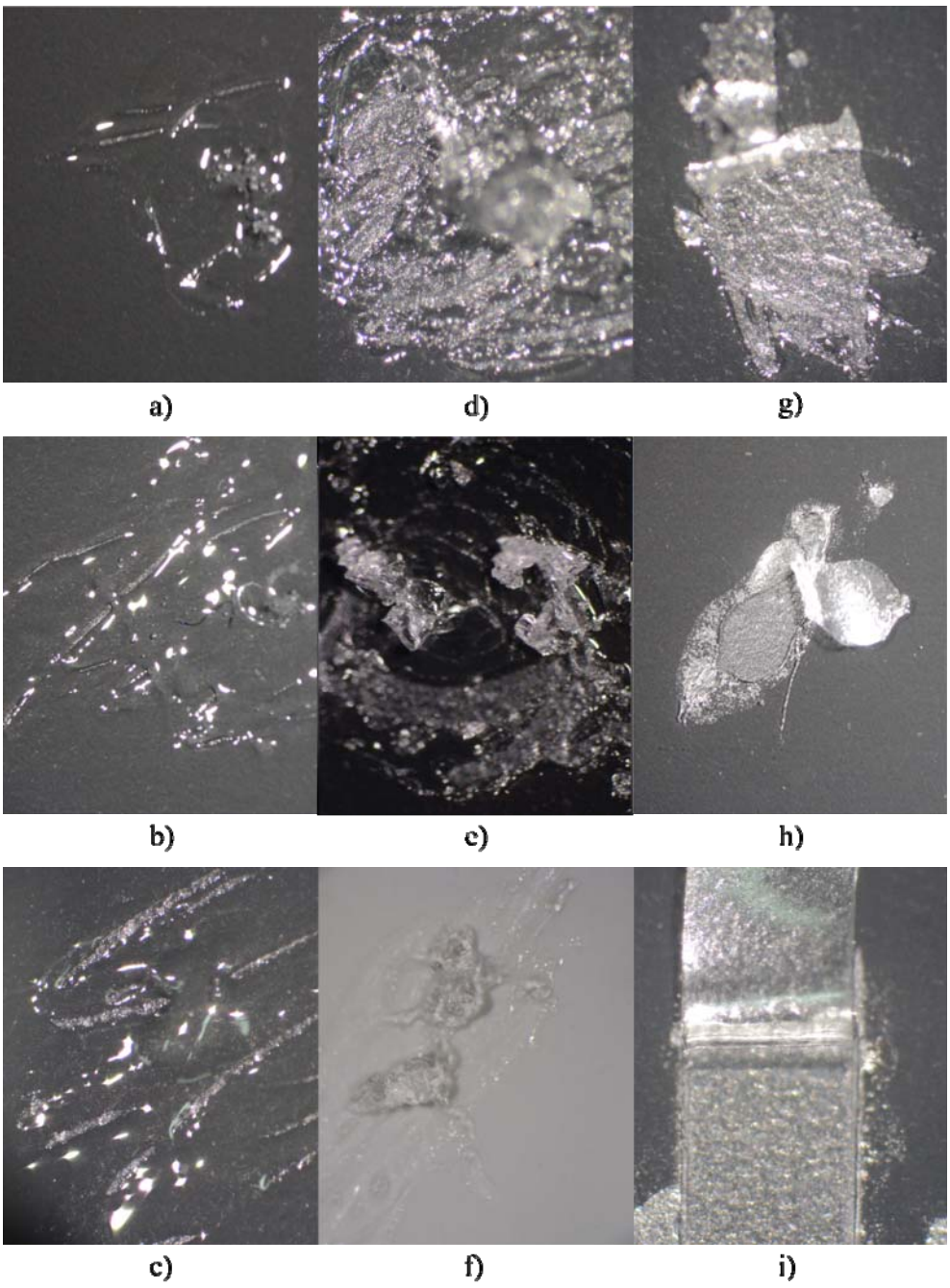

Figure 3-7. Polymerization inhibition of PDMS over PVC substrates.

PDMS polymerization inhibition over PVC substrates is investigated. Figure 3-7 are images that illustrate the degree of PDMS polymerization

inhibition over PVC substrates with respect to the thickness of PDMS dispensed over the substrate. Figures 3-7 a, b, c show full inhibition of polymerization, Figures 3-7 d, e, f show partial polymerization and Figures 3-7 g, h, i show full polymerization over PVC substrates. A rectangular stencil with 1 cm by 1 cm was pasted over a silanized wafer. Precured liquid PDMS was dispensed over the wafer and spin coated with 10 different recipes ranging from 500 rpm to 5000 rpm for 15 seconds with 500 rpm interval. Each recipe started and ended with 500 rpm spinning for 5 seconds each for leveling procedures.

The degree of polymerization inhibition of PDMS over PVC stencils with respect to the thickness was experimentally obtained. The chart in Figure 3-8 shows the relationship between spin-coating recipes and PDMS thickness formed on the PVC stencil. Total inhibition of PDMS was observed when the thickness was less than 20 μm, colored area in blue. When the thickness was in between 80 and 20 μm, partial polymerization was observed, colored area in green. Lastly, when the thickness was greater than approximately 100 μm, inhibition was negated and PDMS fully polymerized, colored area in gray.

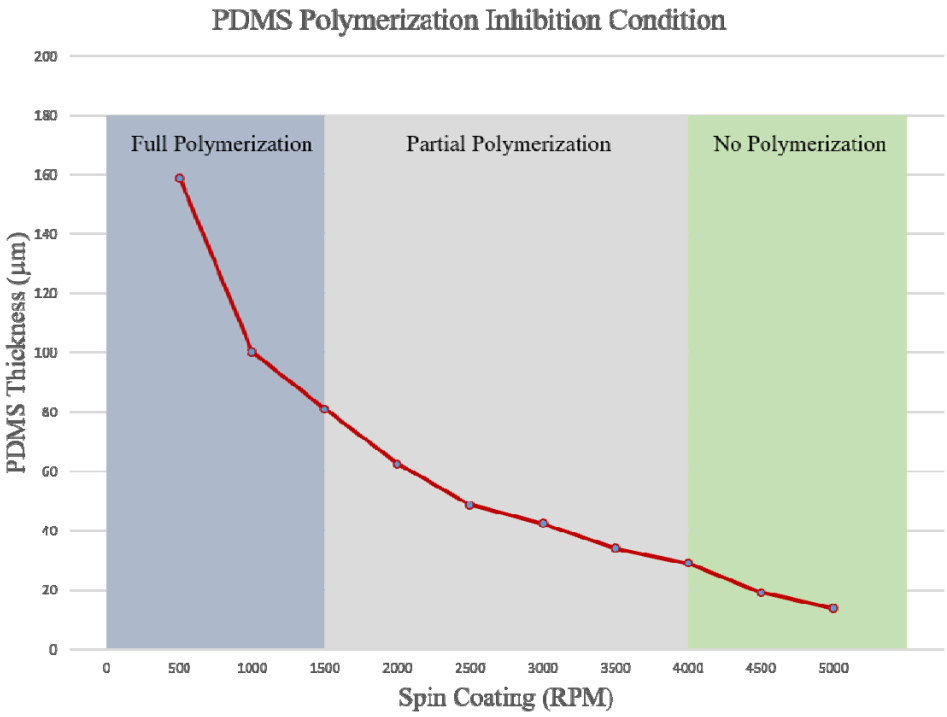

Figure 3-8. The degree of polymerization inhibition with respect to the thickness of PDMS dispensed on the PVC substrate.

3.4. PDMS Etching

The conventional PDMS etching method utilize etching solutions and fluorine based RIE integrated with photolithography patterning. However, these methods either produce etched PDMS surface with substantial surface roughness or lateral etching that cannot be controlled with high precision. The proposed method that utilize PVC stencils and PDMS polymerization inhibition can be used to implement fast and simple fabrication that can produce etched surfaces.

Depending on the thickness of PDMS dispensed on the stencil,

which equals the thickness of the desired etched depth, the degree of inhibition of PDMS polymerization can be obtained. PDMS etching was executable even when PDMS fully polymerized. However, the etching cross-sectional profile differed and depended on the degree of polymerization inhibition. PDMS inhibition occurred only on PDMS directly in contact with the PVC stencil. When PDMS is spin-coated on the pattern pasted surface, both PVC stencil and oxygen plasma treated PDMS surface are coated with fairly equal thickness. After curing, PDMS on the stencil either fully polymerize, partially polymerize, or does not polymerize at all. In cases where polymerization is inhibited, the fully polymerized PDMS on PDMS substrates and the polymerization inhibited PDMS on the PVC stencil form a weak bond directly on top of the stencil boundary. Due to this weak bond that formed directly on top of the boundary, the simple peel off action of the stencil tears the polymerization inhibited PDMS on the weakly bonded boundary. Therefore, when PDMS is spin-coated thin enough for inhibition to occur, the etched surface produces a vertical profile cross-sectional shape. Figure 3-9 shows image of PDMS etched with vertical profile.

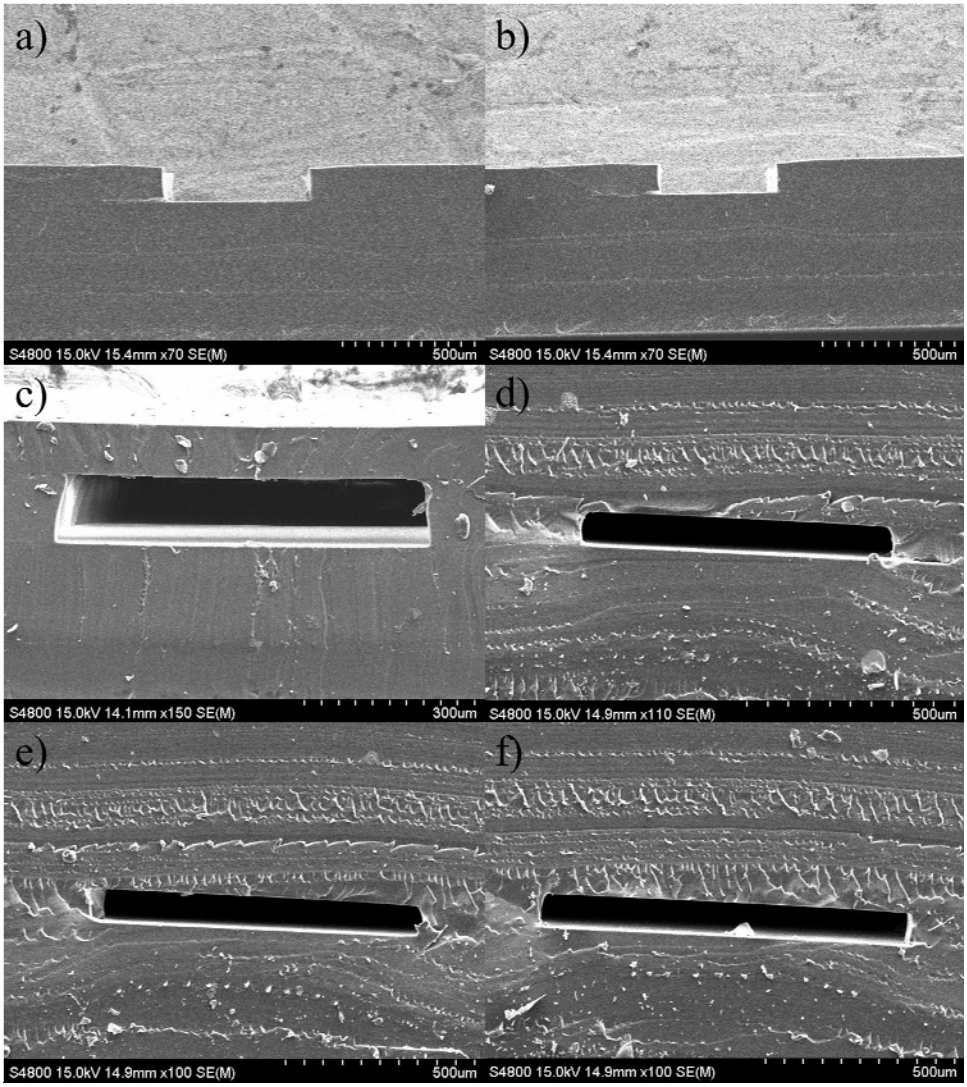

Figure 3-9. SEM images of microchannels' cross-sectional profile. The channels show vertical profile shapes.

Even in cases where PDMS polymerization inhibition is not present, PDMS etching is possible. The weak bond that is present in polymerization inhibited PDMS does not exist here in this condition. Therefore, the same peel off action can develop PDMS etching results. When PDMS is spin-coated thick enough for PDMS polymerization to

fully happen, the PVC stencil is completely encapsulated by fully polymerized PDMS. The first and second PDMS layers spin-coated separately, are bonded irreversibly by oxygen plasma treatment. The same peel off action of the PVC stencil can develop PDMS microgroove for a number of reasons. PDMS is a flexible material with relatively low fracture strength. Moreover, the tensile strength of PDMS is proportional to the thickness. When the PVC stencil is peeled off, the second PDMS layer tears off on the thinnest position. However, the peel off action does not produce a vertical profile channel. The tearing of PDMS produces channels with overcut profile. Figure 3-10 shows a diagram of overcut profile PDMS channels produced using the proposed method.

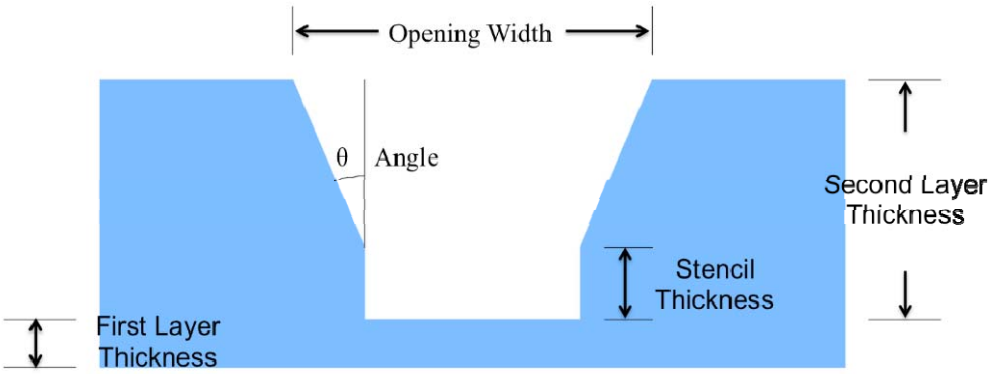

Figure 3-10. Diagram of the overcut profile produced by the proposed PVC stencil fabrication method.

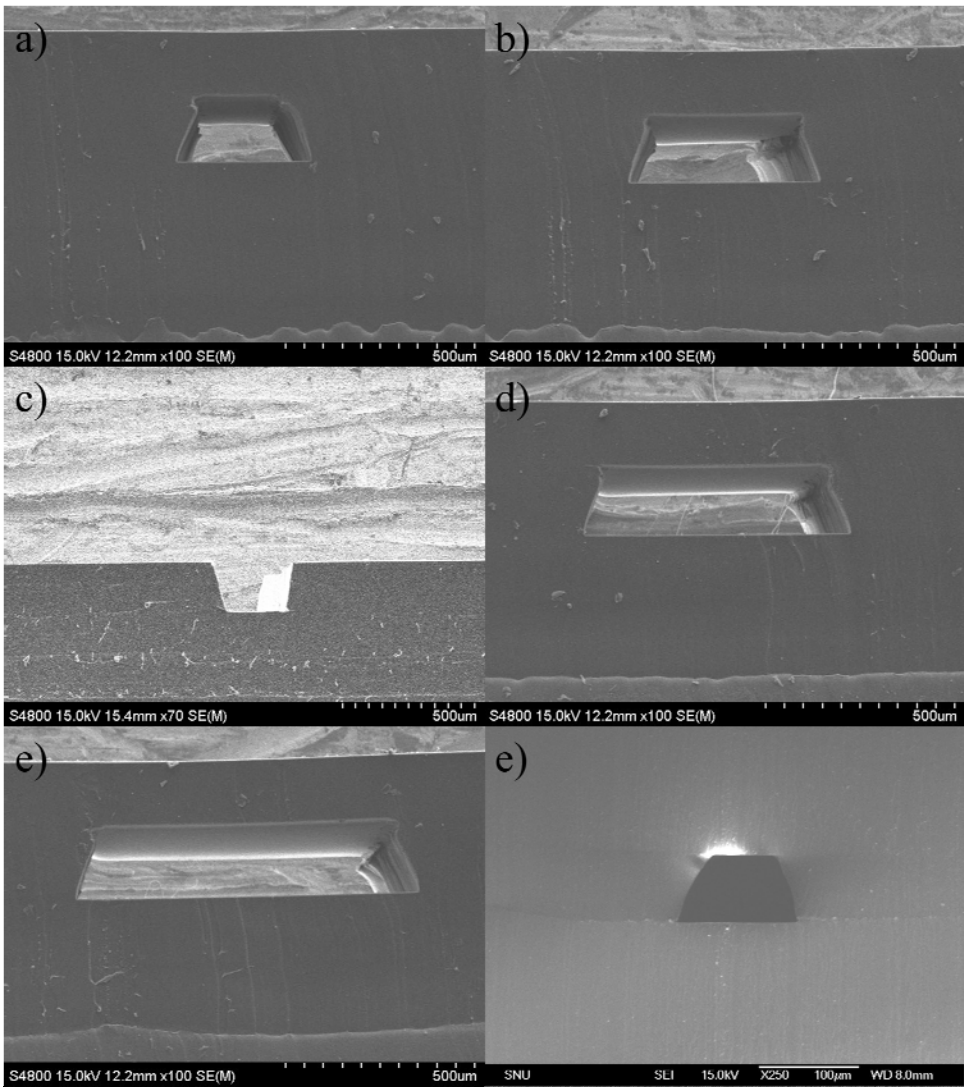

Figure 3-11. SEM images of microchannels' cross-sectional profile. The channels show overcut profile.

The absence of inhibition requires the peel off motion to tear PDMS on the thinnest boundary. The tearing forms a certain angle. This angle, pointed out in Figure 3-10, is proportionate to the stencil width and the thickness of the second PDMS layer. The relationship between the angle, opening width, stencil width, and second PDMS layer is analyzed and the results are filled in Table 3-1.

Table 3-1. Cross-sectional profile of patterned PDMS microchannels

Second-Layer Thickness (μm)		Stencil Design Width (μm)				
		500	400	300	200	100
24	Opening Width (μm)	510.22	411.49	316.32	213.09	92.3
	Angle (°)	0	0	0	0	0
75	Opening Width (μm)	512.23	409.23	318.96	212.60	95.87
	Angle (°)	0	0	0	0	0
165	Opening Width (μm)	541.19	431.69	342.63	250.79	199.60
	Angle (°)	24.16	25.80	24.67	26.60	34.97
302	Opening Width (μm)	630.25	510.41	428.28	366.59	263.78
	Angle (°)	26.54	30.12	32.11	36.88	43.88

To analyze the tearing angle of the cross-sectional profile, multiple thicknesses of second PDMS layer were tested. When the second PDMS layer was thinner than 75 μm, thus polymerization inhibition was present, the cutting angle was 0 degrees. The error in these results were too small and thus had no critical effect. As the thickness increase with thicker second PDMS layer, polymerization inhibition was not present and the cross-sectional shape of the microchannels showed an overcut profile. Analysis in Table 3-1 shows that the cutting angle was proportional to the thickness of the second PDMS layer and inversely proportional to the width of the stencil.

3.5. Three Dimensional Microchannel Fabrication

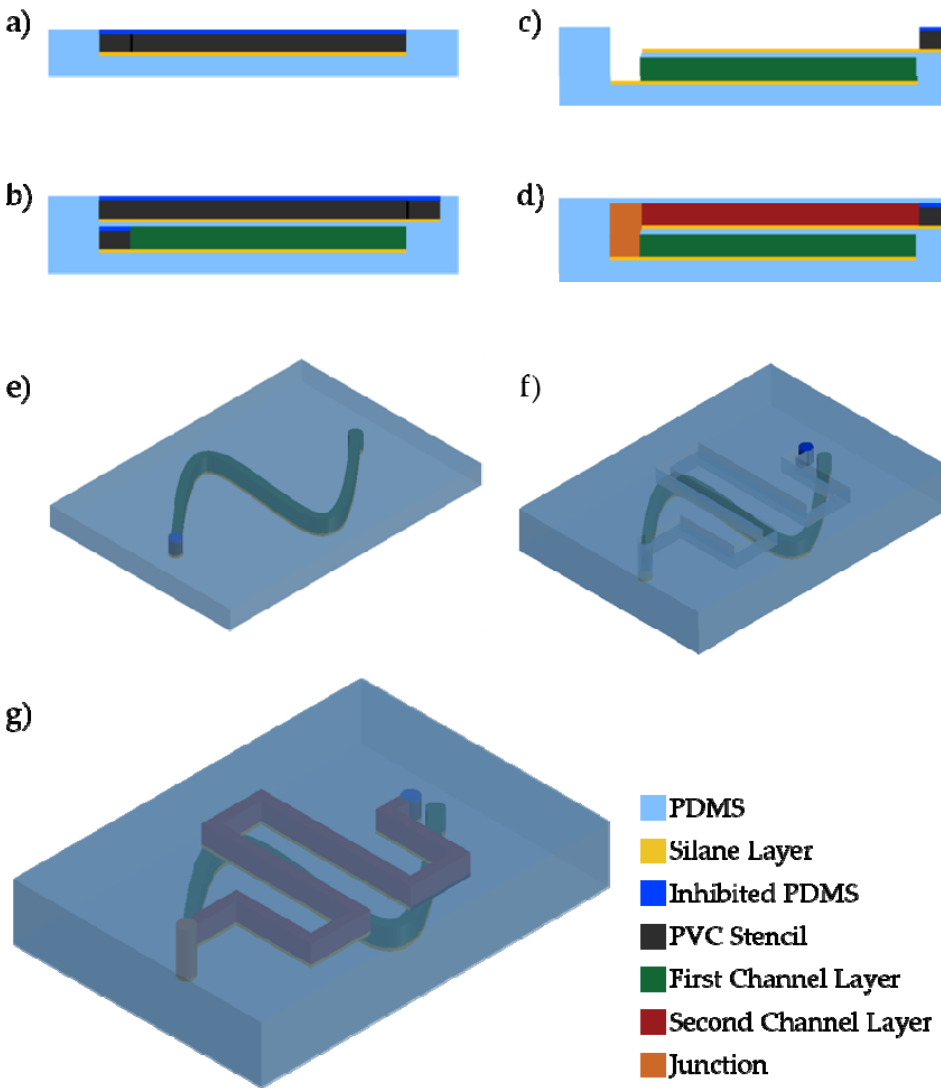

Figure 3-12. Three dimensional microchannel fabrication method.

With the PVC fabrication method, simple and fast fabrication of multilayer microchannel is feasible. Three dimensional microchannel devices are advantageous over the conventional two dimensional in improved observation efficiency, continuous three dimensional motion and integration of more functions. The simplest three dimensional microchannel fabrication method utilize the conventional two

dimensional fabrication method. Photolithography patterning is executed multiple times and bonded via oxygen plasma treatment. This oxygen plasma treatment is a permanent procedure. The essence of bonding to manufacture three dimensional microchannels is the alignment of the connecting junctions in multiple levels. However, plasma bonding is an irreversible procedure where misalignment of the bonding site results in complete failure that requires the procedure to start from step one.

The PVC stencil method can be repeated multiple times. Moreover, the fabrication method is reversible during the critical alignment process. Repeating the PDMS etching procedure with only a few specifications can easily produce PDMS three dimensional microchannels. When the PVC stencil is peeled off, the junction portion of the stencil is still intact. Then, this patterned surface in bonded onto a thin PDMS surface. Now, the second PVC stencil is pasted on top of this layer aligned with the first layer's junction portion of the stencil. Third PDMS layer is dispensed on this layer and stencil. This procedure can be repeated as many times as desired. Thus, developing layers of patterned PDMS microchannels aligning, and integrating can be realized rather easily. Figure 3-13 shows three dimensional PDMS microchannels with two layers. Figure 3-13a is an image of two layers of disconnected PDMS microchannels and Figure 3-13b is an image of two layer of PDMS microchannels connected through a junction. The channels are 150 μm wide and 250 μm deep. Figures 3-13c and d is a magnified image of the two layers of PDMS completely separated by a thin PDMS membrane.

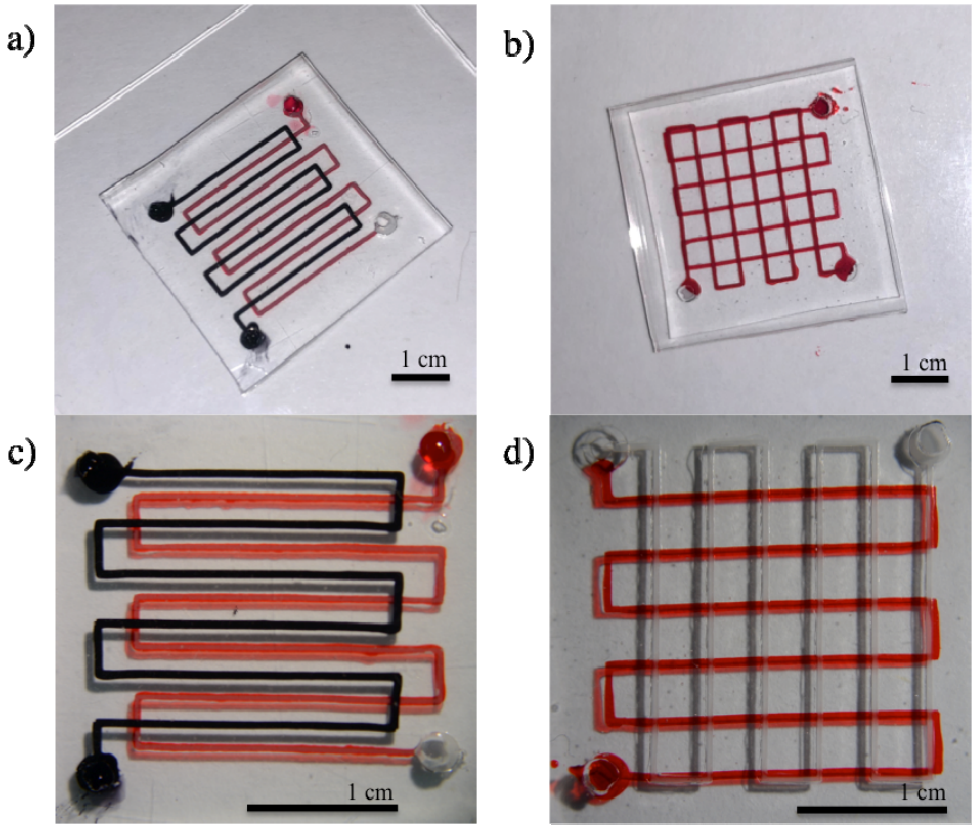

Figure 3-13. Three dimensional microchannels developed using the PVC fabrication method.

3.6. Circular Cross-sectional Microchannel

The selective bonding of PDMS surfaces allow easy fabrication of circular cross-sectional microchannels. The PVC stencil's width determines the diameter of the circular channels. The fabrication process is identical to the chamber fabrication procedure. The stencils are changed to have widths with desired diameter of the channels. Most importantly, only an inlet is required. After selective bonding is implemented, the channel is inflated by injecting olive oil. The substances injected into the channels should be carefully considered

because some substances can diffuse across the PDMS membrane. Substances such as water should not be selected because water will diffuse across the membrane and subsequently, the internal pressure of the channels will decrease. The circular shape of the channels cannot be controlled. Inflated, the inlet is sealed. Then this is then immersed in a PDMS bath and cured. After curing, the cross-sectional images were analyzed to verify the circular shape of the channels.

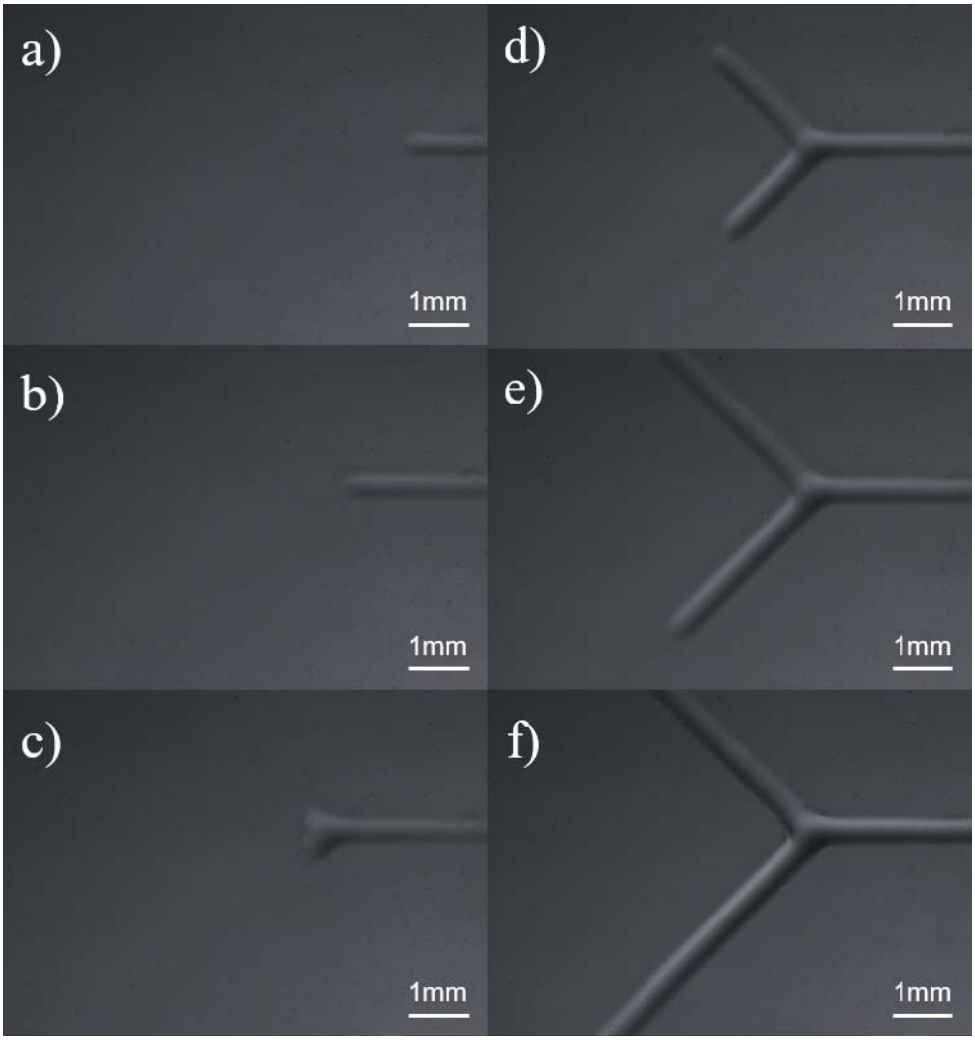

Figure 3-14. Channel inflated by injecting olive oil into the channels with

widths measuring approximately 500 μm.

Figure 3-14 show the inflated microchannels developed using a bifurcated PVC stencil. In Figure 3-14a the channel starts to inflate as the channels are injected with olive oil. Figure 3-15 are SEM images of the cross-sectional images of the circular microchannel. The channel's cross-sectional shape can be controlled by the internal pressure of the channels.

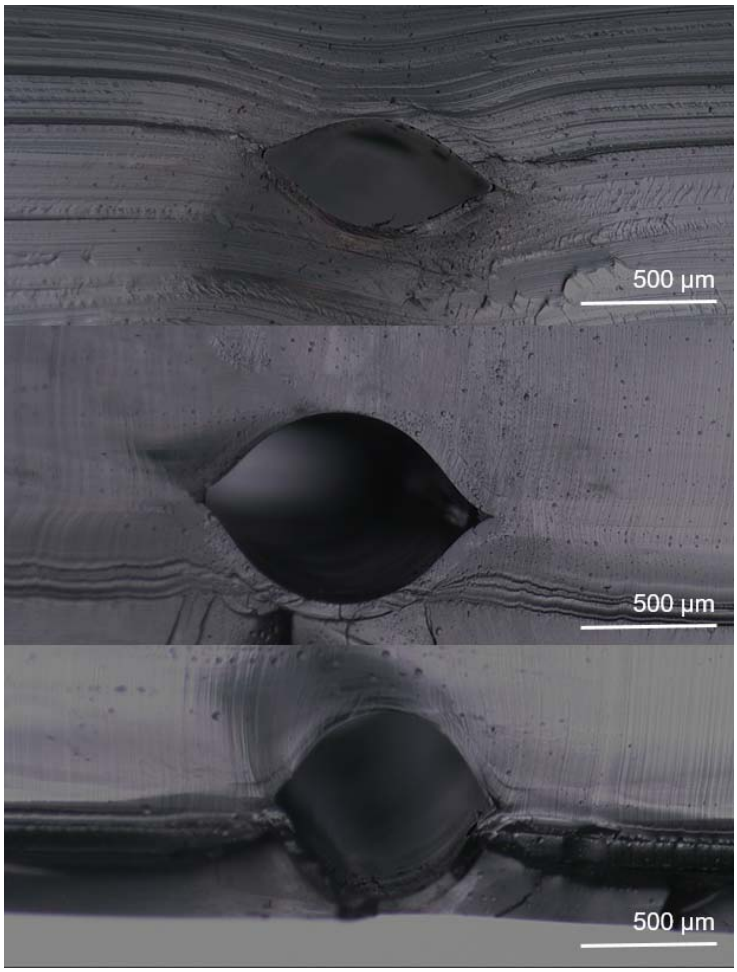

Figure 3-15. Cross-sectional image of circular microchannels.

3.7. Inflatable Chamber Fabrication

Circular inflatable chambers are fabricated using the method introduced in Figure 2-5. The stencils were designed to have an inlet, a circular shaped inflatable chamber, and a thin inflatable microchannel. A Teflon tube connected to a syringe is inserted into the inlet. As the syringe is pushed and DI water is injected, the microchannel inflates first. Substances travel into the chamber through the microchannel subsequently inflating the chamber. As the chamber inflates, the internal pressure continues to increase. Then, the tubing is released. There is no other mechanism that encloses the inlet than the design itself. The substances are bolted by the thin inflatable microchannel that connects the inlet to the chamber. Henceforth, called the bolting microchannel. The inflatable chamber, bolting microchannel and the inlet are all specified in Figure 3-16.

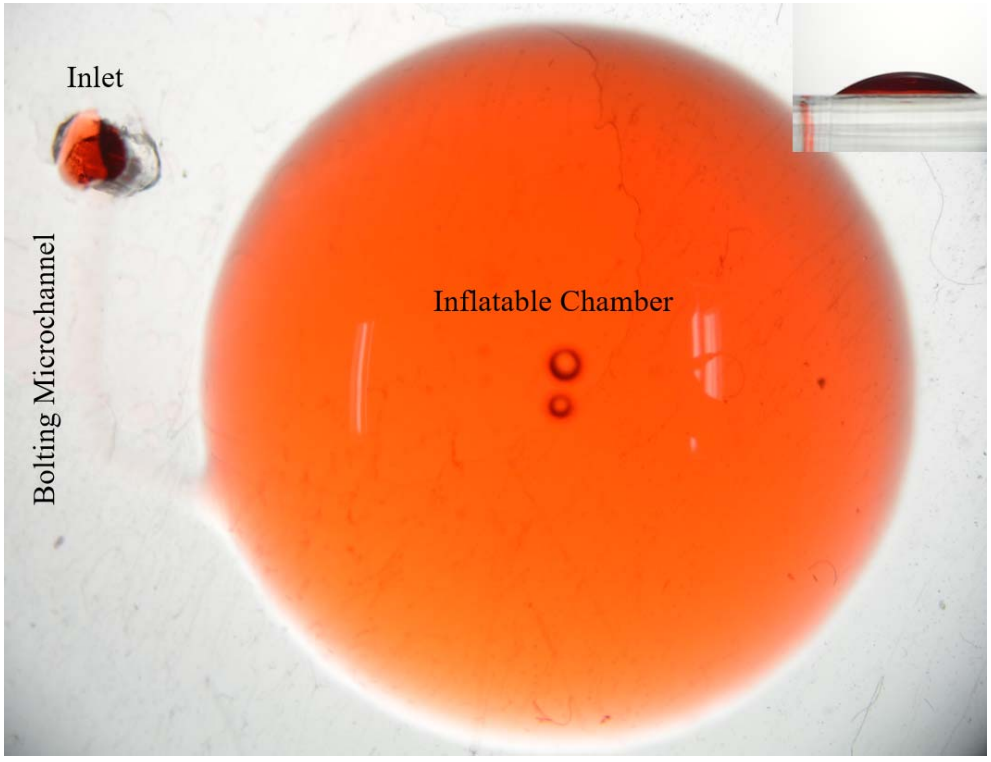

Figure 3-16. Inflated chamber, inlet, and bolting microchannel illustrated by injecting red-dyed DI water into the chamber.

In most cases, the inflated chamber does not produce enough power to inflate the microchannel. However, if the chamber contains too much substance, the inflated membrane can produce enough power to push substances out by inflating the bolting microchannel. Therefore, the maximum tolerable volume of the chamber was measured after the leakage of substances out of the chamber through the inlet completely stopped. In this section, the maximum volume tolerable by the chamber was investigated in relation to the chamber's radius, chamber's membrane thickness, and the bolting microchannel's width and thickness. Here, the chamber and the bolting microchannel's membranes have the

same thickness. Circular stencils with 4 to 8 mm radiuses were used to test the maximum tolerable volume.

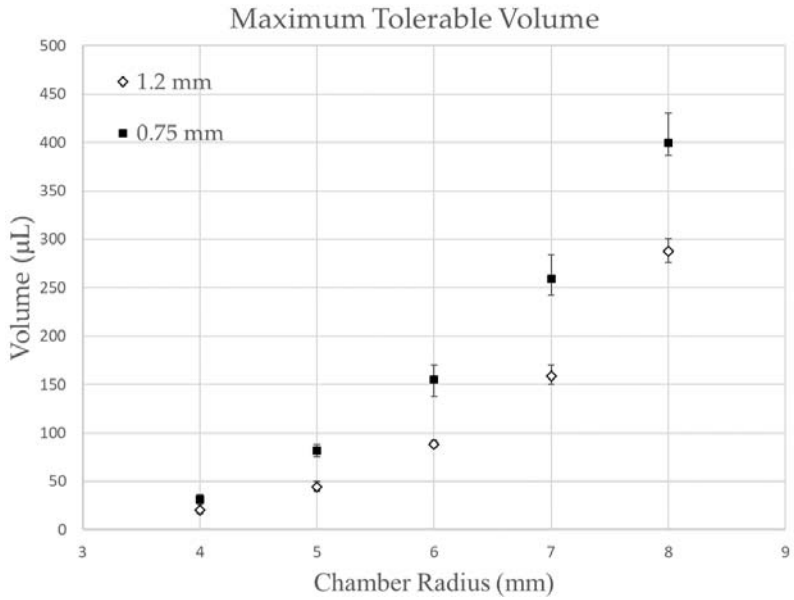

Figure 3-17. Maximum tolerable volume of the circular chamber with respect to the radius of the chamber and the width of the bolting microchannel.

3.8. Conductive PDMS Fabrication

Conductive PDMS fabrication is necessary for the electromagnetic actuation to be feasible. However, conductive coil on flexible materials such as PDMS are lacks durability. Therefore, a mixture of PDMS and silver micro particles were used. Here, a PDMS to silver microparticles in weight ratio of 1:2, 1:3, 1:4, 1:5 were tested to analyze the resistance and the conductivity this PDMS silver composite can produce. With this

composite, a circular shape coil that can produce electromagnetic fields were used to actuate the valve.

Table 3-2. Conductivity and resistivity of metals.

Metal	Conductivity (S/m) at 20°C	Resistivity (Ω·m) at 20°C
Silver	6.30×10^{7}	1.59×10^{-8}
Copper	5.96×10^{7}	1.68×10^{-8}
Gold	4.10×10^{7}	2.44×10^{-8}
Aluminum	3.77×10^{7}	2.65×10^{-8}
Nickel	1.43×10^{7}	6.99×10^{-8}
Iron	1.00×10^{7}	9.7×10^{-8}

Silver microparticles were used for the fabrication of flexible conductive lines that produce magnetic fields to actuated the valve for their high conductivity. Table 3-2 shows metals and their corresponding conductivity and resistivity. Silver has a conductivity of 6.30×10^{7}. The conductive lines that produce magnetic field lines need to have resistances as low as possible to minimize power consumption. Moreover, the metal particles have to be mixed with PDMS, an insulating polymer with a very low conductivity of 2.50×10^{-14}. Therefore, silver microparticles are most adequate for the application. Silver, like many other metal particles, is toxic to the human body. Since PDMS is biocompatible with only mild inflammation while implanted in the body and more importantly, the conductive coil is only used to produce magnetic field, total encapsulation of the conductive lines is critical.

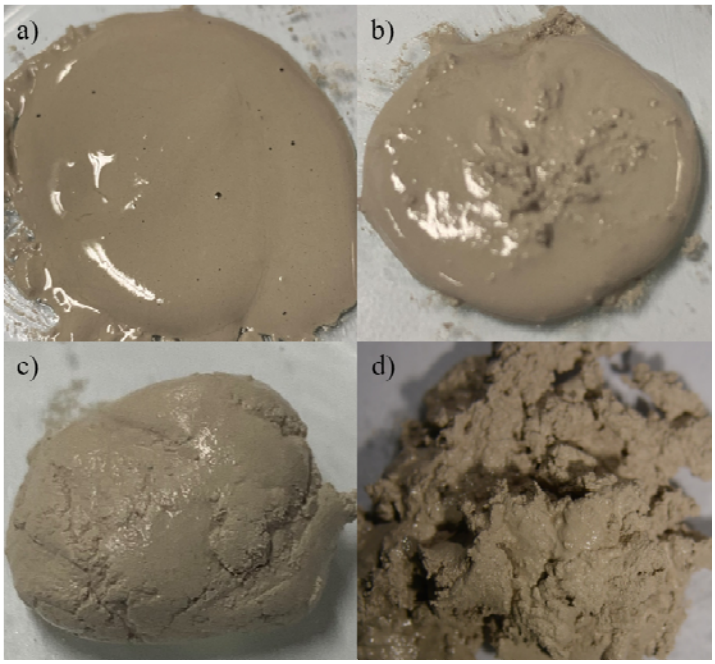

Figure 3-18. Silver microparticles mixed with PDMS with a weight ratio of a) 2:1, b) 3:1, c) 4:1, d) 5:1

Silver microparticles were mixed with PDMS with a weight ratio of 1:2, 1:3, 1:4, and 1:5. Figure 3-18 shows the results of these mixtures with different ratios. For mixtures with 1:2 and 1:3 ratios, the mixture sustains a rather viscous fluid state where patterning conductive lines via microgrooves is still possible. However, the mixture with less silver microparticles have low conductivity and mixing reliability. As the silver microparticles increase in ratio to 1:4 and 1:5, the mixture becomes more and more slurry. To the point, the mixture becomes too lumpy and cannot be used in the patterning process. So, the mixture was mixed with 99.8% ethanol sufficiently to increase the viscosity of the mixture. The mixture was left for the ethanol to evaporate in case it was mixed too much. This

mixture then can be used for the patterning process. For mixtures with higher silver concentration than 1:5, PDMS merely act as a glue that holds the particles together. Therefore, the mixture has high conductivity and the mixing reliability is relatively high, too. To test the conductivity of the mixture, PVC stencils with 1.5 cm in length and 1 mm in width were used to develop PDMS microchannels with equal dimensions and 150 µm deep. 15 to 20 samples were prepared and the average and deviation results were also calculated to show the reliability of its usage. Figure 3-19 shows the a) resistance of each strip of silver-PDMS and b) conductivity calculated from the resistance and the dimensions of the conductive PDMS.

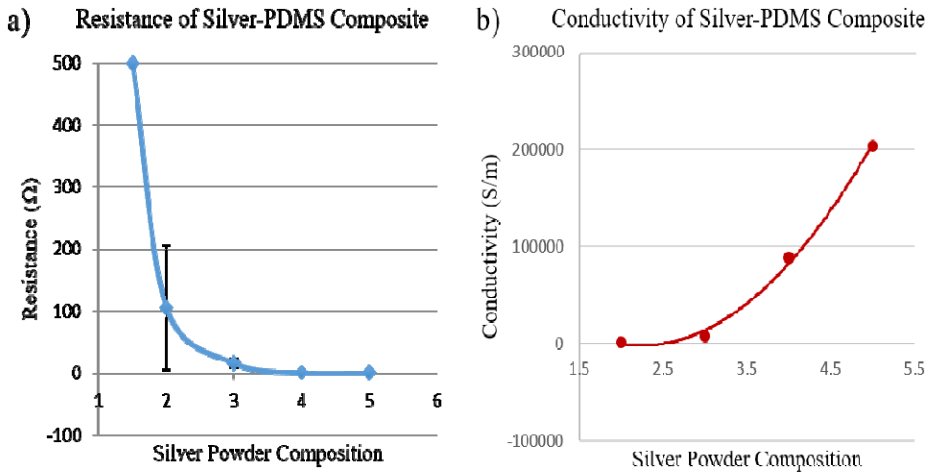

Figure 3-19. a) Resistance of the silver-PDMS conductive lines. b) conductivity of the conductive lines calculated from the resistances.

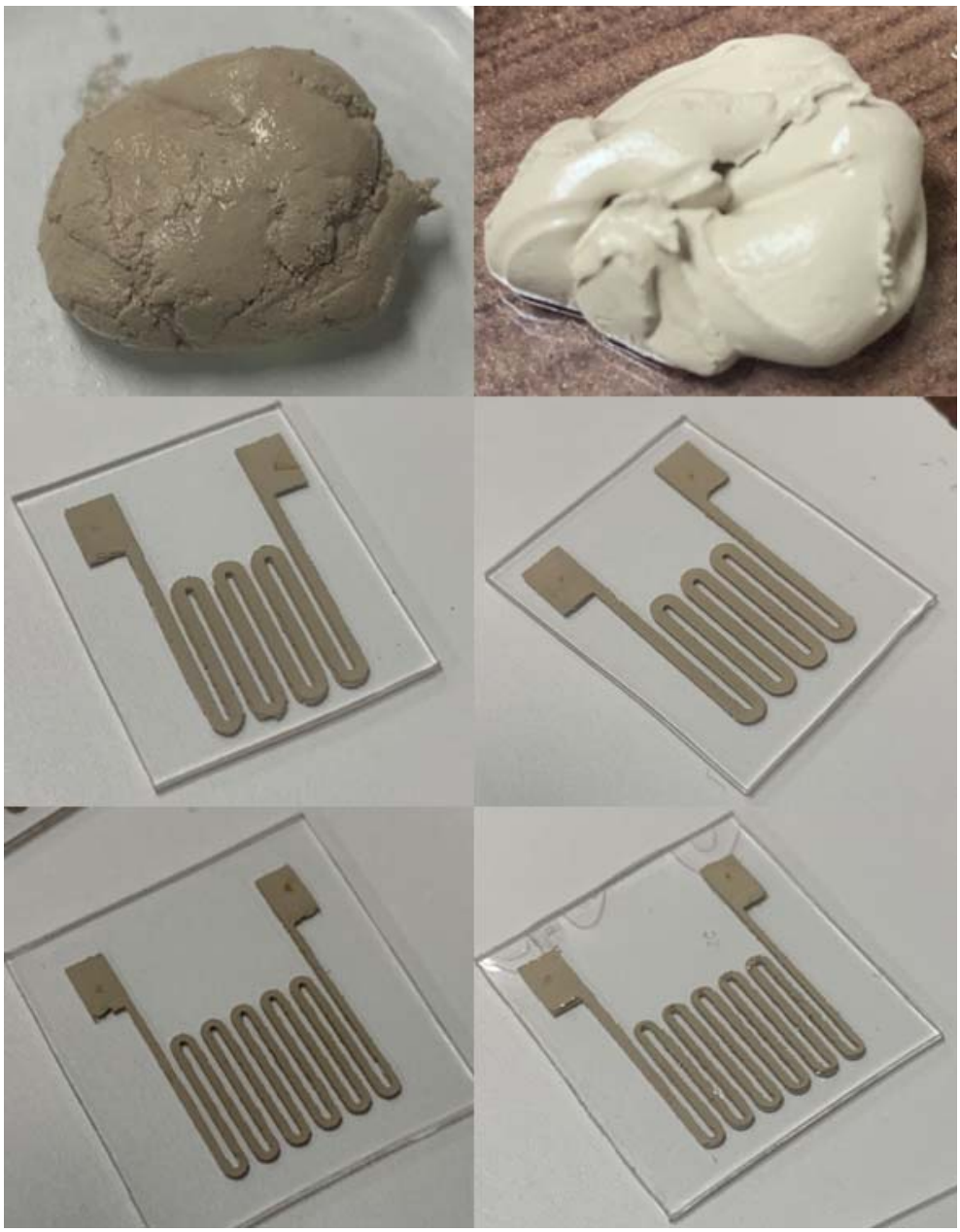

Figure 3-20. Conductive and flexible PDMS fabricated using the proposed fabrication method.

3.9. Drug Delivery Device

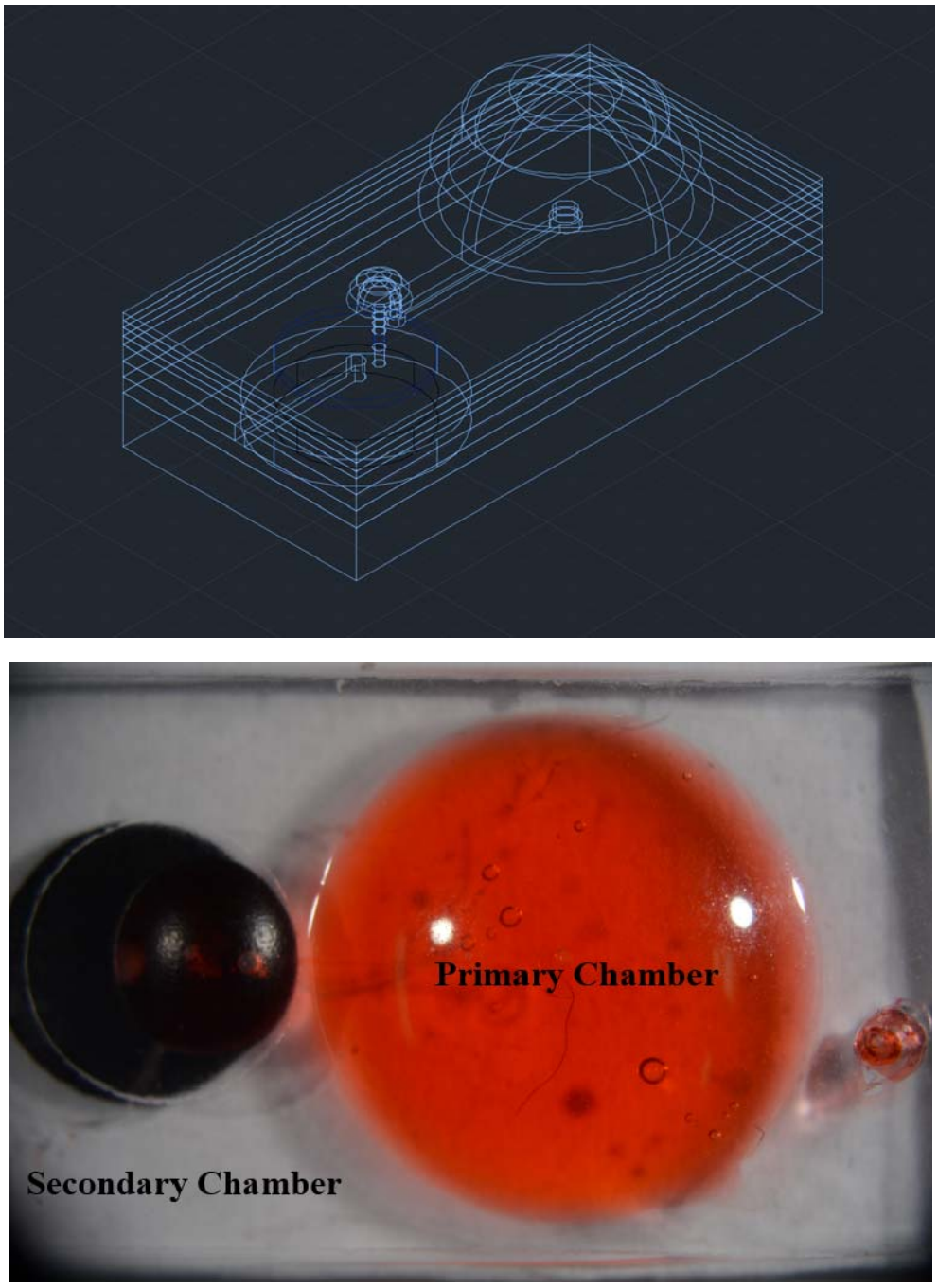

Figure 3-21. Drug Delivery Device

3.9.1. Dimensions and Profile of the Drug Delivery Device

The proposed drug delivery device has a surface area of 3.0 cm by 1.5cm. The overall thickness of the device varied depending on their primary and secondary pump's thickness. The device's overall thickness had to be Three different combinations of primary and secondary pump's membrane thicknesses were tested to find the amount of fluid delivered each time the device was actuated. DI water was chosen to find the released amount at each actuation. DI water was chosen because the main purpose of this drug delivery device was to deliver corticosteroids such as dexamethasone, triamcinolone, prednisolone etc. The actuation was executed using an external magnet. Each actuation lasted for one second.

3.9.2. Fluid Release Amount of the Device

3.9.2.1. Case 1

Table 3-3. Device Dimensions Case 1

	Dimensions
Primary Chamber Radius Thickness	7mm 325 μm
Secondary Chamber Radius Thickness	2 mm 100 μm
Microchannel Length	1 cm

Cross-Sectional Area	100 µm by 95 µm
Bolting Microchannel	750 µm
Initial Volume	220 µL

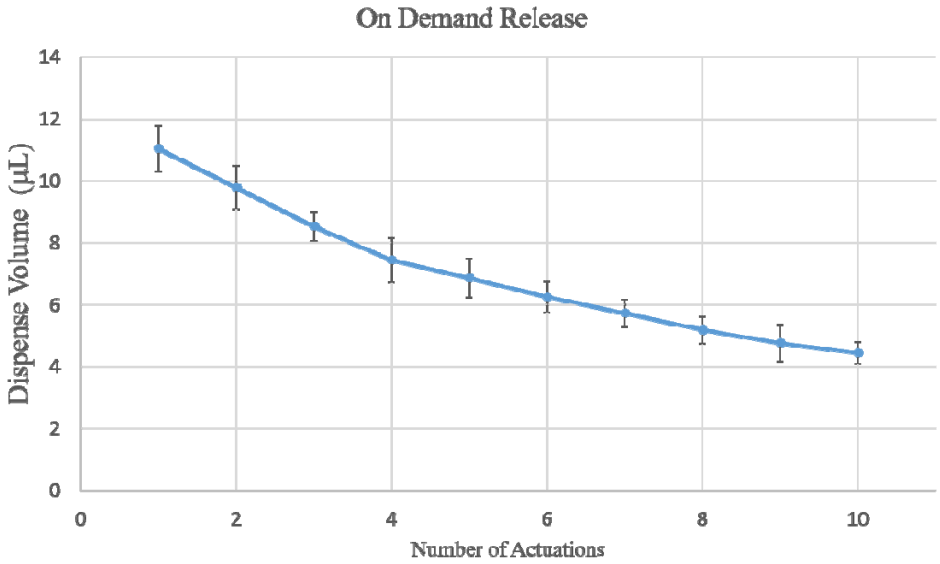

Figure 3-22. DI water delivery at each actuation.

3.9.2.2. Case 2

Table 3-4. Device Dimensions Case 2.

	Dimensions
Primary Chamber Radius Thickness	7mm 325 µm
Secondary Chamber Radius Thickness	2 mm 75 µm
Microchannel Length	1 cm

Cross-Sectional Area	100 µm by 95 µm
Bolting Microchannel	750 µm
Initial Volume	220 µL

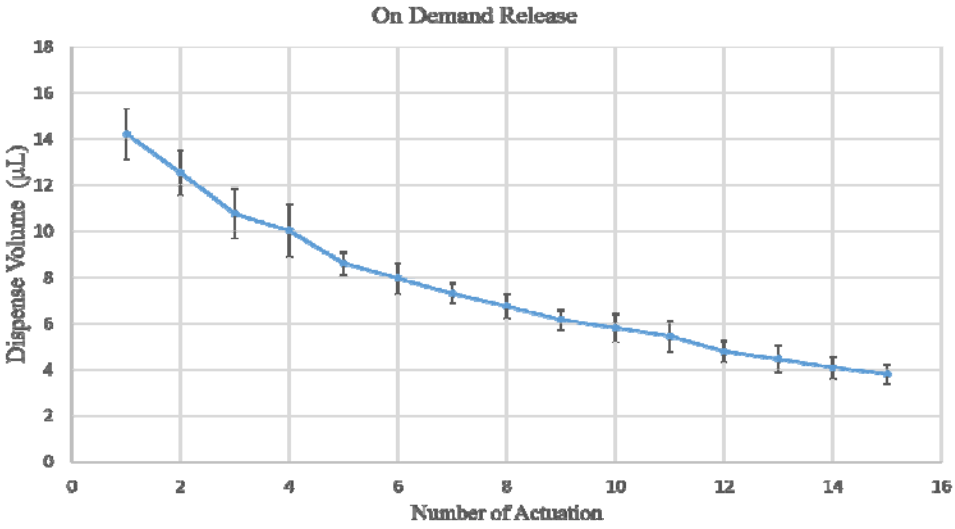

Figure 3-23. DI water delivery at each actuation.

3.9.2.3. Case 3

Table 3-5. Device Dimensions Case 3.

	Dimensions
Primary Chamber Radius Thickness	7mm 250 µm
Secondary Chamber Radius Thickness	2 mm 100 µm
Microchannel Length Cross-Sectional Area	1 cm 100 µm by 95 µm

Bolting Microchannel	750 μm
Initial Volume	270 μL

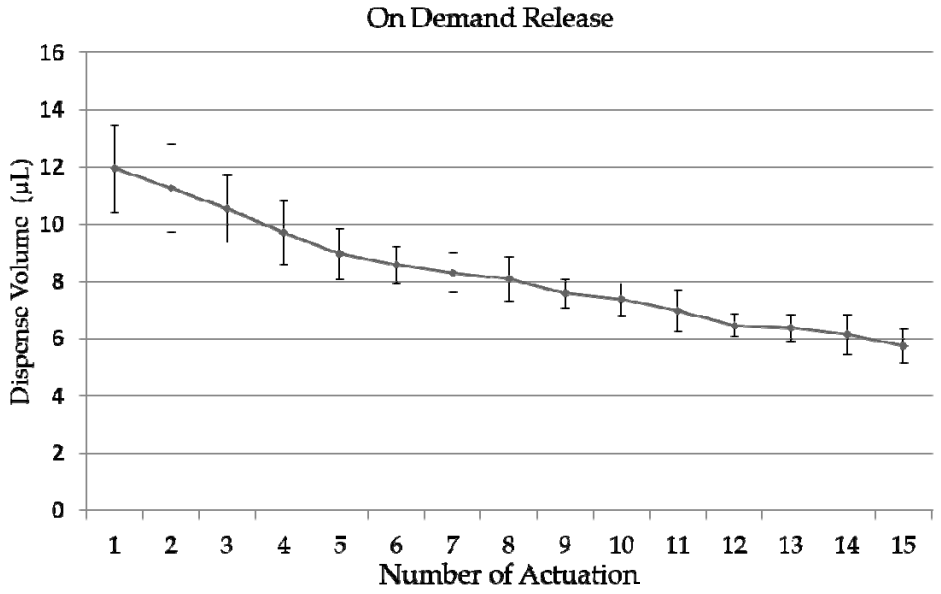

Figure 3-24. DI water delivery at each actuation.

Three cases in section 3.9.2 shows the DI water released amount from the device with different combination of primary and secondary chamber dimensions. Each case was repeated 10 to 15 times where the error bars show the standard deviation values of the dispense rate.

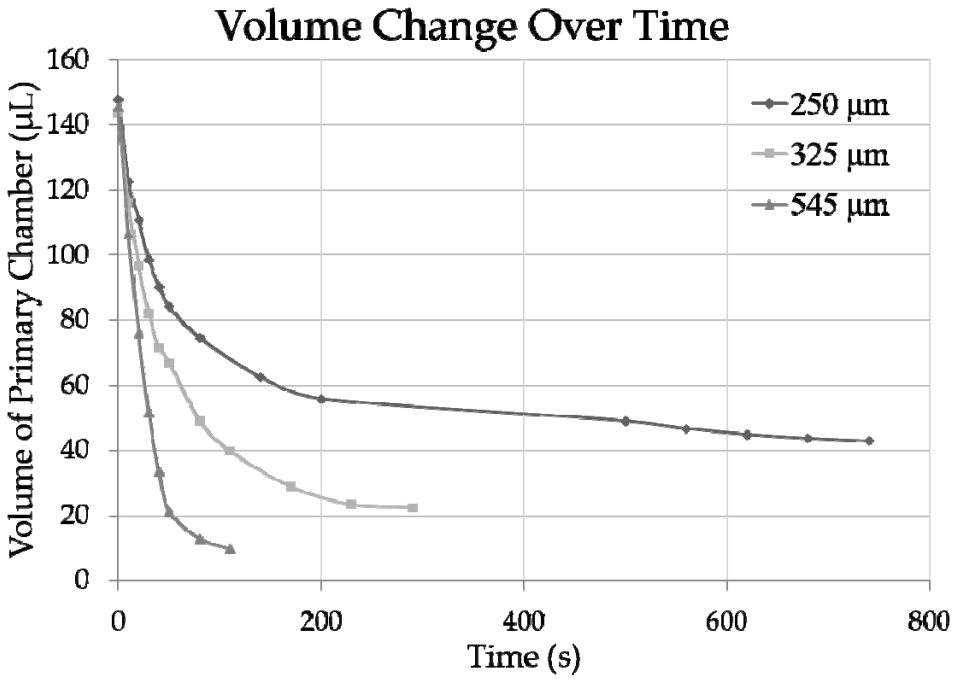

Figure 3-25. Volume change over time when the device only one chamber.

Figure 3-25. shows the volume change of a device with only one chamber over time. Three different dimensions were tested. The chamber had a radius of 7 mm and a bolting microchannel of 750 µm. The thickness of the chambers were 250 µm, 325 µm, and 545 µm. Each chamber was injected with approximately 150 µL of DI water. Similar to many other drug delivery devices, the chamber rapidly pumps out fluids when it is relatively full. As the chamber loses its volume and the internal pressure of the chamber decrease, the chamber quickly saturates reaching zero dispense rate.

Three cases in section 3.9.2 show a relatively controlled dispense amount with equal actuation. It is apparent that the decrease in delivery

amount is inevitable. The released amount of the first and third case reduced to approximately half of the first amount after 10 and 15 actuations. In case of the second, the released amount reached approximately one third after 15 actuations. Since the device is an active control delivery device, this discrepancy can be easily solved by decreasing the release interval

3.10. *In Vitro* Cytotoxicity of the Device

This proposed drug delivery device uses PDMS mainly. However, the use of metal particles such as nickel and silver and the use of neodymium magnet raises questions whether the device is in fact biocompatible when implanted in the body. So, the fabricated device was tested for cytotoxicity with the “ISO 10933-5:2009(E), Part 5: Tests for in vitro cytotoxicity –Annex C: MTT cytotoxicity test” standards. Prior to elution the device was placed in a solution of 70% ethanol and sonicated to wash off dust and other residue. The test was evaluated both qualitatively and quantitatively. Elution was executed using 20 mL of Minimum Essential Medium (MEM) (GIBCO BRL, Cat. No. 11095-080, Lot No. 1858767) solution per 4g of the device. The device was placed in the solution for 24 hours in 37 °C. NCTC clone 929 (L-929) (Korean Cell Line Bank) cell line was used to evaluate the cytotoxicity. The L-929 is the connective tissue from 100 days old male mouse; Mus musculus (C3H/An). This specific cell line was selected because of its sensitivity towards chemical compounds. Moreover, this cell line had

been used extensively in many cytotoxicity experiments. Thus, comparison between the results can be easily realized.

The extract from the elution process was used on the cell line for 24 to 48 hours. The qualitative evaluation was obtained by how much the extract hindered the growth of the cells. The qualitative evaluation of the devices showed a cytotoxicity score of '0'. A cytotoxicity score of 0 proves that the device has no reactivity on the tested cell line. Microtitration test was used to evaluated the device quantitatively. The quantitative evaluation also showed no cytotoxic elements in the device.

Table 3-6. Qualitative cytotoxic evaluation of the drug delivery device

Group	Time	Test Item	Concentration (% (v/v), in media)	Cytotoxicity Score	
				24 hours	48 hours
Media Control	24, 48	MEM	100% Extracts	0	0
Negative Control	24, 48	HDPE	100% Extracts	0	0
Treatment	24, 48	Drug Delivery Device	100% Extracts	0	0
			75% Extracts	0	0
			50% Extracts	0	0
			25% Extracts	0	0
			12.5 Extracts	0	0
Positive Control	24, 48	0.25% ZDBC	100% Extracts	4	4
			50% Extracts	3	3

Table 3-6 shows the qualitative evaluation of the drug delivery device. MEM, High Density Polyethylene (HDPE) for negative control, and 0.25% zinc dibuthyldithiocarbamate (ZDBC) for positive control were also tested at the same time to ensure the evaluation process is valid.

Negative control showed a cytotoxicity score of 0 while positive control showed 3 to 4. The extracts from the drug delivery device were diluted from 100% to 75%, 50%, 25%, and 12.5% consecutively. All diluted extract and the original extract showed a cytotoxicity score of 0. This proves that the device displays no toxic effects.

Table 3-7 shows the quantitative evaluation of the drug delivery device. The process was executed similarly to the qualitative evaluation. Similarly, negative control showed a 75.67% of survival rate while positive control showed 11.97% and 32.50% for 100% and 50% extracts. This value validates the results of the drug delivery device's extracts. Original extract and all four diluted extracts, 75%, 50%, 25%, 12.5% showed a high cell survival rate of 95.40%, 96.46%, 101.60%, 100.17%, and 103.67% correspondingly. This proves qualitatively that the device is nontoxic.

Table 3-7. Quantitative cytotoxic evaluation of the drug delivery device.

Group	Time	Test Item	Concentration (% (v/v), in media)	Absorbance (Mean±SD)	Survival Rate (%)
Media Control	24	MEM	100% Extracts	5.93 ± 0.016	100.00
Negative Control	24	HDPE	100% Extracts	0.449 ± 0.027	75.67
Treatment	24	Drug Delivery Device	100% Extracts	0.566 ± 0.012	95.40
			75% Extracts	0.572 ± 0.016	96.46
			50% Extracts	0.603 ± 0.008	101.60
			25% Extracts	0.594 ±	100.17

				0.005	
			12.5 Extracts	0.615 ± 0.017	103.67
Positive Control	24	0.25% ZDBC	100% Extracts	0.071 ± 0.014	11.97
			50% Extracts	0.193 ± 0.017	32.50

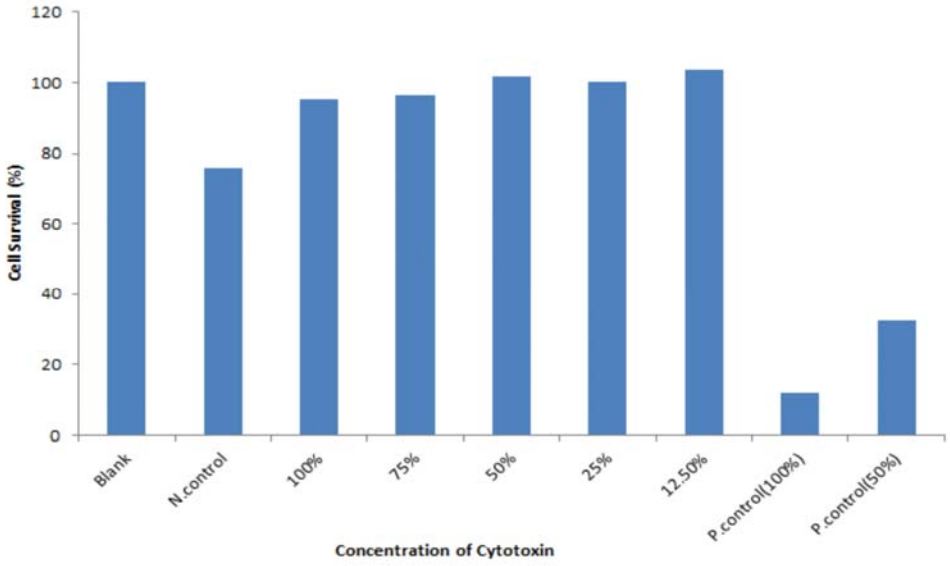

Figure 3-26. Cell Viability of L-929 fibroblasts according to the concentrations of the extracts.

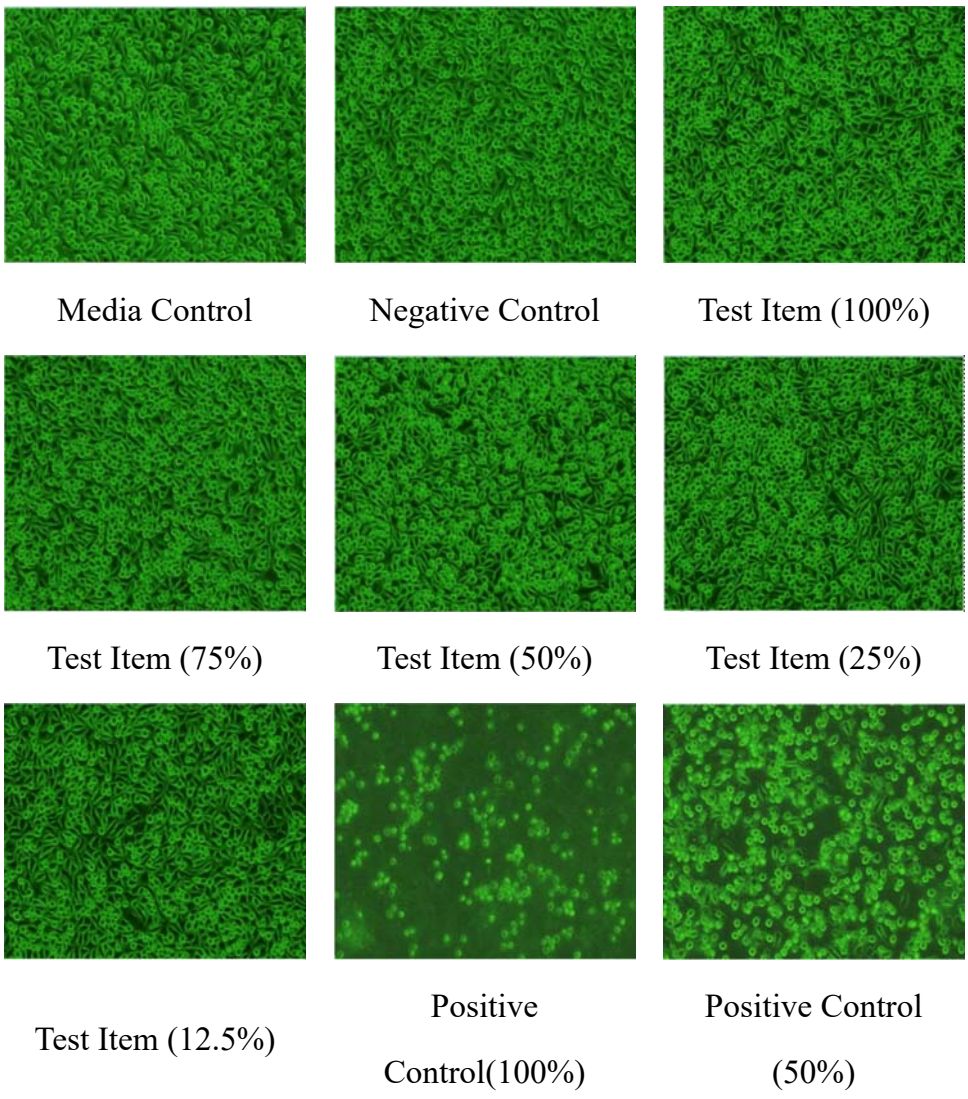

Figure 3- 27. Cell morphology 24 hours after treatment.

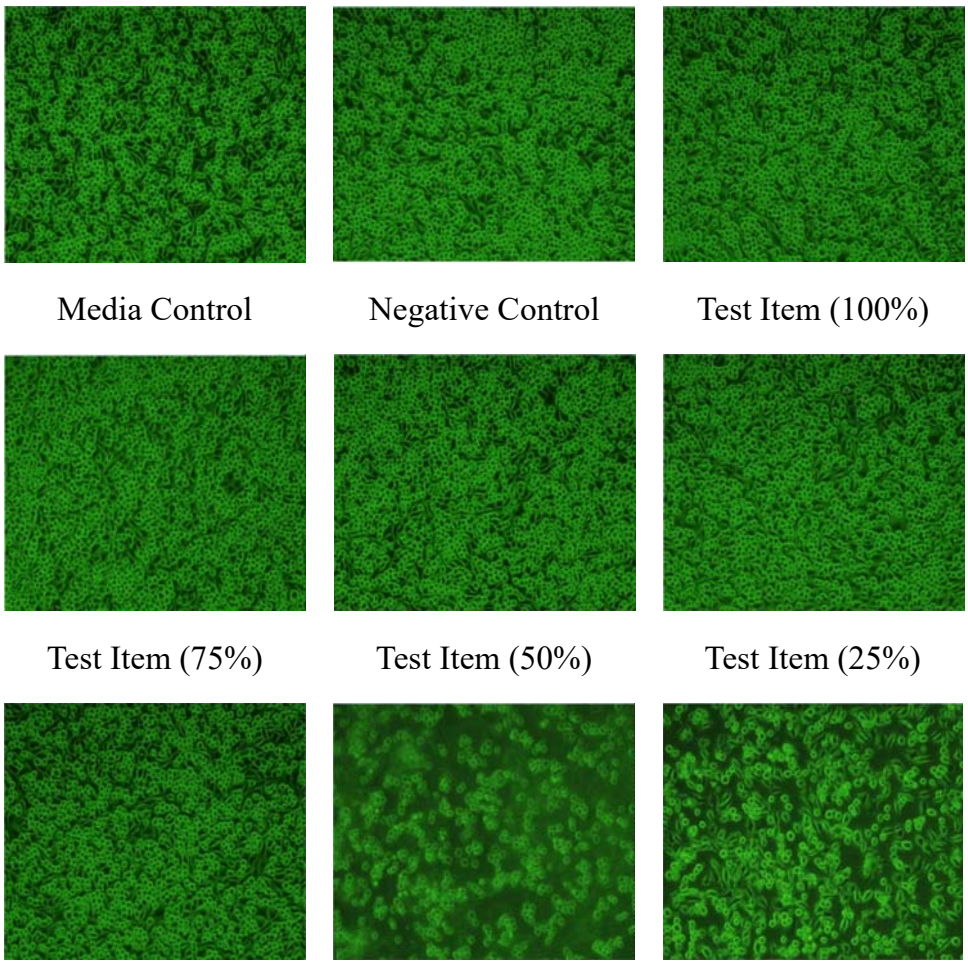

Figure 3-28. Cell morphology 48 hours after treatment.

4. Discussion and Future Work

4.1. Electromagnetic Actuation of the Device

Electromagnetic actuation of the drug delivery device begins with calculating the magnetic field induced by the coil that deflects the valve membrane consequently opening the valve. From Biot-Savart Law, the equation of the magnetic field produced by the circular conductive coil with a radius of r, that carries a current I is:

$$\vec{B} = \frac{\mu_0}{4\pi}\int \frac{I}{r^2} d\vec{l} \times \hat{r} \quad \text{.....(1)}$$

Due to the symmetry of the current produced by the coil, the y component of B is negated. Thus, only x component of the field is present. Therefore, equation (1) can be simplified to:

$$dB_x = \frac{\mu_0}{4\pi}\frac{I}{x^2 + a^2} dl \cos\theta \quad \text{.....(2)}$$

Here,

$$\cos\theta = \frac{a}{r} = \frac{a}{\sqrt{x^2 + a^2}}$$

Hence, equation (2) becomes,

$$B_x = \frac{\mu_0 Ia}{4\pi(x^2 + z^2)^{\frac{3}{2}}}\int_0^{2\pi a} dl = \frac{\mu_0 Ia^2}{2(x^2 + a^2)^{\frac{3}{2}}}$$

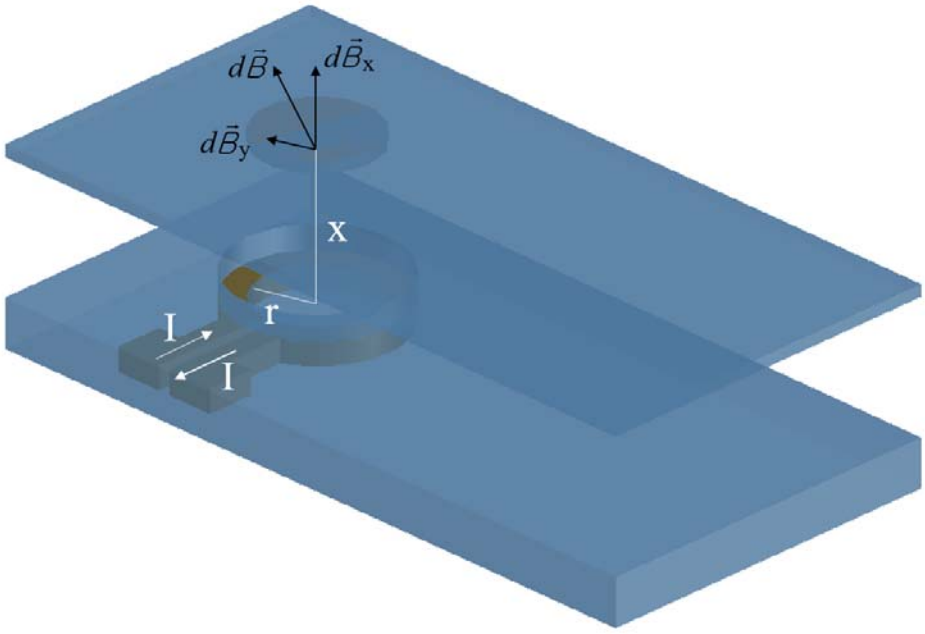

Figure 4-1. Schematic of electromagnetic actuation.

Figure 4-1 show the schematic of the electromagnetic actuation. For visualization purposes, the deflecting membrane is separated from the coil. However, the real device has the two bonded together.

The drawback of this electromagnetic coil and electromagnetic actuation of the device is its durability. To achieve full flexibility, the conductive coil was developed only with PDMS and silver microparticles. 1:4 mixing ratio was selected to be the adequate composition for the electromagnetic coil. However, the conductive coil has very weak durability. The conductive coil had 2 to 4 Ω resistance depending on the thickness and width and size of the designed coil. In this case, even 2 to 4 V of voltage applied to this coil will produce current with 1 to 2 Amperes. As the current flows over 1.5A, the coil starts to burn and the coil's

resistance increase. Consequently, more voltage is required to drive the coil's electromagnetic actuation.

4.2. Drug Delivery Content

The drug delivery device was designed to release corticosteroid drugs, such as dexamethasone, triamcinolone, and prednisolone. Corticosteroids are used to treat many diseases such as allergic disorder, blood disease, certain cancers, eye diseases, dermatologic disease, breathing problems etc. However, to treat these diseases, corticosteroids are injected through a syringe or by oral gavage. These administration methods treat the disease systemically where long-term side effects are inevitable. Some of the long-term side effects are decreased bone density, gastrointestinal bleeding, increased risk of heart disease, thin skin, bruise easily, and slower healing of wounds etc. When these drugs are administered using intravenous methods, 2~8 mg of corticosteroid drugs are necessary every 3 to 6 hours for the concentration to be in the therapeutic range. However, when they are administered locally to specific parts of the body for direct release, only 0.05~0.1 mg every two weeks for percutaneous, 0.8 ~ 5mg every 2 weeks for articular, and 0.8~2.5mg every two weeks for tendon are needed. Fortunately, these drugs are soluble either in, ethanol, dimethyl sulfoxide (DMSO), or water. The reason to why the release amount was tested by DI water is because of these characteristics. DMSO is still in debate on whether the solvent can hard specific parts of the body. The drug content in grams can be calculated from the delivered volume of the substance.

4.3. Comparison with Similar Drug Delivery Devices

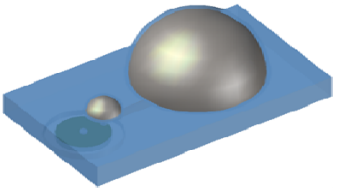

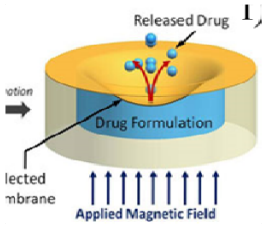

Pirmoradi et al. 2011

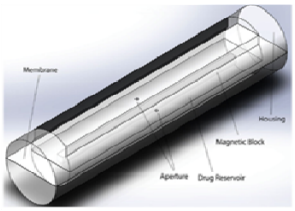

W.J. Sturss et al. 2017

Size	15 mm by 30 mm, 3~4 mm thick	6mm radius, 1 mm thick	2.6mm radius, 12 mm in length
Actuation	External Magnetic Source	External Magnetic Source	External Magnetic Source
Materials	PDMS, Neodymium Magnet, Nickel power	PDMS, Iron oxide powder, Magnet	PDMS, Neodymium magnet,
Reservoir Size	<250 μL	15.7 μL	800 μg
Release	<15μL/s	2.1~3.2 μL	3 μg/h
Reusable	Yes	No	Yes

Figure 4-2. Comparison with other magnetically actuated drug delivery devices.

Figure 4-2 are comparison of three devices with similar actuation mechanisms. All three devices utilize an external magnetic field using a permanent magnet. The fabricated devices use PDMS as their main material and utilize mixture of magnetic particles either as an actuation membrane or a valve component. However, the mechanisms of the devices are rather different. Pirmoradi et al. [115] and W.J. Struss et al. [116] use the magnetic membrane to squeeze the drug reservoir filled with drug substances whereas the proposed device in this thesis uses the magnetic actuation to open the tightly sealed valve. The two previous

devices' actuation deflects a magnetically excitable membrane to push out substances. However, the proposed device merely relieves the pressure contained by the inflated chamber. It is inevitable that all the devices' drug release amounts will decrease as the actuation numbers increase consequently emptying the chamber. However, the two previous devices would require stronger actuation mechanism as the drug reservoir empties.

The proposed drug delivery device could handle 250 μL of liquid substances without leakage happening through either the inlet or the outlet of the device. Moreover, the device can be reused by simply injecting the chamber with more substances using a syringe.

Figure 4-3 is a comparison of the proposed device with other relatively recently developed active control drug delivery devices. All three devices have different actuation mechanisms: magnetic, electrolysis, and thermal. The devices share a concept of an external stimuli triggering the release of drug substances from the chamber. However, while magnetically actuated device has fast response time, the other devices need a few tens of seconds for the release of substance to begin. Again the proposed device can be reused while some are disposable.

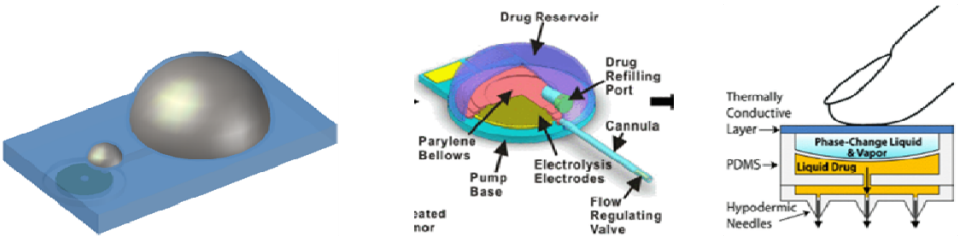

E.Meng et al. 2012 C. Mousoulis et al. 2012

Size	15 mm by 30 mm, 3~4 mm thick	18mm in radius, 3.5mm thick	14 mm by 14mm, 8mm depth
Actuation	External Magnetic Source	Electrolysis (slow response)	Skin contact
Materials	PDMS, Neodymium Magnet, Nickel power	Parylene, epoxy, Pt electrodes, PEEK substrate (rigid)	PDMS, Thermally conductive layer, Phase change liquid
Reservoir Size	<250 μL	560 μL	250 μL
Release	<15μL/s	<7 μL/min	28.8 μL/min
Reusable	Yes	Yes	No

Figure 4-3. Comparison with other active drug delivery device.

4.4. Integration with PDMS Electrodes

This drug delivery device has another advantage. This device is fully made with only PDMS and a mixture of PDMS and metal particle composite. For this reason, integration with PDMS based electrodes can be easily achieved. PDMS based implantable neural electrodes and drug delivery system's integration is important since inflammation reduction is a crucial factor to increase the duration of the electrodes. PDMS based neural electrodes can be implanted in the body on neural tissues for recording and stimulating neural activity. As the use of the electrode's duration increase to days, weeks or months, gliosis may occur. Gliosis is a reactive change of glial cells in response to the damage to the central

nervous system. When not treated, gliosis can form glial scar. Even with PDMS electrodes, when chronically implanted, gliosis can occur within weeks after installation. Usually, neural recording and stimulating electrodes have a fixed impedance. This impedance value is crucial for the signal from the electrodes to be consistent over a long period of time. When gliosis occurs on the contact areas the impedance of the electrode to tissue increase and the signal extracted from the electrode will be different. Integration with drug delivery devices can be a solution. Many researches are in progress where synthetic steroids such as tibolone can suppress the growth of gliosis and scar tissue [136]. Tibolone can be soluble in dimethyl sulfoxide (DMSO) with 15mg/mL. Therefore, liquid substance delivery can also be possible.

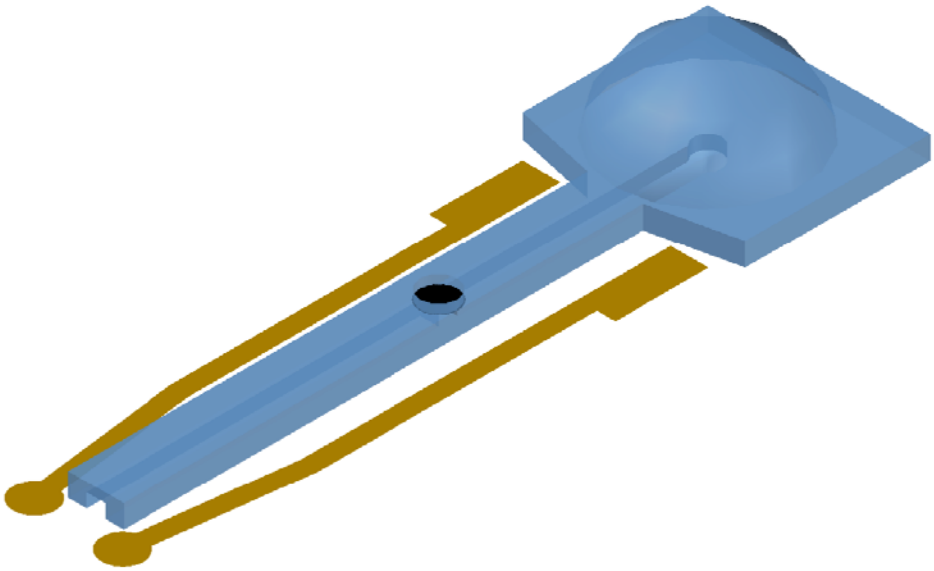

Figure 4-4. Diagram of electrode and drug delivery device integration.

Reference

[1]. Erickson, D., & Li, D. (2004). Integrated microfluidic devices. *Analytica chimica acta*, 507(1), 11-26.

[2]. Sato, K., Hibara, A., Tokeshi, M., Hisamoto, H., & Kitamori, T. (2003). Microchip-based chemical and biochemical analysis systems. *Advanced Drug Delivery Reviews*, *55*(3), 379-391.

[3]. Simpson, P. C., Roach, D., Woolley, A. T., Thorsen, T., Johnston, R., Sensabaugh, G. F., & Mathies, R. A. (1998). High-throughput genetic analysis using microfabricated 96-sample capillary array electrophoresis microplates. *Proceedings of the National Academy of Sciences*, *95*(5), 2256-2261.

[4]. Liu, Y., Ganser, D., Schneider, A., Liu, R., Grodzinski, P., & Kroutchinina, N. (2001). Microfabricated polycarbonate CE devices for DNA analysis. *Analytical Chemistry*, *73*(17), 4196-4201.

[5]. Lee, S. J., & Lee, S. Y. (2004). Micro total analysis system (μ-TAS) in biotechnology. *Applied microbiology and biotechnology*, *64*(3), 289-299.

[6]. Toriello, N. M., Liu, C. N., & Mathies, R. A. (2006). Multichannel reverse transcription-polymerase chain reaction microdevice for rapid gene expression and biomarker analysis. *Analytical chemistry*, *78*(23), 7997-8003.

[7]. Chen, X., Cui, D. F., Wang, L., Wang, M., & Zhao, Q. (2002). Development and characterization of DNA hybridization reaction on

PDMS microchip. *International Journal of Nonlinear Sciences and Numerical Simulation*, *3*(3-4), 211-214.

[8]. Kim, S., Chen, L., Lee, S., Seong, G. H., Choo, J., Lee, E. K., ... & Lee, S. (2007). Rapid DNA hybridization analysis using a PDMS microfluidic sensor and a molecular beacon. *Analytical sciences*, *23*(4), 401-405.

[9]. Heyries, K. A., Loughran, M. G., Hoffmann, D., Homsy, A., Blum, L. J., & Marquette, C. A. (2008). Microfluidic biochip for chemiluminescent detection of allergen-specific antibodies. *Biosensors and Bioelectronics*, *23*(12), 1812-1818.

[10]. Liu, H. B., Ramalingam, N., Jiang, Y., Dai, C. C., Hui, K. M., & Gong, H. Q. (2009). Rapid distribution of a liquid column into a matrix of nanoliter wells for parallel real-time quantitative PCR. *Sensors and Actuators B: Chemical*, *135*(2), 671-677.

[11]. Mata, A., Fleischman, A. J., & Roy, S. (2005). Characterization of polydimethylsiloxane (PDMS) properties for biomedical micro/ nanosystems. *Biomedical microdevices*, *7*(4), 281-293.

[12]. Van Poll, M. L., Zhou, F., Ramstedt, M., Hu, L., & Huck, W. T. (2007). A Self-Assembly Approach to Chemical Micropatterning of Poly (dimethylsiloxane). *Angewandte Chemie International Edition*, *46*(35), 6634-6637.

[13]. Prausnitz, M. R., & Langer, R. (2008). Transdermal drug delivery. *Nature biotechnology*, *26*(11), 1261-1268.

[14]. Lavan, D. A., McGuire, T., & Langer, R. (2003). Small-scale systems for in vivo drug delivery. *Nature biotechnology*, *21*(10), 1184.

[15]. Santini Jr, J. T., Richards, A. C., Scheidt, R., Cima, M. J., & Langer, R. (2000). Microchips as controlled drug-delivery devices. *Angewandte Chemie International Edition*, *39*(14), 2396-2407.

[16]. Santini, J. T. (1999). *A controlled release microchip* (Doctoral dissertation, Massachusetts Institute of Technology).

[17]. Zhang, Y., Chan, H. F., & Leong, K. W. (2013). Advanced materials and processing for drug delivery: the past and the future. *Advanced drug delivery reviews*, *65*(1), 104-120.

[18]. Zhang, Y., Ji, X., & Mohapatra, R. N. (2013). A naturally light sterile neutrino in an asymmetric dark matter model. *Journal of High Energy Physics*, *2013*(10), 104.

[19]. Couvreur, P. (2013). Nanoparticles in drug delivery: past, present and future. *Advanced drug delivery reviews*, *65*(1), 21-23.

[20]. Singh, A., Agarwal, R., Diaz-Ruiz, C. A., Willett, N. J., Wang, P., Lee, L. A., ... & García, A. J. (2014). Nanoengineered Particles for Enhanced Intra-Articular Retention and Delivery of Proteins. *Advanced healthcare materials*, *3*(10), 1562-1567.

[21]. Kochhar, J. S., Goh, W. J., Chan, S. Y., & Kang, L. (2013). A simple method of microneedle array fabrication for transdermal drug delivery. *Drug development and industrial pharmacy*, *39*(2), 299-309.

[22]. Kochhar, J. S., Anbalagan, P., Shelar, S. B., Neo, J. K., Iliescu, C., & Kang, L. (2014). Direct microneedle array fabrication off a photomask to deliver collagen through skin. *Pharmaceutical research*, *31*(7), 1724-1734.

[23]. Judy, J. W. (2001). Microelectromechanical systems (MEMS): fabrication, design and applications. *Smart materials and Structures*, *10*(6), 1115.

[24]. Guo, M., Que, C., Wang, C., Liu, X., Yan, H., & Liu, K. (2011). Multifunctional superparamagnetic nanocarriers with folate-mediated and pH-responsive targeting properties for anticancer drug delivery. *Biomaterials*, *32*(1), 185-194.

[25]. Cheng, R., Meng, F., Deng, C., Klok, H. A., & Zhong, Z. (2013). Dual and multi-stimuli responsive polymeric nanoparticles for programmed site-specific drug delivery. *Biomaterials*, *34*(14), 3647-3657.

[26]. Lo, C. T., Jahn, A., Locascio, L. E., & Vreeland, W. N. (2010). Controlled self-assembly of monodisperse niosomes by microfluidic hydrodynamic focusing. *Langmuir*, *26*(11), 8559-8566.

[27]. Zhang, L., Chan, J. M., Gu, F. X., Rhee, J. W., Wang, A. Z., Radovic-Moreno, A. F., ... & Farokhzad, O. C. (2008). Self-assembled lipid− polymer hybrid nanoparticles: a robust drug delivery platform. *ACS nano*, *2*(8), 1696-1702.

[28]. Owens, D. E., & Peppas, N. A. (2006). Opsonization, biodistribution, and pharmacokinetics of polymeric

nanoparticles. *International journal of pharmaceutics*, *307*(1), 93-102.

[29]. Karnik, R., Gu, F., Basto, P., Cannizzaro, C., Dean, L., Kyei-Manu, W., ... & Farokhzad, O. C. (2008). Microfluidic platform for controlled synthesis of polymeric nanoparticles. *Nano letters*, *8*(9), 2906-2912.

[30]. Andar, A. U., Hood, R. R., Vreeland, W. N., DeVoe, D. L., & Swaan, P. W. (2014). Microfluidic preparation of liposomes to determine particle size influence on cellular uptake mechanisms. *Pharmaceutical research*, *31*(2), 401-413.

[31]. Mathaes, R., Winter, G., Besheer, A., & Engert, J. (2015). Non-spherical micro-and nanoparticles: fabrication, characterization and drug delivery applications. *Expert opinion on drug delivery*, *12*(3), 481-492.

[32]. Geng, Y. A. N., Dalhaimer, P., Cai, S., Tsai, R., Tewari, M., Minko, T., & Discher, D. E. (2007). Shape effects of filaments versus spherical particles in flow and drug delivery. *Nature nanotechnology*, *2*(4), 249-255.

[33]. Kolhar, P., Anselmo, A. C., Gupta, V., Pant, K., Prabhakarpandian, B., Ruoslahti, E., & Mitragotri, S. (2013). Using shape effects to target antibody-coated nanoparticles to lung and brain endothelium. *Proceedings of the National Academy of Sciences*, *110*(26), 10753-10758.

[34]. Studart, A. R., Shum, H. C., & Weitz, D. A. (2009). Arrested coalescence of particle-coated droplets into nonspherical

supracolloidal structures. *The Journal of Physical Chemistry B*, *113*(12), 3914-3919.

[35]. Wang, B., Shum, H. C., & Weitz, D. A. (2009). Fabrication of monodisperse toroidal particles by polymer solidification in microfluidics. *ChemPhysChem*, *10*(4), 641-645.

[36]. Shum, H. C., Abate, A. R., Lee, D., Studart, A. R., Wang, B., Chen, C. H., ... & Weitz, D. A. (2010). Droplet microfluidics for fabrication of non-spherical particles. *Macromolecular rapid communications*, *31*(2), 108-118.

[37]. Panda, P., Ali, S., Lo, E., Chung, B. G., Hatton, T. A., Khademhosseini, A., & Doyle, P. S. (2008). Stop-flow lithography to generate cell-laden microgel particles. *Lab on a Chip*, *8*(7), 1056-1061.

[38]. Nagai, N., Kaji, H., Onami, H., Katsukura, Y., Ishikawa, Y., Nezhad, Z. K., ... & Nakazawa, T. (2014). A Platform for Controlled Dual-Drug Delivery to the Retina: Protective Effects against Light-Induced Retinal Damage in Rats. *Advanced healthcare materials*, *3*(10), 1555-1560.

[39]. Lo, R., Li, P. Y., Saati, S., Agrawal, R. N., Humayun, M. S., & Meng, E. (2009). A passive MEMS drug delivery pump for treatment of ocular diseases. *Biomedical microdevices*, *11*(5), 959.

[40]. Zachkani, P., Jackson, J. K., Pirmoradi, F. N., & Chiao, M. (2015). A cylindrical magnetically-actuated drug delivery device proposed for minimally invasive treatment of prostate cancer. *RSC Advances*, *5*(119), 98087-98096.

[41]. Pirmoradi, F. N., Jackson, J. K., Burt, H. M., & Chiao, M. (2011). A magnetically controlled MEMS device for drug delivery: design, fabrication, and testing. *Lab on a Chip*, *11*(18), 3072-3080.

[42]. Yi, Y., Zaher, A., Yassine, O., Buttner, U., Kosel, J., & Foulds, I. G. (2015, April). Electromagnetically powered electrolytic pump and thermo-responsive valve for drug delivery. In *Nano/Micro Engineered and Molecular Systems (NEMS), 2015 IEEE 10th International Conference on* (pp. 5-8). IEEE.

[43]. Pawinanto, R. E., Yunas, J., Majlis, B. Y., Bais, B., & Said, M. M. (2015). Fabrication and testing of electromagnetic MEMS microactuator utilizing PCB based planar microcoil. *ARPN J. Eng. Appl. Sci*, *10*(18), 8399-8403.

[44]. Bourouina, T., Bossebuf, A., & Grandchamp, J. P. (1997). Design and simulation of an electrostatic micropump for drug-delivery applications. *Journal of Micromechanics and Microengineering*, *7*(3), 186.

[45]. Chung, A. J., Huh, Y. S., & Erickson, D. (2009). A robust, electrochemically driven microwell drug delivery system for controlled vasopressin release. *Biomedical microdevices*, *11*(4), 861-867.

[46]. Santus, G., & Baker, R. W. (1995). Osmotic drug delivery: a review of the patent literature. *Journal of Controlled Release*, *35*(1), 1-21.

[47]. Verma, R. K., Krishna, D. M., & Garg, S. (2002). Formulation aspects in the development of osmotically controlled oral drug delivery systems. *Journal of controlled release*, *79*(1), 7-27.

[48]. Herrlich, S., Spieth, S., Messner, S., & Zengerle, R. (2012). Osmotic micropumps for drug delivery. *Advanced drug delivery reviews*, *64*(14), 1617-1627.

[49]. Said, M. M., Yunas, J., Pawinanto, R. E., Majlis, B. Y., & Bais, B. (2016). PDMS based electromagnetic actuator membrane with embedded magnetic particles in polymer composite. *Sensors and Actuators A: Physical*, *245*, 85-96.

[50]. Morimoto, Y., Mukouyama, Y., Habasaki, S., & Takeuchi, S. (2016). Balloon pump with floating valves for portable liquid delivery. *Micromachines*, *7*(3), 39.

[51]. Riahi, R., Tamayol, A., Shaegh, S. A. M., Ghaemmaghami, A. M., Dokmeci, M. R., & Khademhosseini, A. (2015). Microfluidics for advanced drug delivery systems. *Current Opinion in Chemical Engineering*, *7*, 101-112.

[52]. Rahimi, S., Sarraf, E. H., Wong, G. K., & Takahata, K. (2011). Implantable drug delivery device using frequency-controlled wireless hydrogel microvalves. *Biomedical microdevices*, *13*(2), 267-277.

[53]. Yanagisawa, K., Kuwano, H., & Tago, A. (1995). Electromagetically driven microvalve. *Microsystem Technologies*, *2*(1), 22-25.

[54]. Bae, B., Kee, H., Kim, S., Lee, Y., Sim, T., Kim, Y., & Park, K. (2003). In vitro experiment of the pressure regulating valve for a

glaucoma implant. *Journal of Micromechanics and Microengineering*, *13*(5), 613.

[55]. Oh, K. W., Rong, R., & Ahn, C. H. (2001). In-line micro ball valve through polymer tubing. In *Micro Total Analysis Systems 2001* (pp. 407-408). Springer Netherlands.

[56]. Fu, C., Rummler, Z., & Schomburg, W. (2003). Magnetically driven micro ball valves fabricated by multilayer adhesive film bonding. *Journal of Micromechanics and microengineering*, *13*(4), S96.

[57]. Choi, J. W., Oh, K. W., Thomas, J. H., Heineman, W. R., Halsall, H. B., Nevin, J. H., ... & Ahn, C. H. (2001, January). An integrated microfluidic biochemical detection system with magnetic bead-based sampling and analysis capabilities. In *Micro Electro Mechanical Systems, 2001. MEMS 2001. The 14th IEEE International Conference on* (pp. 447-450). IEEE.

[58]. Choi, J. W., Oh, K. W., Han, A., Wijayawardhana, C. A., Lannes, C., Bhansali, S., ... & Helmicki, A. J. (2001). Development and characterization of microfluidic devices and systems for magnetic bead-based biochemical detection. *Biomedical microdevices*, *3*(3), 191-200.

[59]. Schaible, J., Vollmer, J., Zengerle, R., Sandmaier, H., & Strobelt, T. (2001). Electrostatic microvalves in silicon with 2-way-function for industrial applications. In *Transducers' 01 Eurosensors XV* (pp. 900-903). Springer Berlin Heidelberg.

[60]. van der Wijngaart, W., Ask, H., Enoksson, P., & Stemme, G. (2002). A high-stroke, high-pressure electrostatic actuator for valve applications. *Sensors and Actuators A: Physical*, *100*(2), 264-271.

[61]. Teymoori, M. M., & Abbaspour-Sani, E. (2005). Design and simulation of a novel electrostatic peristaltic micromachined pump for drug delivery applications. *Sensors and Actuators A: Physical*, *117*(2), 222-229.

[62]. Yang, X. E., Holke, A., Jacobson, S. A., Lang, J. H., Schmidt, M. A., & Umans, S. D. (2004). An electrostatic, on/off microvalve designed for gas fuel delivery for the MIT microengine. *Journal of Microelectromechanical Systems*, *13*(4), 660-668.

[63]. Kirby, B. J., Shepodd, T. J., & Hasselbrink, E. F. (2002). Voltage-addressable on/off microvalves for high-pressure microchip separations. *Journal of Chromatography A*, *979*(1), 147-154.

[64]. Jerman, H. (1994). Electrically activated normally closed diaphragm valves. *Journal of Micromechanics and Microengineering*, *4*(4), 210.

[65]. Rich, C. A., & Wise, K. D. (2003). A high-flow thermopneumatic microvalve with improved efficiency and integrated state sensing. *Journal of Microelectromechanical Systems*, *12*(2), 201-208.

[66]. Takao, H., Miyamura, K., Ebi, H., Ashiki, M., Sawada, K., & Ishida, M. (2005). A MEMS microvalve with PDMS diaphragm and two-chamber configuration of thermo-pneumatic actuator for integrated blood test system on silicon. *Sensors and Actuators A: Physical*, *119*(2), 468-475.

[67]. Kim, J. H., Na, K. H., Kang, C. J., Jeon, D., & Kim, Y. S. (2004). A disposable thermopneumatic-actuated microvalve stacked with PDMS layers and ITO-coated glass. *Microelectronic Engineering*, *73*, 864-869.

[68]. Tamanaha, C. R., Whitman, L. J., & Colton, R. J. (2002). Hybrid macro–micro fluidics system for a chip-based biosensor. *Journal of Micromechanics and Microengineering*, *12*(2), N7.

[69]. Li, B., Chen, Q., Lee, D. G., Woolman, J., & Carman, G. P. (2005). Development of large flow rate, robust, passive micro check valves for compact piezoelectrically actuated pumps. *Sensors and Actuators A: Physical*, *117*(2), 325-330.

[70]. Bien, D. C. S., Mitchell, S. J. N., & Gamble, H. S. (2003). Fabrication and characterization of a micromachined passive valve. *Journal of micromechanics and microengineering*, *13*(5), 557.

[71]. Hu, M., Du, H., Ling, S. F., Fu, Y., Chen, Q., Chow, L., & Li, B. (2003). A silicon-on-insulator based micro check valve. *Journal of micromechanics and microengineering*, *14*(3), 382.

[72]. Chung, S., Kim, J. K., Wang, K. C., Han, D. C., & Chang, J. K. (2003). Development of MEMS-based cerebrospinal fluid shunt system. *Biomedical Microdevices*, *5*(4), 311-321.

[73]. Nguyen, N. T., & Truong, T. Q. (2004). A fully polymeric micropump with piezoelectric actuator. *Sensors and Actuators B: Chemical*, *97*(1), 137-143.

[74]. Nguyen, N. T., Truong, T. Q., Wong, K. K., Ho, S. S., & Low, C. L. N. (2003). Micro check valves for integration into polymeric

microfluidic devices. *Journal of Micromechanics and Microengineering*, *14*(1), 69.

[75]. Santra, S., Holloway, P., & Batich, C. D. (2002). Fabrication and testing of a magnetically actuated micropump. *Sensors and Actuators B: Chemical*, *87*(2), 358-364.

[76]. Olsson, A., Stemme, G., & Stemme, E. (2000). Numerical and experimental studies of flat-walled diffuser elements for valve-less micropumps. *Sensors and Actuators A: Physical*, *84*(1), 165-175.

[77]. Tsai, J. H., & Lin, L. (2002). A thermal-bubble-actuated micronozzle-diffuser pump. *Journal of microelectromechanical systems*, *11*(6), 665-671.

[78]. Andersson, H., Van Der Wijngaart, W., Nilsson, P., Enoksson, P., & Stemme, G. (2001). A valve-less diffuser micropump for microfluidic analytical systems. *Sensors and Actuators B: Chemical*, *72*(3), 259-265.

[79]. Jang, W. I., Choi, C. A., Jun, C. H., Kim, Y. T., & Esashi, M. (2004). Surface micromachined thermally driven micropump. *Sensors and Actuators A: Physical*, *115*(1), 151-158.

[80]. Laser, D. J., & Santiago, J. G. (2004). A review of micropumps. *Journal of micromechanics and microengineering*, *14*(6), R35.

[81]. Woias, P. (2005). Micropumps—past, progress and future prospects. *Sensors and Actuators B: Chemical*, *105*(1), 28-38.

[82]. Nguyen, N. T., & Wereley, S. T. (2002). *Fundamentals and applications of microfluidics*. Artech House.

[83]. Yang, X., Grosjean, C., Tai, Y. C., & Ho, C. M. (1998). A MEMS thermopneumatic silicone rubber membrane valve. *Sensors and Actuators A: Physical*, *64*(1), 101-108.

[84]. Baechi, D., Buser, R., & Dual, J. (2002). A high density microchannel network with integrated valves and photodiodes. *Sensors and Actuators A: Physical*, *95*(2), 77-83.

[85]. Kohl, M., Dittmann, D., Quandt, E., & Winzek, B. (2000). Thin film shape memory microvalves with adjustable operation temperature. *Sensors and Actuators A: Physical*, *83*(1), 214-219.

[86]. Pemble, C. M., & Towe, B. C. (1999). A miniature shape memory alloy pinch valve. *Sensors and Actuators A: Physical*, *77*(2), 145-148.

[87]. Reynaerts, D., Peirs, J., & Van Brussel, H. (1997). An implantable drug-delivery system based on shape memory alloy micro-actuation. *Sensors and Actuators A: Physical*, *61*(1-3), 455-462.

[88]. Qin, D., Xia, Y., & Whitesides, G. M. (2010). Soft lithography for micro-and nanoscale patterning. *Nature protocols*, *5*(3), 491.

[89]. Park, J., Kim, H. S., & Han, A. (2009). Micropatterning of poly (dimethylsiloxane) using a photoresist lift-off technique for selective electrical insulation of microelectrode arrays. *Journal of Micromechanics and Microengineering*, *19*(6), 065016.

[90]. Adrega, T., & Lacour, S. P. (2010). Stretchable gold conductors embedded in PDMS and patterned by photolithography: fabrication

and electromechanical characterization. *Journal of Micromechanics and Microengineering*, *20*(5), 055025.

[91]. Thangawng, A. L., Swartz, M. A., Glucksberg, M. R., & Ruoff, R. S. (2007). Bond–detach lithography: a method for micro/nanolithography by precision PDMS patterning. *small*, *3*(1), 132-138.

[92]. Kane, R. S., Takayama, S., Ostuni, E., Ingber, D. E., & Whitesides, G. M. (1999). Patterning proteins and cells using soft lithography. *Biomaterials*, *20*(23), 2363-2376.

[93]. Liu, H. B., & Gong, H. Q. (2009). Templateless prototyping of polydimethylsiloxane microfluidic structures using a pulsed CO2 laser. *Journal of Micromechanics and Microengineering*, *19*(3), 037002.

[94]. Rahimi, R., Ochoa, M., Donaldson, A., Parupudi, T., Dokmeci, M. R., Khademhosseini, A., ... & Ziaie, B. (2015). A Janus-paper PDMS platform for air? liquid interface cell culture applications. *Journal of Micromechanics and Microengineering*, *25*(5), 055015.

[95]. Li, M., Li, S., Wu, J., Wen, W., Li, W., & Alici, G. (2012). A simple and cost-effective method for fabrication of integrated electronic-microfluidic devices using a laser-patterned PDMS layer. *Microfluidics and nanofluidics*, *12*(5), 751-760.

[96]. Garra, J., Long, T., Currie, J., Schneider, T., White, R., & Paranjape, M. (2002). Dry etching of polydimethylsiloxane for

microfluidic systems. *Journal of Vacuum Science & Technology A: Vacuum, Surfaces, and Films*, *20*(3), 975-982.

[97]. Balakrisnan, B., Patil, S., & Smela, E. (2009). Patterning PDMS using a combination of wet and dry etching. *Journal of Micromechanics and Microengineering*, *19*(4), 047002.

[98]. Mata, A., Fleischman, A. J., & Roy, S. (2005). Characterization of polydimethylsiloxane (PDMS) properties for biomedical micro/nanosystems. *Biomedical microdevices*, *7*(4), 281-293.

[99]. Zhou, J., Ellis, A. V., & Voelcker, N. H. (2010). Recent developments in PDMS surface modification for microfluidic devices. *Electrophoresis*, *31*(1), 2-16.

[100]. Choi, J. S., Piao, Y., & Seo, T. S. (2013). Fabrication of a circular PDMS microchannel for constructing a three-dimensional endothelial cell layer. *Bioprocess and biosystems engineering*, *36*(12), 1871-1878.

[101]. Wang, G. J., Hsueh, C. C., Hsu, S. H., & Hung, H. S. (2007). Fabrication of PLGA microvessel scaffolds with circular microchannels using soft lithography. *Journal of micromechanics and microengineering*, *17*(10), 2000.

[102]. Wilson, M. E., Kota, N., Kim, Y., Wang, Y., Stolz, D. B., LeDuc, P. R., & Ozdoganlar, O. B. (2011). Fabrication of circular microfluidic channels by combining mechanical micromilling and soft lithography. *Lab on a Chip*, *11*(8), 1550-1555.

[103]. Guo, Y., Li, L., Li, F., Zhou, H., & Song, Y. (2015). Inkjet print microchannels based on a liquid template. *Lab on a Chip*, *15*(7), 1759-1764.

[104]. He, Y., Qiu, J., Fu, J., Zhang, J., Ren, Y., & Liu, A. (2015). Printing 3D microfluidic chips with a 3D sugar printer. *Microfluidics and Nanofluidics*, *19*(2), 447-456.

[105]. Kim, J. M., Im, C., & Lee, W. R. (2017). Plateau-Shaped Flexible Polymer Microelectrode Array for Neural Recording. *Polymers*, *9*(12), 690.

[106]. Larmagnac, Alexandre, et al. "Stretchable electronics based on Ag-PDMS composites." *Scientific reports* 4 (2014): 7254.

[107]. Jiang, Y., Wang, H., Li, S., & Wen, W. (2014). Applications of micro/nanoparticles in microfluidic sensors: a review. *Sensors*, *14*(4), 6952-6964.

[108]. Chen, Z., Xi, J., Huang, W., & Yuen, M. M. (2017). Stretchable conductive elastomer for wireless wearable communication applications. *Scientific reports*, *7*(1), 10958.

[109]. Lo, R., Li, P. Y., Saati, S., Agrawal, R., Humayun, M. S., & Meng, E. (2008). A refillable microfabricated drug delivery device for treatment of ocular diseases. *Lab on a Chip*, *8*(7), 1027-1030.

[110]. Lee, S. M., Kim, J. H., Byeon, H. J., Choi, Y. Y., Park, K. S., & Lee, S. H. (2013). A capacitive, biocompatible and adhesive electrode for long-term and cap-free monitoring of EEG signals. *Journal of neural engineering*, *10*(3), 036006.

[111]. Lee, H., Lee, B. P., & Messersmith, P. B. (2007). A reversible wet/dry adhesive inspired by mussels and geckos. *Nature*, *448*(7151), 338.

[112]. Wood, K. C., Zacharia, N. S., Schmidt, D. J., Wrightman, S. N., Andaya, B. J., & Hammond, P. T. (2008). Electroactive controlled release thin films. *Proceedings of the National Academy of Sciences*, *105*(7), 2280-2285.

[113]. Ma, Y., & Pidaparti, R. M. (2014). Simulation of Drug-Loaded Nanoparticles Transport Through Drug Delivery Microchannels. *Journal of Nanotechnology in Engineering and Medicine*, *5*(3), 031002.

[114]. Rahimi, S., Sarraf, E. H., Wong, G. K., & Takahata, K. (2011). Implantable drug delivery device using frequency-controlled wireless hydrogel microvalves. *Biomedical microdevices*, *13*(2), 267-277.

[115]. Pirmoradi, F. N., Jackson, J. K., Burt, H. M., & Chiao, M. (2011). A magnetically controlled MEMS device for drug delivery: design, fabrication, and testing. *Lab on a Chip*, *11*(18), 3072-3080.

[116]. Struss, W. J., Tan, Z., Zachkani, P., Moskalev, I., Jackson, J. K., Shademani, A., … & Chiao, M. (2017). Magnetically-actuated drug delivery device (MADDD) for minimally invasive treatment of prostate cancer: An in vivo animal pilot study. The Prostate, 77(13), 1356-1365.

[117]. Gensler, H., Sheybani, R., Li, P. Y., Mann, R. L., & Meng, E. (2012). An implantable MEMS micropump system for drug delivery in small animals. Biomedical microdevices, 14(3), 483-496.

[118]. Chung, A. J., Huh, Y. S., & Erickson, D. (2009). A robust, electrochemically driven microwell drug delivery system for controlled vasopressin release. *Biomedical microdevices*, *11*(4), 861-867.

[119]. Kim, Y. C., Park, J. H., & Prausnitz, M. R. (2012). Microneedles for drug and vaccine delivery. *Advanced drug delivery reviews*, *64*(14), 1547-1568.

[120]. Herrlich, S., Spieth, S., Messner, S., & Zengerle, R. (2012). Osmotic micropumps for drug delivery. *Advanced drug delivery reviews*, *64*(14), 1617-1627.

[121]. Bodas, D., & Khan-Malek, C. (2007). Hydrophilization and hydrophobic recovery of PDMS by oxygen plasma and chemical treatment—An SEM investigation. *Sensors and Actuators B: Chemical*, *123*(1), 368-373.

[122]. Verbaan, F.J.; Bal, S.M.; van den Berg, D.J.; Dijksman, J.A.; van Hecke, M.; Verpoorten, H.; van den Berg, A.; Luttge, R.; Bouwstra, J.A. Improved piercing of microneedle arrays in dermatomed human skin by an impact insertion method. J. Control. Release 2008, 128, 80–88.

[123]. Yuzhakov, V.V. The AdminPenTM microneedle device for painless & convenient drug delivery. Drug Deliv. Technol. 2010, 10, 32–36.

[124]. Lyon, B.J.; Aria, A.I.; Gharib, M. Fabrication of carbon nanotube-polyimide composite hollow microneedles for transdermal drug delivery. Biomed. Microdevices 2014, 16, 879–886.

[125]. Hwang, H., Kim, D. G., Jang, N. S., Kong, J. H., & Kim, J. M. (2016). Simple method for high-performance stretchable composite conductors with entrapped air bubbles. *Nanoscale research letters*, *11*(1), 14.

[126]. Liu, M., Sun, J., Sun, Y., Bock, C., & Chen, Q. (2009). Thickness-dependent mechanical properties of polydimethylsiloxane membranes. *Journal of micromechanics and microengineering*, *19*(3), 035028.

[127]. Jang, S. H., Park, Y. L., & Yin, H. (2016). Influence of coalescence on the anisotropic mechanical and electrical properties of nickel powder/polydimethylsiloxane composites. *Materials*, *9*(4), 239.

[128]. Nanni, G., Petroni, S., Fragouli, D., Amato, M., De Vittorio, M., & Athanassiou, A. (2012). Microfabrication of magnetically actuated PDMS–Iron composite membranes. *Microelectronic Engineering*, *98*, 607-609.

[129]. Carlborg, C. F., Haraldsson, T., Cornaglia, M., Stemme, G., & van der Wijngaart, W. (2010). A high-yield process for 3-D large-scale integrated microfluidic networks in PDMS. Journal of microelectromechanical systems, 19(5), 1050-1057.

[130]. ALZET® Osmotic Pumps, http://www.alzet.com27-8-2011

[131]. Rohloff, C. M., Alessi, T. R., Yang, B., Dahms, J., Carr, J. P., & Lautenbach, S. D. (2008). DUROS® Technology delivers peptides and proteins at consistent rate continuously for 3 to 12 months. *Journal of diabetes science and technology*, *2*(3), 461-467.

[132]. Intarcia Therapeutics, Inc., http://www.intarcia.com27-8-2011

[133]. S. Herrlich, S. Spieth, R. Nouna, R. Zengerle, L.I. Giannola, D.E. Pardo-Ayala, E. Federico, P. Garino, Ambulatory Treatment and Telemonitoring of Patients with Parkinson's Disease, in: R. Wichert, B. Eberhardt (Eds.), Springer, Dordrecht, 2011, pp. 295–305.

[134]. S. Herrlich, T. Lorenz, M. Marker, S. Spieth, S. Messner, R. Zengerle, Miniaturized osmotic pump for oromucosal drug delivery with external readout station, Proc.of IEEE-EMBC, Boston, 2011, pp. 8380–8383.

[135]. Koh, K. S., Chin, J., Chia, J., & Chiang, C. L. (2012). Quantitative studies on PDMS-PDMS interface bonding with piranha solution and its swelling effect. Micromachines, 3(2), 427-441.

[136]. Crespo-Castrillo, A., Yanguas-Casás, N., Arevalo, M. A., Azcoitia, I., Barreto, G. E., & Garcia-Segura, L. M. (2018). The Synthetic Steroid Tibolone Decreases Reactive Gliosis and Neuronal Death in the Cerebral Cortex of Female Mice After a Stab Wound Injury. *Molecular neurobiology*, 1-17.

초록

의료 분야의 발전에 따라 수많은 약들이 개발되어 왔지만 아직까지 투여 방법은 경구 투여 방법과 정맥에 바로 주입하는 주사기를 통한 방법으로만 지속되고 있다. 경구 투여와 정맥 주사는 투여 방법이 쉽다는 이유 때문에 아직도 주로 쓰이지만 특정 부위 또는 목표 세포에만 약물을 전달하는 것은 어렵다. 효율적인 약물 전달은 최소독성혈중농도 (MTC) 와 최소유효혈중농도 (MEC) 사이를 유지하도록 약물을 적정량 그리고 적정 기간을 두고 전달해야 한다. 현재에도 흔히 쓰이는 약물 전달 방식은 이러한 효율적인 약물 요법의 조건들을 만족하지 못한다. 그러므로 경구 투약이나 주사에 의한 투여 방법의 단점들을 보완할 수 있는 약물 전달 기기들이 활발히 연구되고 있다.

국소 부위에 설치하는 약물 전달 기기들은 약물 전달이 필요한 부위에 설치되는 방법으로 공간적인 제어를 실현한다. 이러한 전달 기기들이 만족해야 하는 조건들은 적정량의 약물, 정확한 시간에 그리고 저전력으로 구동이 가능해야 한다는 것이다. 이 모든 조건들은 대부분의 약물 전달 기기들이 가지고 있는 밸브와 펌프를 통해 달성할 수 있다. 본 논문에서 제안하는 약물 전달 기기는 풍선과 같이 부풀고 수축이 가능한 약물 저장소 구조를 제작하는 방법을 제안하여 전력이 필요한 펌프가 없이도 약물 전달이 가능하게 하였다. 이 펌프는 자기장 혹은 전자기장의 유무에 따라 구동되는 밸브를 만들어 약물 전달은 이 밸브를

열고 닫는 것만으로 가능하게 하였다. 이 밸브는 평상시에 닫혀 있는 형태로 열릴 때만 전력을 사용하여 전력 사용량을 최소화 하였다.

이 약물 전달 기기의 제작은 Polydimethylsiloxane (PDMS) 와 PDMS 와 금속 기반의 마이크로 입자의 합성물로만 이루어지도록 하였다. PDMS 패터닝은 일반적으로 Micro Electromechanical Systems (MEMS) 의 포토리소그래피 (photolithography) 와 식각 (etching) 방식을 통해 이루어진다. 하지만 이런 방식은 여러층과 복잡한 구조를 만들려면 여러 단계 그리고 긴 시간 동안의 공정 시간이 필요하다. 본 논문에서는 사진석판술이나 식각과 같은 결과를 낳을 수 있는 새로운 PDMS 공정 방법을 산소 플라즈마 표면처리 (oxygen plasma treatment), 자기조립분자막 (self-assembled monolayer) 그리고 폴리염화 비닐 시트지 패터닝을 사용해 약물 전달 기기 제작법을 제안한다.

자기조립분자막은 PDMS 와 PDMS 간의 접착이 이루어지지 않게 하기 위한 막을 분자 단위의 두께로 제작하는 방법이다. 반대로 산소 플라즈마 표면처리는 PDMS 간의 접착이 더 효과적으로 이루어지게 하는 방식이다. 자기조립분자막과 산소 플라즈마 표면처리를 조합하여 폴리염화비닐 패턴을 통해 선택적 표면 접착을 실행하였다. 폴리염화비닐 패턴은 칼로 잘라내는 자동 플로터 (blade plotter) 와 레이저로 잘라내는 다이오드 펌핑 고체 레이저 (diode pumped solid state laser) 두 기기로 제작하였다. 선택적 표면 접착 방법은 약물 저장소를 만드는데 사용하였다. 더 나아가, 폴리염화비닐과 PDMS 의

중합 억제 관련성을 조사하여 PDMS 식각을 실현하였다. PDMS 식각은 약물 저장소와 밸브를 연결하는 마이크로 채널을 만드는데 사용하였다. 이 약물 전달 기기의 약물 전달량은 기기의 약물 저장소의 크기, 막 두께, 저장소를 빠져나가는 마이크로 채널의 단면적 크기 등 복합적인 요소에 따라 달라진다. 약물 전달 시기를 제어하는 것은 자기장 또는 전자기장을 통해 구동되는 마이크로 밸브이다. 이 밸브는 저전력 구동이 가능하도록 평상시에는 닫혀 있도록 설계되었다.

약물의 전달 시기를 조절하는 밸브는 외부 자기장으로 구동 될 수 있도록 제작되었다. 이 밸브는 얇은 니켈 마이크로 입자와 PDMS 로 섞은 얇은 막에 네오디뮴 자석이 접합되어 있어 평소에는 닫혀있는 상태를 유지하다 자기장으로 구동되어 당겨지는 힘에 의해 열리는 구조를 가지고 있다. 자기 구동은 막이 당겨지는 방향으로 자석을 위치시켜 밸브가 열리게 할 수 있다.

마지막으로, 제작된 약물 전달 기기는 생체 적합성을 분석하기 위해 용출물 실험과 세포 독성 실험을 진행하였다. PDMS 는 높은 생체적합성을 가지는 물질로 판명된 물질이다. 하지만 PDMS 만 쓰지 않고 금속 마이크로 입자를 섞은 PDMS 와 네오디뮴 자석도 사용하였기에, 또 이 기기는 피부에 접합하여 사용하거나 약물이 전달되어야 하는 체내에 설치하는 방식으로 사용 되기 때문에 생체 적합성 실험을 진행하였다. 더 나아가, 이 기기의 중요한 구성 요소인 밸브와 펌프의 내구성도 조사되었다. 반복적인 실험으로 약물 전달량의 변화가 없는지 또는 밸브에서 누출이 이루어지지 않는지도 실험하였다.

주요어: 폴리염화비닐 스텐실, PDMS 경화 억제, 단층과 다층 PDMS 패터닝, 전도성 폴리머, 약물전달 기기

학번: 2012-30933